DEVELOPMENT OF A PROBABILISTIC CHANNEL FLOOD ROUTING METHOD FOR STORMWATER MANAGEMENT ANALYSIS

By

CHUAN LI, B.Eng.

(Sichuan University, China)

A Thesis

Submitted to the School of Graduate Studies

In Partial Fulfillment of the Requirements

For the Degree

Master of Applied Science

McMaster University

MASTER OF APPLIED SCIENCE (2008) McMaster University

(Civil Engineering) Hamilton, Ontario

TITLE:	Development of a Probabilistic Channel Flood Routing Method for Stormwater Management Analysis
AUTHOR:	Chuan Li, B.Eng. (Sichuan University, China)
SUPERVISOR:	Professor Y. Guo, PhD, P.Eng.
NUMBER OF PAGES:	ix, 125.

Abstract

An approach to incorporate the effect of flood routing through a channel reach for use with the analytical probabilistic stormwater models (APSWM) was developed earlier in 2005. That earlier approach relied on adding the Muskingum K value of the channel reach into the catchment time of concentration and treating the whole drainage area including the channel reach as a lumped catchment. This is insufficient since other factors such as the X value in the Muskingum routing method also affects the routing results. In this study, a new approach to incorporate the routing effect of channel reaches in APSWM was developed where not only the K value but also the X value of a channel reach are considered. A number of continuous simulations were conducted to verify the proposed approach. It was demonstrated that the proposed approach performs better than the earlier one.

Acknowledgements

I would like to thank Dr. Yiping Guo, my supervisor, for his guidance and patience. This thesis would not have been possible without him. Many thanks also go to Dr. David Hansen at Dalhousie University who led me to the door of the professionals and helped me a lot during my earlier graduate studies in Canada. Dr. Hansen actually co-supervised me during my graduate studies both at McMaster University and Dalhousie University. I am grateful to Mr. Zhengji Zhuge, who did a great job on his research, which was the starting point of my thesis.

Finally, I would like to give my thanks to my wife, Qiuling Wang, who endured this long process with me, always offering support and love.

TABLE OF CONTENTS

LIST OF TABLES

LIST OF FIGURES

CHAPTER 1: Introduction

1.1 Watershed Planning and Stormwater Management

Urbanization and other changes of land use in a watershed may result in an increase of surface runoff volume and peak stormwater discharge. Watershed planning refers to the watershed-based policy making and more detailed design or setting of performance criteria for activities related to flood mitigation, water quality improvement, and ecosystem rehabilitation [*MOE*, 2003]. Construction of buildings, roads, subdivisions and industrial parks converts originally pervious lands into impervious areas. This conversion will cause a number of stormwater- related problems if it is not dealt with properly. These problems may include, (1) increased flood frequency and magnitude; (2) accelerated erosion of streams; (3) deteriorated water quality; and (4) reduced base flows in downstream rivers [*DeBarry*, 2004]. The conversion of natural land into agricultural land may cause similar problems. Stormwater management is the planning for and control of drainage from urban areas and agricultural fields in order to maximize the benefits of stormwater and minimize its adverse environmental impacts [*MOE*, 2003]. In the past, stormwater management emphasized only the construction of hydraulic structures such as retention ponds that simply slow down the delivery of stormwater to downstream water bodies. More recently, stormwater management has required an integrated approach for the best management of both stormwater quantity and quality.

Urban stormwater also poses a challenge to downstream existing municipal sewerage systems. Expanding urban areas require greater capacities of stormwater conveyance facilities and the treatment plants that treat combined sewage. Options of expanding the existing downstream sewerage system, replacing the dysfunctional system, and building a new system, all require the municipality to spend huge sums of money. Hence, a good stormwater management strategy should be based on not only engineering consideration, but also financial and social impacts. Stormwater best management practices (BMPs) are therefore widely adopted for the quantity and quality control of runoff by many municipalities. As a result, stormwater management on a watershed-basis and implemented together with watershed planning are highly promoted. To facilitate watershed planning and stormwater management, hydrologic models are used as the basic tool for setting up and verifying the conformance of various management criteria.

Hydrologic models are numerical models that simulate the hydrological processes occurring within a watershed in response to precipitation inputs. The processes commonly simulated by hydrologic models include rainfall-runoff transformation, catchment and channel routing, and reservoir or detention pond flow routing. The results from hydrologic models may be used for flood forecasting, stormwater facility real-time control, stormwater facility design analysis, watershed/master drainage plan analysis, etc. Design storm models and continuous simulation models are commonly used for these purposes. In the following sections, more details are provided about design storm models and continuous simulation models as they are applied to watershed planning and stormwater management. Subsequently, an alternative modeling approach is introduced.

1.2 Design Storm Models

Design storm models are single event hydrologic models that use synthetic or actual storms as input rainfall sources to simulate hydrologic processes occurring on the watershed of interest. The synthetic or actual storms which are used to establish a consistent and uniform design criterion are referred to as design storms. Design storms are widely used in engineering practice, as not only can they be easily constructed and standardized for regulatory purposes, but are also believed to provide conservative outputs [*Huber*, 1993]. The following paragraphs describe the parameters that determine a typical design storm detailed characteristics.

1) *Storm Duration*: Storm duration is the duration in hours of the design storm. For regulation and design purposes, the duration of a design storm should typically be equal to or longer than the time of concentration of the catchment. Only when the storm

duration is equal to or longer than the catchment time of concentration, will runoff from the entire catchment contribute to the design point. Normally storm durations of 1-3 hours are satisfactory for small urban watersheds. Large watersheds require the use of long duration storms (up to 24 hours).

2) *Storm Depth*: Storm depth is the total precipitation depth at a point which is a function of storm frequency and storm duration. Rainfall intensity-duration-frequency (IDF) curves provide average rainfall intensity for various storm durations and selected recurrence intervals. The IDF curves published by Atmospheric Environment Services (AES) of Environment Canada are available for more than one thousand stations across Canada. IDF information can be expressed in the forms of a table, a set of curves or equations. The required design storm depths can be calculated from IDFs by multiplying the average intensity with the selected storm duration for a specific recurrence interval.

3) *Time Distribution*: Time distribution of a storm refers to the variation of precipitation intensity over its duration and is another important factor in determining the timing and the magnitude of the resulting peak flow. The selection of representative hyetographs should proceed with caution, since the choice will significantly affect the shape and peak discharge of the resulting runoff hydrograph. The design storm hyetograph should follow the recorded storm distribution patterns or be based on the worst-possible storm patterns. The commonly used Chicago, AES, Huff-Quarter Storms

have their own unique distribution patterns [*Adams & Papa*, 2000]. Triangular distribution is also widely used due to its simple pattern.

Design storm models are used widely in watershed planning to establish site-specific flood and water quality control criteria and stormwater management for the hydrologic design of various stormwater management facilities. Although the design storm method is very popular, its shortcomings cannot be ignored because they may limit the applicability of design storms for some purposes or under some special circumstances. Firstly, the assumption of the same exceedance frequency between the input design storm and output peak flow has not been proven to be true. Secondly, the selected rainfall volume and duration are not the real volume and duration of actual storm events. There is no way of associating a unique frequency to the volumes of design storms which have the same exceedance frequency but different durations. Thirdly, the design storm hyetograph cannot be considered with only one unique frequency, the characteristics (duration, volume, density etc.) within a hyetograph may have different frequency distributions [*Adams & Papa*, 2000].

1.3 Continuous Simulation Models

Unlike design storm models, continuous simulation models use actual historical rainfall records as input to perform rainfall-runoff transformations and other hydrologic calculations continuously for a long time (from 1 year up to 100 years). The basic hydrologic mechanisms simulated by continuous simulation models are similar to those simulated by design storm models, but continuous simulations include the modeling of evapotranspiration during dry periods and continuous accounting of soil moisture. Continuous simulations can generate more accurate results than design storm modeling because long-term rainfall records are employed as direct input and frequency analyses are performed on the simulation output to obtain the required information on the frequency of occurrence of runoff volume and peak discharge rate.

However, continuous simulations have their associated costs for the accuracies gained. Firstly, the longer the period, the more the missing data in the historical rainfall records. Secondly, the short calculation time steps for a long-term continuous simulation consume more computer time, especially when evaluating multiple design scenarios and conducting sensitivity analyses on input parameters. Thirdly, separate frequency analyses need to be made on continuous simulation results. This would cost additional time. To overcome these drawbacks, some simplifications may have to be made but those simplifications decrease the accuracy of the finial outputs.

At present, long-term rainfall records are typically provided with hourly temporal resolution from the AES of Environment Canada. Continuous simulations are therefore usually run using hourly time step, which is not as refined as 5-minute to 15-minute time steps used in design storm modeling, particularly for some small urban catchments. Although several interpolation methods have been developed to meet the requirements of refined temporal resolution for continuous simulation, the accuracy that they provide is questionable.

1.4 Analytical Probabilistic Stormwater Models

Analytical probabilistic stormwater models include the set of analytical equations developed by *Guo* and *Adams* [1998a, b; 1999a, b]. Recently these analytical equations were coded into a computer program named APSWM at McMaster University [*Guo*, 2004]. APSWM provides an expedient solution to those analytical equations. Unlike design storm modeling or continuous simulation, APSWM uses analytical expressions to estimate peak discharge and runoff volume for various return periods. Since the entire spectrum of rainfall conditions are taken into consideration in deriving the analytical expressions, the results from APSWM are expected to be close to those from continuous simulations. In other words, APSWM possesses the accuracy of continuous simulation but is more efficient to use than design storm modeling.

APSWM considers natural rainfall events in their entirety. Each natural rainfall event is characterized by its rainfall event volume (v) and rainfall event duration (t), as well as the inter-event time (b) following that rainfall event. A typical rainfall record can then be viewed as comprising a time series of each of the above characteristics. Generally the time series of v, t and b can represent the major statistical characteristics of the historical rainfall record, since the detailed rainfall intensity variations within each rainfall event do not have significant impacts [*Guo* and *Adams* 1998a]. The v, t and b series can be used to plot their respective histograms and fitted with theoretical distribution curves. An average annual number of storm events (θ) can also be calculated from a historical rainfall record. It has been found that exponential probability density functions (PDF) often fit the v, t and b probability density histograms (PDH) satisfactorily [*Eagleson*, 1972, 1978; *Howard*, 1976; *Adams et al.*, 1986; *Adams and Papa*, 2000].

The exponential distributions for rainfall event characteristics can be expressed as follows:

$$f_V(v) = \zeta e^{-\zeta v}, v \ge 0 \quad \text{where} \quad \zeta = \frac{1}{\bar{v}} \quad (\text{mm}^{-1})$$

$$f_T(t) = \lambda e^{-\lambda t}, t \ge 0 \quad \text{where} \quad \lambda = \frac{1}{\bar{t}} \quad (\text{hr}^{-1})$$

$$f_B(b) = \psi e^{-\psi b}, b \ge 0 \quad \text{where} \quad \psi = \frac{1}{\bar{b}} \quad (\text{hr}^{-1})$$

where ζ, λ, and ψ are distribution parameters. For a specific location, the four parameters ζ, λ, ψ, and θ need to be known in order to use the probabilistic models to describe local rainfall characteristics. In this respect, design storms of various return periods used for stormwater management planning and design are replaced by these four parameters in APSWM. The value of the three distribution parameters may be estimated from $\bar{v}$, $\bar{t}$, and $\bar{b}$, respectively; where $\bar{v}$ is the average event volume, $\bar{t}$ is the average event duration, and $\bar{b}$ is the average interevent time determined from the rainfall record. Thus, instead of requesting users to input design storms or a time series of historical rainfall record, APSWM requires users to input $\bar{v}$, $\bar{t}$, $\bar{b}$ and θ for the location of interest.

One of the major differences between APSWM and conventional stormwater models in modelling the catchment rainfall-runoff processes is that APSWM considers these processes storm-event by storm-event and does not perform any time-step by time-step calculations. The triangular hydrograph assumptions incorporated in APSWM particularly resemble the unit hydrograph methodology used in conventional stormwater models. The difference is that in conventional stormwater models, the time step length is the duration over which a unit (1 cm or 1 in) of excess rainfall generates a unit hydrograph. While in APSWM, the duration over which a unit of excess rainfall resulting in a triangular unit hydrograph is the duration of the rainfall event itself and varies from event to event. APSWM's simple formulation for catchment rainfall-runoff routing ensures that v's and t's of similar magnitudes would generate runoff volumes and peak discharges of similar magnitudes. Although large errors may result from APSWM's simple formulation when the peak discharge from individual storms is forecast, the errors are largely random and should be less important in studying the frequency distributions of peak discharges. If the interest is the frequency distributions rather than the values for individual events, APSWM's simple formulation may be accurate enough.

The other major difference between APSWM and conventional stormwater models is that land areas upstream of a point where runoff information is needed are modeled in APSWM as a single catchment for the proper tracing of input and output probabilities. While in using conventional stormwater models, the same land area may be treated as comprised of several subcatchments combined and/or linked with channel reaches, runoff generation and/or routing may be calculated separately for each subcatchment and channel reach. It is recognized that some accuracy may be lost because of the use of the lumped runoff generation and routing scheme in APSWM. However, for small drainage areas typical of stormwater management studies, this loss of accuracy may be insignificant.

To explicitly represent the effect of a channel reach on downstream peak discharge's frequency of occurrence, APSWM takes in some of the parameters describing the channel reach and modifies the upstream catchment's time of concentration to account for the effect of the reach based on the physical characteristics of reach. In that sense, although no separate numerical reach routing calculations are performed in APSWM, ASPWM still carries out probabilistic reach routing calculations. The current channel routing module in APSWM is based on the method proposed by *Zhuge* [2005]. The channel reach's Muskingum K value is calculated based on the reach's physical characteristics and is incorporated into the APSWM analytical equations so that the storm wave travel time through the reach can be added in the total time of concentration of the upstream catchment. The comparison with design storm modeling showed that this approach is capable of representing some of the reach routing effects in APSWM.

1.5 Thesis Objective and Organization

At present, APSWM is mostly used for research purposes. It is still necessary to improve APSWM so that it can eventually be accepted and used in engineering practice. In this study, the probabilistic channel reach routing mechanism that is currently used in APSWM is reviewed and a new approach is proposed and tested. The objective of developing this new probabilistic reach routing method is to eliminate some of the shortcomings of the method proposed by *Zhuge* [2005]. Verification of this new method is accomplished through comparison with continuous simulation rather than design storm modeling.

Provided below is a brief overview of the following chapters of this thesis.

- Chapter 2 – Rainfall Statistics for Use in APSWM

Describes the basics of event-based rainfall data analysis. Interevent time definition (IETD) and threshold of rainfall event volume (TRV) as required in the event-based analysis are introduced. The Halifax and Toronto long-term rainfall records are used as examples of analyses to determine the required rainfall statistics.

- Chapter 3 – Verification of APSWM Catchment Runoff Routing

Verifies the catchment runoff routing method used in APSWM. Six hypothetical catchments are used to represent a variety of catchment conditions. These catchments are modeled by both APSWM and HEC-HMS. Different overland flow routing methods were used by HEC-HMS, comparisons with APSWM results establish the approximate relationship between the catchment's time of concentration as used in HEC-HMS and the same catchment's time of concentration as used in APSWM.

- Chapter 4 – A New Probabilistic Channel Flood Routing Method

Presents a new channel routing method that can be used in APSWM. Detailed descriptions and theoretical derivations are provided. The influence of Muskingum-Cunge's K and X values are both incorporated in the new method. Various catchment and downstream routing reach combinations are chosen to verify the applicability of the new method.

- Chapter 5 – Conclusions and Recommendations for Further Research

Summarizes the findings of this thesis and provides the suggestions for further research.

CHAPTER 2: Rainfall Statistics for APSWM

2.1 Inter-Event Time Definition (IETD)

A long-term rainfall record collected at a gauge station is comprised of rainfall pulses and dry periods. Individual storm events may be isolated from this record. A minimum period without rainfall or interevent time definition (IETD) is introduced to distinguish consecutive rainfall events. If the dry period between two rainfall pulses is less than IETD, the two pulses are considered as belonging to the same storm event; otherwise the two pulses are considered as belonging to different storm events. Thus, the number of storm events and other statistics will be different if different IETDs are used.

Adams and *Papa* [2000] illustrate that autocorrelation analysis is one way of determining a suitable IETD. Autocorrelation is the correlation of data at one point in time with the same data at an earlier point in time and can be expressed as follows:

$$r_k = \frac{\sum (y_t - \bar{y})(y_{t-k} - \bar{y})}{\sum (y_t - \bar{y})^2} \tag{2.1}$$

where y is the observed rainfall intensity, k is the lag time between two observations. The lag time needs to be long enough for consecutive storm events and to be statistically independent (i.e., r_k should be close to 0). The lag time that results in a low enough r_k value may be used as IETD.

Another method of determining a suitable IETD is to compare the observed relative frequency histogram (RFH) obtained based on a specific IETD and its best-fit theoretical exponential PDF curve. The comparison can be made visually or by checking coefficient of correlation (COC) between the theoretical and empirical probability densities. If the COC is equal to or approximately equal to unity, the exponential curve will fit the observed probability density histogram (PDH) the best and the corresponding IETD should be used. COC can be calculated as:

$$COC = \frac{COV(X,Y)}{\sigma_x \cdot \sigma_y} \tag{2.2}$$

where $$COV(X,Y) = \frac{1}{n}\sum(x_i - \mu_x)(y_i - \mu_y)$$

X and Y are the empirical and theoretical probability densities, respectively, each regarded as a random variable; x_i, y_i are the n realizations of the random variable X and Y respectively; and u_x and u_y are the means of X and Y respectively.

The examination of the relationship between IETD and the average annual number of rainfall events is another method of determining a suitable IETD. A suitable IETD may be selected as that after which increases in the IETD do not result in significant changes in the annual number of events observed.

For urban catchments, IETDs between 2 to 6 hours are recommended, since rainfall characteristics become less sensitive when IETD increases over 6 hours [*Guo & Adams*, 1998a]. An appropriate IETD should be obtained with statistical analysis using some of the above-mentioned methods.

2.2 Threshold of Rainfall Event Volume (TRV)

A rainfall record usually includes many small rainfall events. *Guo* and *Adams* [1998a] found that the exponential PDF would fit the observed relative frequency histogram better if some of the small rainfall events (e.g., volume $\leq$ 1 mm) are discarded. Small rainfall events do not generate any runoff and can be excluded from further analyses. It is therefore necessary to determine an appropriate threshold of rainfall event volume (TRV) in the analysis so that events with volumes less than this threshold are discarded. In this study, various combinations of IETD and TRV are used to determine the most suitable combination.

2.3 Long-term Rainfall Data Preparation

A 41-year hourly historical rainfall record (1956-1998, with 1957 and 1992 missing) from the Halifax Shearwater station (AES #8205090, Latitude: 44.63; Longitude: -63.5; Elevation: 50.9 m) and a 56-year hourly historical rainfall record (1939-1998, with 1940, 1956-1958 missing) from the Toronto Yonge Street station (AES #6158350, Latitude: 43.67; Longitude: -79.4; Elevation: 112.5 m) were used to represent the climates in the Maritimes and Southern Ontario. In order to avoid snowfall and snowmelt calculations, data from November through March were not included; each year rainfall data series starts from April 1st and ends on October 31st.

Interpolation is used to fill gaps in rainfall data series. It was found that there were some days' when hourly data are missing. Since the corresponding daily rainfall data are available from AES' website, the missing hourly data can be added using interpolation within the 24 hours of the day with the daily total equaling the daily total found from AES' website. It is assumed that a linear relationship exists between each hour rainfall and the daily total rainfall. Based on this assumption and the daily total rainfall, the hourly distribution of daily rainfall is estimated from hourly climate condition data. For instance, if the hourly climate condition is "*Drizzle*", then no more than 0.5 mm rainfall depth is given to that hour; if the hourly climate condition is "*Shower*", then no more than 2 mm rainfall depth is given to that hour. Although the estimated values are somewhat arbitrary and not precise, the outputs are not affected significantly considering the small number of missing days (less than 5%).

2.4 APSWM Rainfall Statistics Calculation

A Visual Basic Application (VBA) for Microsoft EXCEL was developed to perform the rainfall event separation and other related calculations. The rainfall statistical calculations were performed using this VBA program.

APSWM requires the input of four rainfall statistics: i.e., average rainfall volume ($\bar{v}$), average rainfall duration ($\bar{t}$), average inter-event time ($\bar{b}$), and average annual number of storm events (θ). By selecting an IETD and TRV values, the VBA program calculates the average values of the annual number of events, volume and duration of events and interevent times. Table 2.1 and Table 2.2 list the rainfall statistics for Halifax and Toronto respectively, obtained using different IETD and TRV combinations.

Table 2.1 APSWM Rainfall Statistics for the Halifax Shearwater Station

Halifax Statistics	Rainfall Event Threshold = 0 mm			
	IETD = 2 hr	**IETD = 4 hr**	**IETD = 6 hr**	**IETD = 9 hr**
ψ	0.021156965	0.017106517	0.015211547	0.013814446
ζ	0.143477517	0.114839046	0.10119198	0.090926127
θ	85.90243902	68.75609756	60.58536585	54.43902439
λ	0.241630077	0.173423562	0.139951547	0.114602588
Halifax Statistics	**Rainfall Event Threshold = 1 mm**			
	IETD = 2 hr	**IETD = 4 hr**	**IETD = 6 hr**	**IETD = 9 hr**
ψ	0.012738702	0.011530569	0.010893167	0.010339334
ζ	0.089648972	0.079411131	0.073957533	0.069247912
θ	52.29268293	46.73170732	43.68292683	41
λ	0.168288854	0.128772095	0.107690458	0.091046959
Halifax Statistics	**Rainfall Event Threshold = 2 mm**			
	IETD = 2 hr	**IETD = 4 hr**	**IETD = 6 hr**	**IETD = 9 hr**
ψ	0.010093796	0.009565171	0.009188287	0.008907937
ζ	0.073529096	0.067608421	0.063845695	0.060871927
θ	41.70731707	39	37.07317073	35.53658537
λ	0.146970348	0.115226634	0.097323601	0.083333333

Table 2.2 APSWM Rainfall Statistics for the Toronto Yonge St. Station

Toronto	Rainfall Event Threshold = 0 mm			
Statistics	IETD = 2 hr	IETD = 4 hr	IETD = 6 hr	IETD = 9 hr
ψ	0.018923992	0.015709547	0.014161232	0.012799489
ζ	0.191753941	0.157921644	0.141306227	0.126457608
θ	91.08928571	75.01785714	67.125	60.07142857
λ	0.283704116	0.208849118	0.1701752	0.135552242
Toronto	**Rainfall Event Threshold = 1 mm**			
Statistics	**IETD = 2 hr**	**IETD = 4 hr**	**IETD = 6 hr**	**IETD = 9 hr**
ψ	0.011778974	0.010843901	0.01027655	0.00966094
ζ	0.124731467	0.112503659	0.105241365	0.097538425
θ	57.23214286	52.16071429	49.01785714	45.58928571
λ	0.207618061	0.160812596	0.134433616	0.109195894
Toronto	**Rainfall Event Threshold = 2 mm**			
Statistics	**IETD = 2 hr**	**IETD = 4 hr**	**IETD = 6 hr**	**IETD = 9 hr**
ψ	0.009319607	0.00882608	0.008563709	0.008223189
ζ	0.103237973	0.095060207	0.090553118	0.085299916
θ	45.55357143	42.71428571	41.08928571	39.01785714
λ	0.184855072	0.144890666	0.122185641	0.09964429

2.5 Selection of Suitable IETD and TRV

In Tables 2.1 and 2.2, there are 12 IETD and TRV combinations for both Halifax and Toronto. The resulting rainfall statistics were then substituted to the theoretical exponential distributions. Theoretical PDF curves were obtained and compared with observed relative frequency histogram (RFH). The coefficient of correlation between PDF and RFH can be calculated using Eq. (2.2).

Table 2.3 shows the coefficients of correlation (COC) resulting from 12 IETD and TRV combinations for Halifax and Toronto. The coefficients in Table 2.3 are the average values of the coefficients of correlation for volume v, duration t and interevent time b. It was found that when IETD is equal to 9 hours and TRV is equal to 1 mm, the theoretical PDF curves provide the best fit for Halifax and Toronto. *Guo* and *Adams* [1998a] found that when IETD = 6 hr and TRV =1 mm, the theoretical PDF curves fit the Toronto Pearson International Airport rainfall data the best. In this study, however, the COC using an IETD of 6 hr is 0.9935 and the COC using an IETD of 9 hr is 0.9939, only a very small difference exists between the IETD of 6 hr and the IETD of 9 hr for the Toronto Yonge Street rainfall data. Therefore, the results with IETD of 6 hr and 9 hr are both acceptable for the Toronto area. Figures 2.1 to 2.6 present the fitting plots for Toronto using an IETD of 6 hrs and TRV of 1mm, and plots for Halifax using an IETD of 9 hrs and TRV of 1mm.

Table 2.3 Correlation Coefficient for IETD and TRV combinations

IETD (hr)	TRV (mm)	Correlation Coefficient	
		Halifax	Toronto
2	0	0.93047209	0.949218301
4	0	0.929675697	0.960824531
6	0	0.940345847	0.968883325
9	0	0.940160395	0.969277012
2	1	0.941220797	0.971841338
4	1	0.966382139	0.986482424
6	1	0.944717896	0.99345537
9	1	0.970599999	0.993872341
2	2	0.908243235	0.91746648
4	2	0.941927771	0.948381454
6	2	0.945326178	0.960972079
9	2	0.941863028	0.960593455

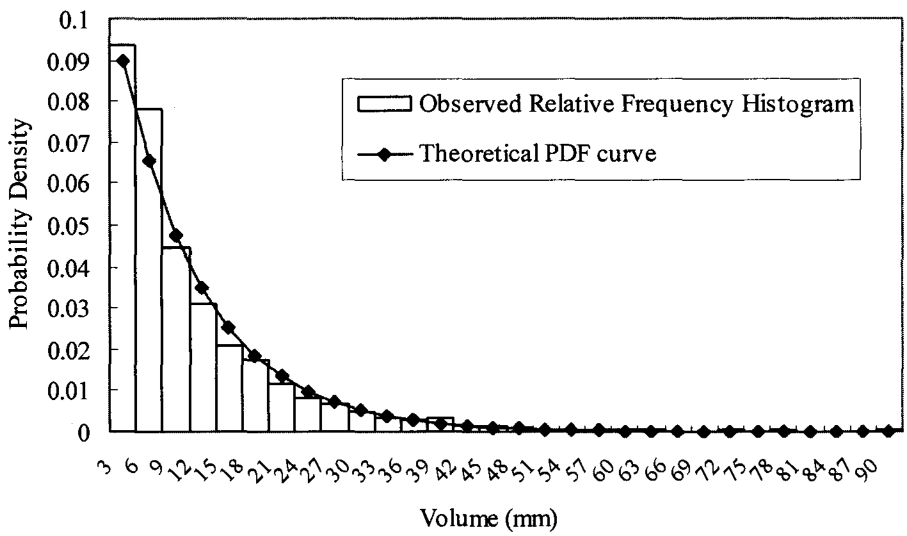

Figure 2.1 PDF Curve Fitting for Rainfall Event Volume (Toronto, IETD = 6 hr; TRV = 1 mm)

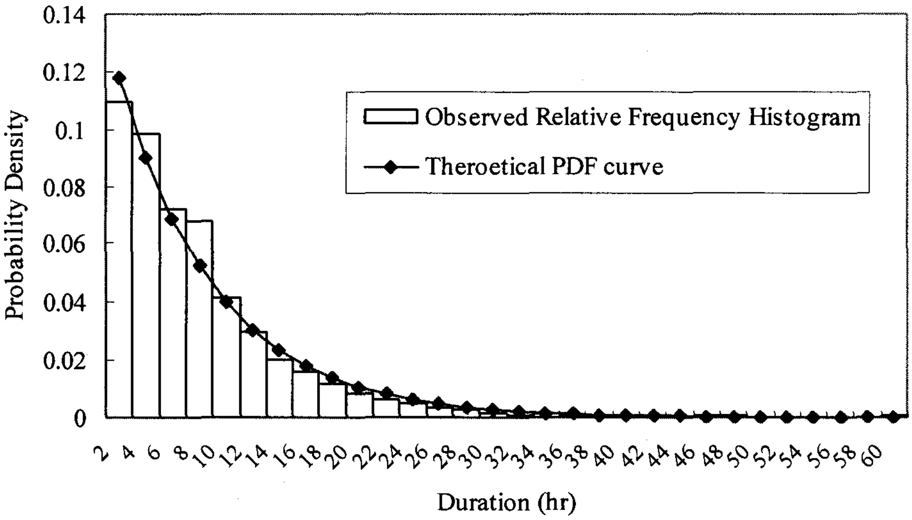

Figure 2.2 PDF Curve Fitting for Rainfall Event Duration (Toronto, IETD = 6 hr; TRV = 1 mm)

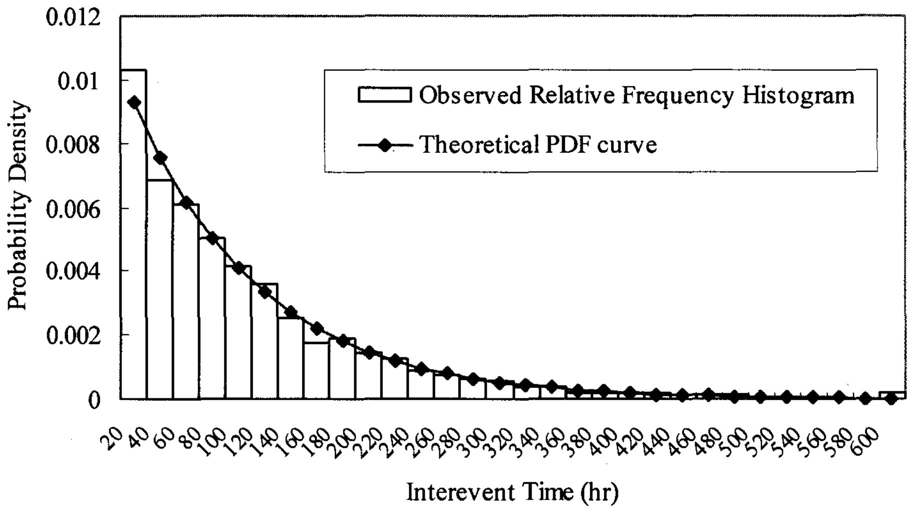

Figure 2.3 PDF Curve Fitting for Interevent Time (Toronto, IETD = 6 hr; TRV = 1 mm)

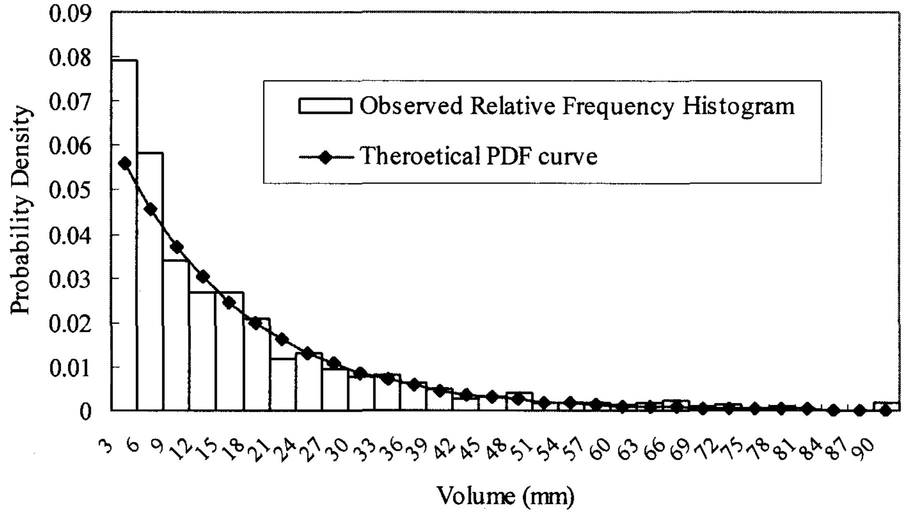

Figure 2.4 PDF Curve Fitting for Rainfall Event Volume (Halifax, IETD = 9 hr; TRV = 1 mm)

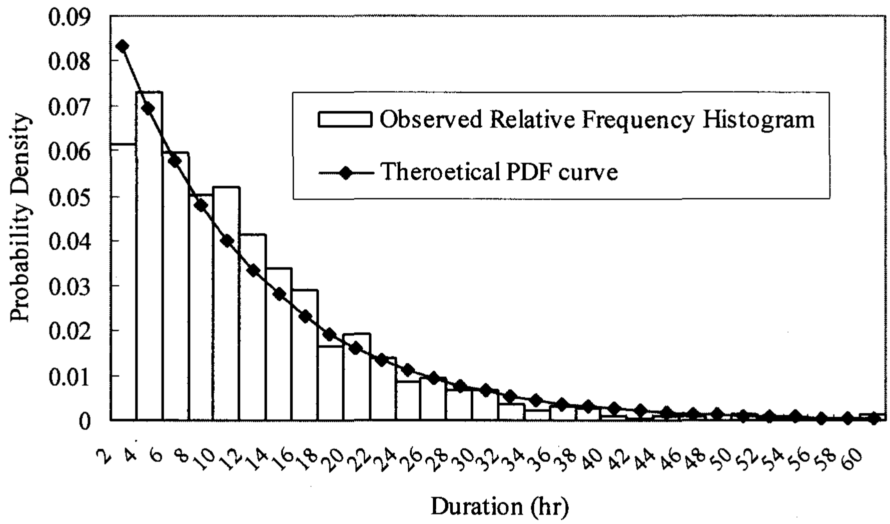

Figure 2.5 PDF Curve Fitting for Rainfall Event Duration (Halifax, IETD = 9 hr; TRV = 1 mm)

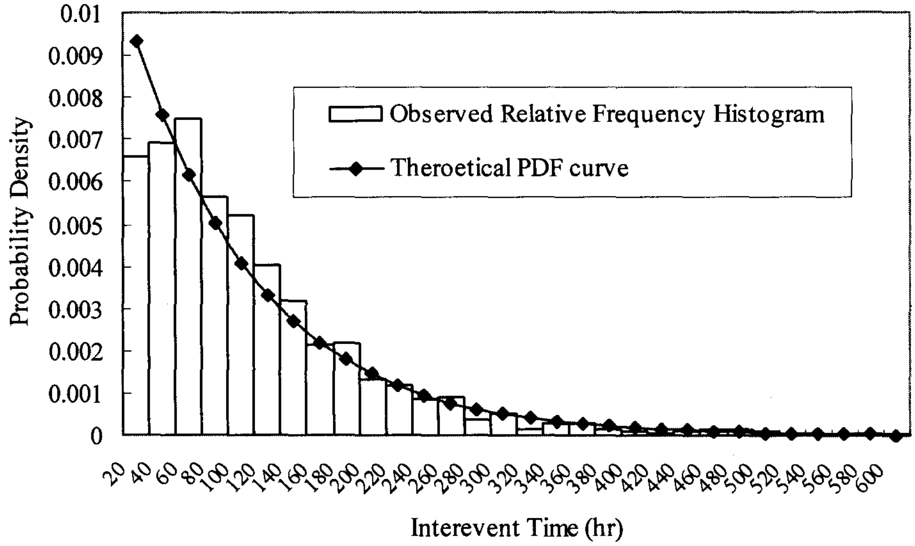

Figure 2.5 PDF Curve Fitting for Interevent Time (Halifax, IETD = 9 hr; TRV = 1 mm)

It can be seen from these figures that when TRV = 1mm, IETD = 9 hour for Halifax and IETD = 6 hour for Toronto are selected, the agreement between the PDF and RFH is graphically acceptable as well. Thus, these IETD and TRV values along with their corresponding rainfall statistics are used for catchment and channel routing analyses in Chapters 3 and 4.

CHAPTER 3: Verification of APSWM Catchment Runoff Routing

3.1 Catchment Setup

Catchment is the basic hydrologic unit that is used in hydrologic calculations related to rainfall-runoff transformation. Based on their areas, three categories of catchments (i.e., small, midsize, and large) are possible [*Ponce*, 1989]. For urban stormwater management, small catchments are often encountered. In a small catchment, rainfall can be assumed to be uniformly distributed in space; storm duration usually exceeds time of concentration; runoff is primarily produced by overland flow and channel storages are negligible. Catchments with areas less than 2.5 km^2 or 250 ha are normally considered small catchments, although criteria other than area may also be used to judge if a catchment can be categorized as small.

In this study, before developing and testing out more advanced probabilistic channel routing method for use in APSWM, the catchment runoff routing method of APSWM was verified further. To this end, six hypothetical small catchments were made up to represent various urban conditions. The physical characteristics of these catchments are listed in Table 3.1. *Guo* and *Adams* [1998a] and *Zhuge* [2005] conducted hydrological modeling for three of the six catchments (i.e., catchments *A*, *B*, and *C*) using Toronto Pearson International Airport rainfall data and found that results from APSWM are fairly close to those from SWMM (continuous simulation) and MIDUSS (design storm modeling). Three more hypothetical catchments (i.e., catchments *D*, *E*, and *F*) have been added in this study in order to cover a longer range of times of concentration, as well as a wider range of soil conditions. HEC-HMS version 3.0.1 [*USACE*, 2005] was used for continuous simulations and APSWM version 1.0 [*Guo*, 2006] was employed for analytical calculations.

Table 3.1 Physical Characteristics of the Test Catchments

Catchment	A	B	C	D	E	F
Area (ha)	30	4	40	47	22	101
Imperviousness (%)	100	20	70	50	100	0
Impervious Portion Flow Length (m)	750	10	800	400	290	0
Pervious Portion Flow Length (m)	0	40	343	380	0	830
Soil Type	Silt	Clay	Sand & Gravel	Gravel	Sand & Silt	Silt & Clay
Slope	0.01	0.005	0.005	0.005	0.008	0.03
Impervious Area Manning's *n*	0.014	0.013	0.02	0.015	0.02	0.015
Pervious Area Manning's *n*	0.25	0.25	0.25	0.1	0.1	0.1
Initial Deficit (mm)	3	3	3	4	4	4
Maximum Storage (mm)	17.7	8.5	21.8	37.2	22.4	12.4
Constant Infiltration Rate (mm/hr)	3.6	0.36	36	55	16	2.7
Impervious Depression Storage (mm)	4.5	4.5	4.5	4	4	4

Average Initial Loss (mm)	20.7	11.5	24.8	41.2	26.4	16.4
Average t_c Used in APSWM (hr)	1.65	1.97	2.62	0.85	0.75	1.34
Storage Coefficient (hr)	0.99	1.182	1.572	0.125	0.125	0.125

3.1.1 Time of Concentration

One of the most important parameters in catchment routing is time of concentration (t_c), which is defined as the travel time of a water particle from the most hydraulically remote point to the outlet. There are two types of t_c formulae. Those that express t_c as a function of catchment characteristics only are referred to as Type I; those that express t_c as a function of both catchment characteristics and rainfall intensity are referred to as Type II formulas. The kinematic wave formula [*Singh*, 1996] which is a Type II formula is adopted by APSWM:

$$t_c = 0.116 \frac{(Ln)^{0.6}}{i_e^{0.4} S^{0.3}} \tag{3.1}$$

where L is the overland length (m), n is the Manning's roughness coefficient, i_e is the effective rainfall intensity (mm/hr), and S is the average overland slope (dimensionless). The units of t_c in Eq. (3.1) are hours. Eq. (3.1) may be used for sheet flow when channel flows cannot be modeled, and this equation is valid for a maximum length of 90 m over impervious areas and 30 m over pervious areas. If the overland flow length is beyond these limits, the Friend's equation [*Ponce*, 1989] can be used to estimate t_c:

$$t_c = \frac{0.71nL^{0.333}}{S^{0.2}} \qquad (3.2)$$

Where t_c is in hours and L is in meters.

This way, both the type II kinematic wave equation and the type I Friend's equation are included to APSWM to estimate t_c. An urban catchment usually comprises pervious and impervious areas, so the time of concentration of an urban catchment is the sum of the flow travel time over the pervious and impervious planes. In addition to estimating t_c values based on catchment characteristics, APSWM also allows users to directly specify t_c values. If a user chooses this option, the user input t_c values will overwrite APSWM estimated t_c values.

Constant t_c values are used for catchments modeled by APSWM [*Guo and Adams*, 1998b]. The constant overland flow time is obtained by using the kinematic wave formula together with a long-term average effective rainfall intensity characteristic of the location and the catchment. This is justified because it is believed that t_c variations from storm to storm are small compared to t_c variations attributable to other factors (e.g., catchment geometric shape, slope, length, and soil type). It is found that the results from APSWM using a constant t_c are very close to the results from design storm modeling where t_c changes as rainfall intensity changes [*Quader and Guo*, 2005].

3.1.2 Loss Methods Available in HEC-HMS

Based on the water balance theory, the water mass movement in a hydrologic cycle can be represented by the following equation [*Viessman & Lewis*, 1996]:

$$P - R - G - E - T = \Delta S \tag{3.3}$$

where P is the amount of precipitation in the study area; R is the net amount of surface runoff out of the area; G is the net amount of groundwater flow out of the area; E is the total evaporation from the area; T is the total transpiration from the area and ΔS is the change in water mass stored in that area. HEC-HMS uses Eq. (3.3) and calculates runoff volume by computing the volume of water that is intercepted, infiltrated, stored, evaporated, or transpired and subtracting them from the precipitation [*USACE*, 2000]. There are several loss models incorporated in HEC-HMS 3.0.0 and later versions:

- Initial and constant loss model
- Deficit and constant loss model
- SCS curve number loss model
- Green and Ampt loss model
- Soil moisture accounting loss model

Among these models, only *Deficit and Constant* (D&C) loss model and *Soil Moisture Accounting* (SMA) loss model can be used for the continuous simulation, the other models are more suitable for single event simulations. The D&C loss model is selected for this study in view of the complexities of the SMA loss model. The basic concept of D&C loss model is that the maximum potential rate of precipitation loss f_c is constant throughout a rainfall event. So the excess rainfall can be represented by:

$$R = \begin{cases} P - f_c, & if \ \ P > f_c \\ 0, & Otherwise \end{cases} \tag{3.4}$$

where R is the excess rainfall depth or runoff volume in depth at the current time step, P is the average precipitation depth at the current time step. The initial loss I_a is added to the loss model to represent interception and depression storage losses. Thus, incorporating initial loss, Eq. (3.4) can be written as:

$$R = \begin{cases} 0, & if \ \ \sum P < I_a \\ P - f_c, & if \ \ \sum P > I_a \ \ and \ \ P > f_c \\ 0, & if \ \ \sum P > I_a \ \ and \ \ P < f_c \end{cases} \tag{3.5}$$

Here $\sum P$ is the accumulated precipitation.

As for the antecedent conditions, before individual rainfall events if the soil in the watershed is dry, then the initial loss I_a will reach its maximum value, contrarily I_a will approach zero when the soil is totally saturated. In a continuous simulation, the soil moisture condition varies between dry and wet cycle. I_a is calculated automatically by HEC-HMS.

3.1.3 Surface Runoff Routing Methods Available in HEC-HMS

HEC-HMS provides several direct runoff routing methods to simulate the processes of overland flow and interflow:

- Clark's unit hydrograph
- Snyder's unit hydrograph
- SCS unit hydrograph
- User-specified unit hydrograph
- Kinematic wave

The *Unit Hydrograph* (UH) approach is a simple linear model that can be used to derive the hydrograph resulting from any excess rainfall [*Chow*, 1988]. A unit hydrograph is the hydrograph resulting from rainfall with 1 inch (or 1 cm) depth for a selected duration. Clark's UH and User-specified UH (Triangular or Rectangular UH) are used in this study to further evaluate the surface runoff routing method used in APSWM.

The original Clark's UH is based on the Time-Area theory combined with a hypothetical linear reservoir to account for the catchment's storage effect [*Clark*, 1945]. The continuity equation for a reservoir is:

$$I - O = \frac{dS}{dt} \tag{3.6}$$

where I is inflow and O is outflow of the hypothetical linear reservoir. dS/dt is the rate of change in storage. Under the linear reservoir assumption:

$$S_t = KQ_t \tag{3.7}$$

Combine Eq. (3.6) and Eq. (3.7) and represent it in finite difference form:

$$\frac{I_1 + I_2}{2} - \frac{O_1 + O_2}{2} = K\frac{Q_2 - Q_1}{\Delta t} \tag{3.8}$$

Solve for Q_2:

$$Q_2 = C_0 \frac{I_1 + I_2}{2} + C_1 Q_1 \tag{3.9}$$

where

$$C_0 = \frac{2\Delta t}{2K + \Delta t} \tag{3.10}$$

$$C_1 = \frac{2K - \Delta t}{2K + \Delta t} \tag{3.11}$$

K is the storage coefficient of the hypothetical reservoir, and it is often approximated by the watershed's lag time.

In HEC-HMS, the time-area relationship for Clark's UH is generalized as:

$$\frac{A_t}{A} = \begin{cases} 1.414\left(\dfrac{t}{t_c}\right)^{1.5} & \text{for } t \le \dfrac{t_c}{2} \\ 1 - 1.414\left(1 - \dfrac{t}{t_c}\right)^{1.5} & \text{for } t \ge \dfrac{t_c}{2} \end{cases} \tag{3.12}$$

where A_t is cumulative watershed area contributing at time t; A is total watershed area; t_c is time of concentration [*USACE*, 2000]. Thus, users just need to input t_c and K to use the Clark's UH option of HEC-HMS.

3.1.4 Loss and Runoff Routing Methods Available in APSWM

The conventional rainfall-runoff transformation process is represented in APSWM as well. Runoff comes from rainfall with deduction of hydrologic losses during a rainfall event. Some rainfalls are intercepted by vegetation and structures and eventually evaporate to the atmosphere; some are used to fill the depression areas of the catchment; some infiltrate the soil and replenish the groundwater. The remaining rainfall becomes runoff. The interception loss and depression storage loss of rainfall are combined as one loss in APSWM, i.e., pervious and impervious area depression storages. APSWM has also included the option of use any of the commonly used infiltration models including *Horton's* model, *Green-Ampt* model, *SCS Curve Number* model, *Initial and Constant Loss* model. For urban catchments, the total runoff volumes can be calculated as the combination of runoff generated from pervious and impervious areas. The following expressions illustrate this:

$$v_r = \begin{cases} 0 & , \quad v \le S_{di} \\ h(v - S_{di}) & , \quad S_{di} < v \le S_{il} + f_c t \\ v - S_d - f_c(1-h)t & , \quad v > S_{il} + f_c t \end{cases} \tag{3.13}$$

where v_r is the total runoff volume; v_{ri} and v_{rp} are the runoff volume from impervious and pervious areas of the urban catchment, respectively; h is the fraction of impervious areas within that urban catchment; S_{di} is the depression storage of impervious areas; S_{il} is the initial losses of pervious areas; $S_d = hS_{di} + (1 - h)S_{il}$, is the area-weighted depression storage of the impervious areas and the initial losses of the pervious areas of the urban catchment; f_c is the ultimate infiltration capacity of the pervious area; t is the duration and v is the volume of the input rainfall event. In this study, the *Initial and Constant Loss* model is selected to match with the one selected in HEC-HMS continuous simulations. The average initial loss in APSWM, i.e., $S_{il} = S_{dp} + S_{iw}$, which is sum of depression storage (S_{dp}) plus initial soil wetting infiltration depth (S_{iw}), is considered equivalent to the *Maximum Storage* as defined and used in HEC-HMS. The constant infiltration loss rate f_c in APSWM is equivalent to constant loss rate in HEC-HMS.

The mathematical frequency distribution functions for runoff event volume and peak discharge have been derived by *Guo and Adams* [1998 a&b]. The probability of exceedance for runoff event volume (v_r) is expressed as follows:

$$G_{V_R}(v_r) = \begin{cases} \exp(-\zeta S_{di}) & , \quad v_r = 0 \\ \exp(-\zeta S_{di} - \frac{\zeta}{h} v_r) & , \quad 0 < v_r \le hS_{dd} \\ \frac{\lambda}{\lambda + \zeta f_c - \zeta f_c h} \exp(-\zeta S_d - \zeta v_r) + \\ \frac{\zeta f_c (1-h)}{\lambda + \zeta f_c - \zeta f_c h} \exp\left[-\zeta S_{di} + \frac{\lambda}{f_c} S_{dd} - \frac{1}{h}(\zeta + \frac{\lambda}{f_c}) v_r \right] & , \quad v_r > hS_{dd} \end{cases}$$

(3.14)

where S_{dd} is the difference between the initial losses in the pervious area and depression storage in the impervious area (i.e., $S_{il} - S_{di}$). The relationship between return period (T_R) and the probability of exceedance, $G_{V_R}(v_r)$, is as follows:

$$T_R = \frac{1}{\theta G_{V_R}(v_r)} \tag{3.15}$$

where θ is the annual average number of rainfall events.

Each runoff hydrograph is assumed to be triangular in APSWM. This is an important assumption and is the basis for routing calculations in APSWM. Also as shown in Figure 3.1, the duration of rainfall events is estimated as $t + t_c$, thus the peak discharge rate can be obtained based on the geometry as follows:

$$Q_p = \frac{2v_r}{t + t_c} \tag{3.16}$$

where t is the duration of the rainfall event, and t_c is the catchment time of concentration.

In order to obtain the exceedance probability of peak discharge, two types of catchments are defined. The catchments where $f_c < S_{dd}/t_c$ are identified as Type I catchments. The peak discharge exceedance probability for Type I catchments can be expressed as:

$$P[Q_p > q_p] = \begin{cases} \dfrac{2h\lambda}{2h\lambda + \zeta q_p} \exp(-\zeta S_{di} - \dfrac{\zeta t_c}{2h} q_p) & , \quad q_p < 2 f_c h \\ \dfrac{2\lambda\zeta(1-h)(q_p - 2f_c h)}{(2h\lambda + \zeta q_p)(2\lambda + \zeta q_p + 2f_c\zeta - 2hf_c\zeta)} \exp\left[-\dfrac{(\zeta S_{il} - \lambda t_c - f_c\zeta t_c)q_p - 2f_c\zeta h S_{di} + 2\lambda h S_{dd}}{q_p - 2f_c h} \right] & \\ + \dfrac{2\lambda}{2h\lambda + \zeta q_p} \exp(-\zeta S_{di} - \dfrac{\zeta t_c}{2h} q_p) & , \quad 2f_c h < q_p < \dfrac{2hS_{dd}}{t_c} \\ \dfrac{\lambda}{\lambda + \zeta(\dfrac{q_p}{2} + f_c - f_c h)} \exp(-\zeta S_d - \dfrac{\zeta t_c}{2} q_p) & , \quad q_p \geq \dfrac{2hS_{dd}}{t_c} \end{cases}$$

(3.17)

The catchments where $f_c \geq S_{dd}/t_c$ is identified as Type II catchments. The peak discharge exceedance probability for Type II catchments can be expressed as:

$$P[Q_p > q_p] = \begin{cases} \dfrac{2h\lambda}{2h\lambda + \zeta q_p} \exp(-\zeta S_{di} - \dfrac{\zeta t_c}{2h} q_p) & , \quad q_p < \dfrac{2hS_{dd}}{t_c} \\ \dfrac{2\lambda\zeta(1-h)(2f_c h - q_p)}{(2h\lambda + \zeta q_p)(2\lambda + \zeta q_p + 2f_c\zeta - 2hf_c\zeta)} \exp\left[-\dfrac{(\zeta S_{il} - \lambda t_c - f_c\zeta t_c)q_p - 2f_c\zeta h S_{di} + 2\lambda h S_{dd}}{q_p - 2f_c h} \right] & \\ + \dfrac{2\lambda}{2\lambda + \zeta(q_p + 2f_c - 2f_c h)} \exp(-\zeta S_d - \dfrac{\zeta t_c}{2h} q_p) & , \quad \dfrac{2hS_{dd}}{t_c} < q_p < 2f_c h \\ \dfrac{\lambda}{\lambda + \zeta(\dfrac{q_p}{2} + f_c - f_c h)} \exp(-\zeta S_d - \dfrac{\zeta t_c}{2} q_p) & , \quad q_p \geq 2f_c h \end{cases}$$

(3.18)

where Q_p is a specific peak discharge while q_p is a random variable. Similarly the return period (T_R) of peak discharge also can be calculated as follows:

$$T_R = \frac{1}{\theta P[Q_p > q_p]} \tag{3.19}$$

This way, APSWM calculates the runoff volume and peak discharge of desired return periods using Equations (3.14) through (3.18). Comparing with conventional stormwater models, APSWM does not conduct time-step by time-step calculations, but it gives similar results for many test cases [*Guo* and *Adams*, 1998; *Quader* and *Guo*, 2005; *Zhuge*, 2005].

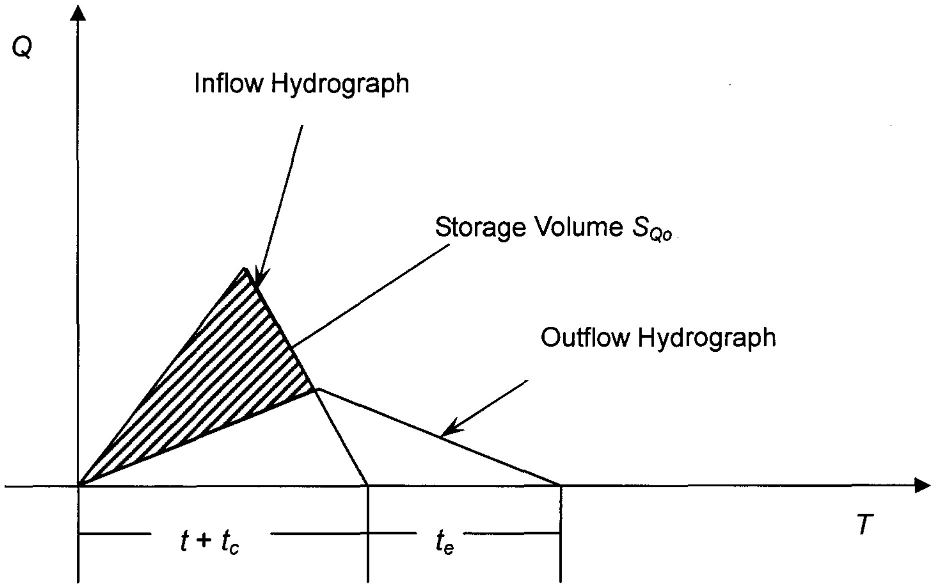

Figure 3.1 APSWM Catchment and Detention Pond Routing Hydrograph

3.2 Catchment Peak Discharge Analysis

Since peak discharges of various return periods are often used as the criteria for sizing stormwater infrastructures, and APSWM results have so far never been compared with HEC-HMS results, by comparing APSWM and HEC-HMS results for a series of test catchments, a better understanding of APSWM and conventional modeling methods may be obtained.

3.2.1 HEC-HMS Continuous Simulations

As mentioned in Chapter 2, this study uses two Canadian cities' (i.e., Halifax and Toronto) rainfall historical record as the input meteorological data. Each rainfall data set is applied to six hypothetical catchments separately, thus each catchment has two sets of peak discharges. There are 41 years of hourly rainfall data from Halifax, and 56 years of hourly records from Toronto. HEC-HMS uses the DSS (Data Storage System) file system to manage the massive amount of data, so the long records can be processed in a very efficient way.

Different from event simulations, continuous simulations account for soil moisture conditions during dry as well as wet conditions to simulate runoff from rainfall events in hourly intervals over long time periods. The *Initial and Constant Loss* method is used in both HEC-HMS and APSWM models. In HEC-HMS, *Initial Deficit* represents the initial condition of a catchment, and equals to the total amount of water needed to saturate the soil to its *Maximum Storage* capacity. The *Constant Loss Rate* is the average infiltration rate after the soil is saturated.

Unit Hydrograph (UH) method was selected in HEC-HMS simulations. Three UH methods: Clark's, Triangular and Rectangular UHs are used in HEC-HMS. The surface runoff routing method in APSWM is somewhat similar to triangular UH but not really the same. In APSWM it is event-based while conventional UH methods perform routing calculations time-step by time-step. Future versions APSWM may incorporate more surface routing options.

The time step for continuous simulation is 15 minutes, which is a fairly acceptable value considering the long period of time simulated. The storage coefficient or Clark's *K* value is selected as the minimum allowable value of 0.125 hour. This is for the purpose of minimizing differences between the catchment as simulated by HEC-HMS and that simulated by APSWM. Since the storage effect is not separately considered in APSWM, but as a part of the catchment time of concentration.

Frequency analysis is conducted with the HEC-HMS simulated long-term flow series to estimate peak discharge frequency of occurrence. The recurrence interval is based on the probability that the given event will be equaled or exceeded in any given year. In this study, peak discharge corresponding to 2, 5, 10, 25, 50, 100-year return periods are determined in frequency analysis using continuous simulation results. For a given recurrence interval *T*, the corresponding peak discharge can be calculated by the following frequency factor equation [*Viessman & Lewis*, 1996]:

$$\log Q = \overline{\log Q} + z(s_{\log s}) \tag{3.20}$$

In Eq. (3.20), Q is the required peak discharge; $\overline{\log Q}$ and $s_{\log s}$ are the mean and standard deviation of log-transformed annual maximum discharges respectively, z is the frequency factor, which is a function of T and the coefficient of skewness of the log-transformed annual maximum discharges. In using Eq. (3.20), Log Pearson Type III distributions are assumed.

Base flow is not considered in HEC-HMS modeling, because base flows are usually low for small catchments and may not influence hydrographs significantly during storm periods. The current version of APSWM considers surface runoff only. A base flow function may be added in future APSWM versions.

3.2.2 APSWM Calculations

Similar to HEC-HMS, the *Initial and Constant Loss* method is used in APSWM. As stated in 3.1.4, the value of *Average Initial Losses* S_{il} is the sum of pervious area depression storage S_{dp} and initial soil wetting infiltration depth S_{iw}, i.e., $S_{il} = S_{dp} + S_{iw}$. *Constant Infiltration Loss Rate* is the infiltration rate after the soil is saturated.

APSWM incorporates the function of estimating time of concentration, which relies on the kinematic wave equation and Friend's equation to perform calculations.

However in this study, t_c in APSWM is directly inputted by the user to ensure equivalence between HEC-HMS and APSWM. It was found that the t_c used in APSWM should be 1.5 times the sum of the t_c used in HEC-HMS and the storage coefficient of 0.125 hours. This is mainly based on the observations of HEC-HMS simulated hydrographs. Through extensive experiments, the actual catchment time of concentration defined as the duration between the last point of input hyetograph and the last point of outflow hydrograph is approximately equal to 1.5 times t_c, where t_c is the HEC-HMS input time of concentration value. Figure 3.2 gives an example of the input hyetograph and output hydrograph by using Clark's UH.

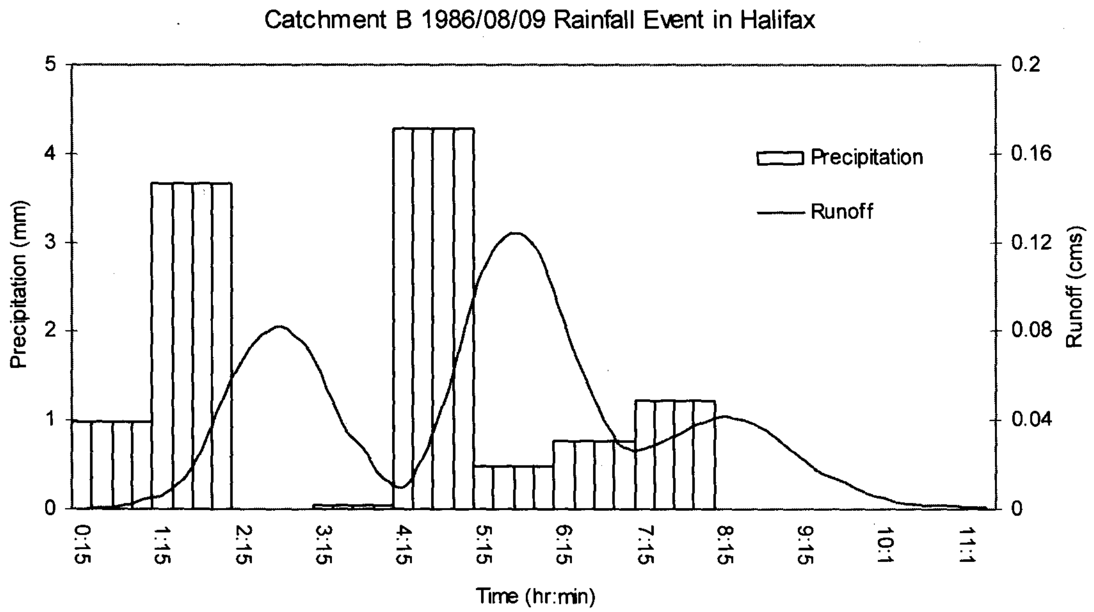

Figure 3.2 Typical Input Hyetograph and Output Hydrograph from HEC-HMS Simulations Using Clark's UH

Comparing Clark's UH in HEC-HMS with the corresponding triangular hydrograph in APSWM, the fact that 1.5 times t_c should be used in APSWM can also be demonstrated by examining the geometry of the hydrographs. Assuming that rainfall is uniformly distributed over the catchment, the resulting hydrograph varies proportionally in accordance with the time-area curve. In Figure 3.3, a sample hydrograph is plotted to represent the situation when t_c = 1 time unit and one unit of rainfall occurred instantaneously at time zero. The arch curve of *ABC* represents the resulting runoff hydrograph before routing through the hypothetical reservoir if Clark's UH is used, and the triangle area *ABD* represents the resulting APSWM hydrograph. The area of triangle *ABD* must equal to the area under arch *ABC*, therefore the sum of sub areas *I* (*AB*) and *II* (*BC*) must equal to triangular area *III* (*BCD*). Using Eq. (3.12) to calculate sub-areas *I* and *II*, it can be shown that the length of *AD* must be 1.5 to ensure that triangular sub-area *BCD* is equal to the sum of sub-areas *I* and *II*. As a result, the t_c in triangular APSWM hydrograph must be at least 1.5 times the t_c in Clark's UH in order to have the same peak discharge.

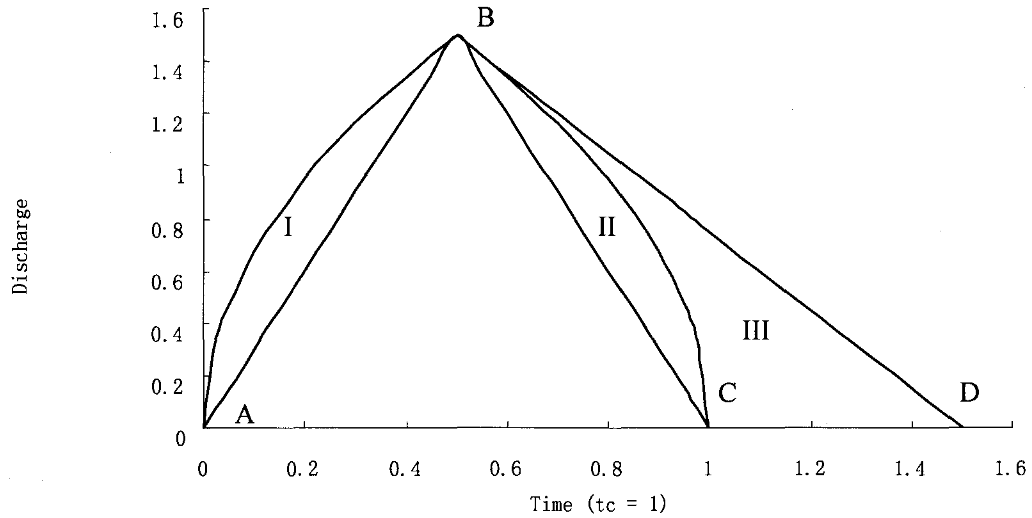

Figure 3.3 HEC-HMS Clark's Hydrograph vs. APSWM Hydrograph

3.3 Comparison Results

The six test catchments are divided into two groups: Group *ABC* (catchments *A*, *B*, and *C*) and Group *DEF* (catchments *D*, *E*, and *F*). Halifax rainfall data are used for Group *ABC*, and Toronto rainfall data are used for Group *DEF*. As a priori, it is believed that time of concentration is a significant factor that influences the hydrograph shape and consequently the peak discharge frequency distribution. With a variety of t_c values included, the comparison studies conducted here are more comprehensive than previous studies. HEC-HMS introduces a storage coefficient *K* to account for storage effects. *K* is the only parameter of the hypothetical linear reservoir located at the outlet of the catchment. APSWM considers the whole catchment as a lumped unit. The peak discharge attenuation effect of a catchment can be accounted for by adding a value that is between K and $2K$ to the travel time (or t_c as input to HEC-HMS) models to obtain the t_c that should be input to APSWM. The validity of this is demonstrated in *Guo* and *Adams* (1999). The values of peak discharge for various return periods may still not be the same even by properly considering all the differences in APSWM and HEC-HMS modeling. Since HEC-HMS is widely used in engineering practice, and continuous simulation results are accepted as more accurate than design storm or APSWM results, comparison between APSWM results and HEC-HMS continuous simulation results may help improve APSWM in the future.

3.3.1 Comparison for Catchment in Group ABC

Three sets of comparisons were conducted for each catchment in group *ABC*. The first set of comparison focused on the observed time of concentration (i.e., the duration between the input hyetograph and the output hydrograph ending time, measured from selected single storm events from the HEC-HMS continuous simulation using Clark's UH); the second set of comparisons concentrates on HEC-HMS Clark's UH; and the third set of comparisons focuses on triangular and rectangular UH. APSWM uses the same routing approach with parameter t_a (i.e., time of concentration for APSWM). Through these comparisons, a suitable t_a range may be obtained so that APSWM results are similar to HEC-HMS results.

3.3.1.1 Catchment A

Fig. 3.4 shows the comparison where the observed t_c from HEC-HMS is used as t_a in APSWM. The average value of the observed t_c from HEC-HMS is 5.08 hour, so this value was used as t_a in APSWM. Fig. 3.4 shows that the peak discharge curves from HEC-HMS results (dashed line) and APSWM results (solid line) have the same trend and similar slope. The average discrepancy is 7.75% based on the 6 return periods of interest.

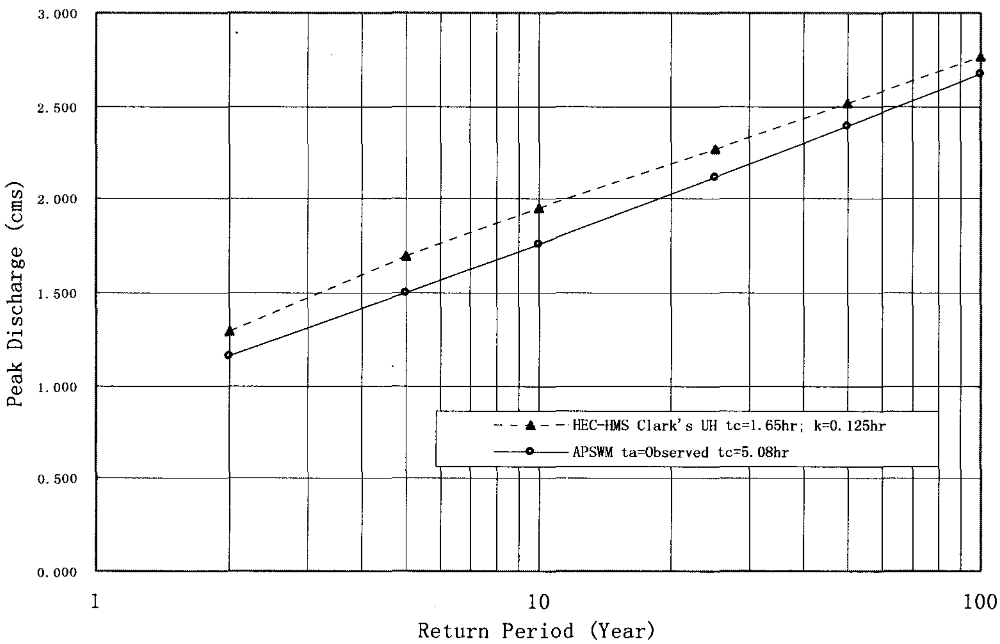

Figure 3.4 Catchment *A*, Routing Comparison Set A-1 (Observed t_c)

Fig. 3.5 illustrates the influence of Clark's UH storage coefficient *K*. The *K* value was selected to be (1) $K = 0.6t_c = 0.99$ hr (usually considered as lag time), (2) $K = 0.167t_c = 0.275$ hr and (3) $K = 0.125$ hr for 3 runs of HEC-HMS continuous simulations, meanwhile t_a in APSWM is chosen as $t_a = 1.5(t_c + 2K)$ by using the same *K* values for 3 runs to examine if the results are close enough. So there are a total of 6 curves in Fig. 3.5. The results show that APSWM models (solid lines) generated greater peak discharges than HEC-HMS models (dashed lines) (e.g., when $K = 0.125$ hr, the average difference between these two models is 46.58%. To reduce the difference, a longer t_a seems to be necessary. Nevertheless, the extent of the influence of the storage coefficient K on peak discharge rates of various return periods seems to be captured well by APSWM. In the following comparisons, longer t_a values are tried and selected.

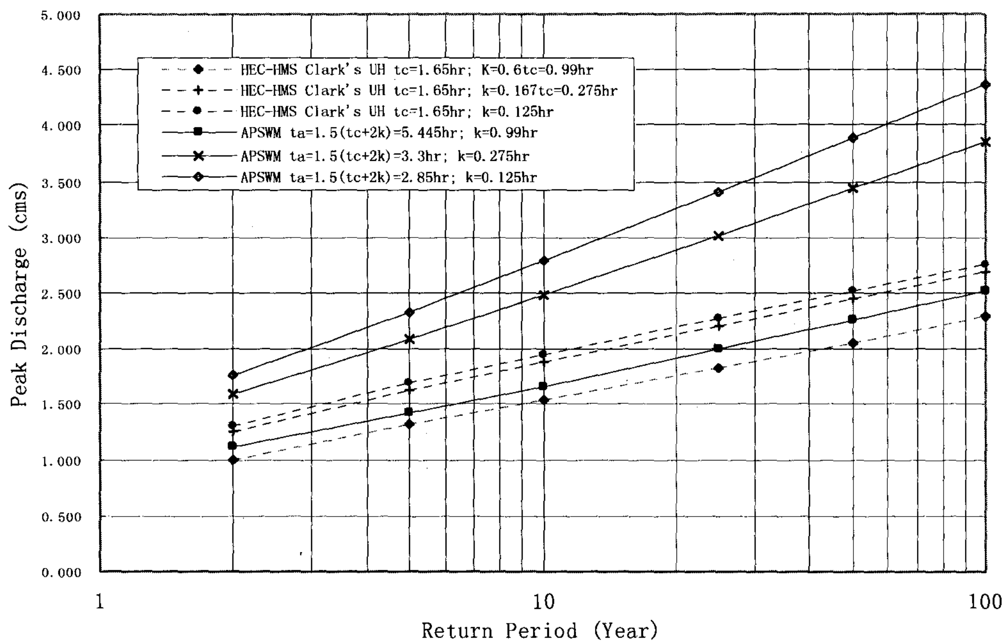

Figure 3.5 Catchment *A*, Routing Comparison Set A-2 (Clark's UH)

Fig. 3.6 presents the results when triangular UH and rectangular UH are adopted in HEC-HMS. The time of concentration t_c in either triangular UH or rectangular UH is 1.65 hours, the same as t_c in Clark's UH. Accordingly t_a in APSWM was selected as $t_a = 2t_c = 3.3$ hr, $t_a = 2.5t_c = 4.125$ hr and $t_a = 3t_c = 4.95$ hr. The results indicate that peak discharge values from HEC-HMS triangular UH are about 15% greater than those from rectangular UH, and APSWM models (solid lines) generated close results with $t_a = 2.5t_c$ and $t_a = 3t_c$ as compared to triangular UH and rectangular UH HEC-HMS results, respectively.

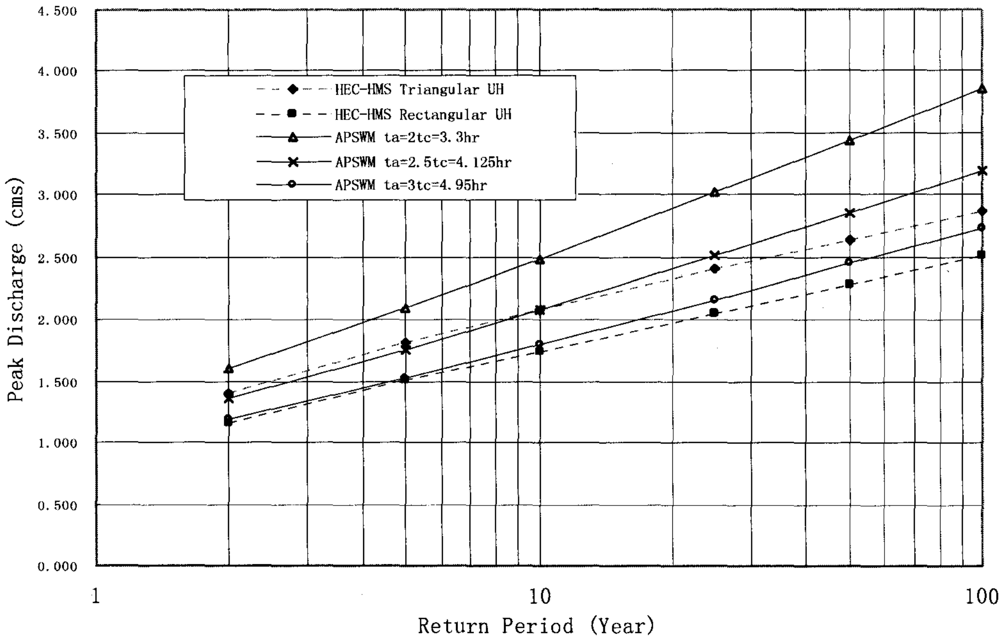

Figure 3.6 Catchment *A*, Routing Comparison Set A-3 (Triangular & Rectangular UH)

3.3.1.2 Catchment B

Similar to catchment *A*, Fig. 3.7 shows the comparison of using observed t_c from HEC-HMS as t_a for catchment *B* in APSWM. The average observed t_c in HEC-HMS is 4.33 hour, so this value is used as t_a in APSWM and compared with HEC-HMS results. It was found that the peak discharge curves of HEC-HMS (dashed line) and APSWM (solid line) are very close especially for low return periods (T = 2, 5, 10-year). The average discrepancy is 2.7% based on the 6 return periods of interest.

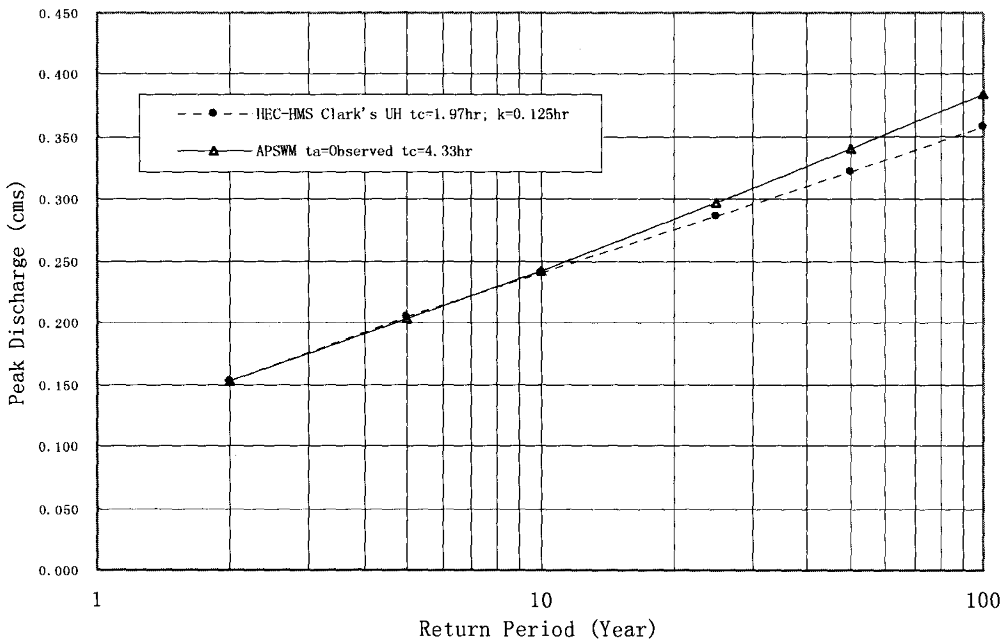

Figure 3.7 Catchment *B*, Routing Comparison Set B-1 (Observed t_c)

Fig. 3.8 illustrates the influence of Clark's UH storage coefficient *K*. The *K* value was selected as (1) $K = 0.6t_c = 1.182$ hr, (2) $K = 0.167t_c = 0.328$ hr and (3) $K = 0.125$ hr for 3 runs of HEC-HMS continuous simulations, meanwhile t_a in APSWM was chosen as $t_a = 1.5(t_c + 2K)$ by using the same *K* values. The results show that APSWM model results (solid lines) have the same trend as HEC-HMS model results (dashed lines). There is a 26.36% difference when $K = 0.125$ hr between these two models. However the discrepancy will be much less if one uses $t_a = 2(t_c + 2K)$ (not in the figure), only 0.63% difference will result (See Table 3.2).

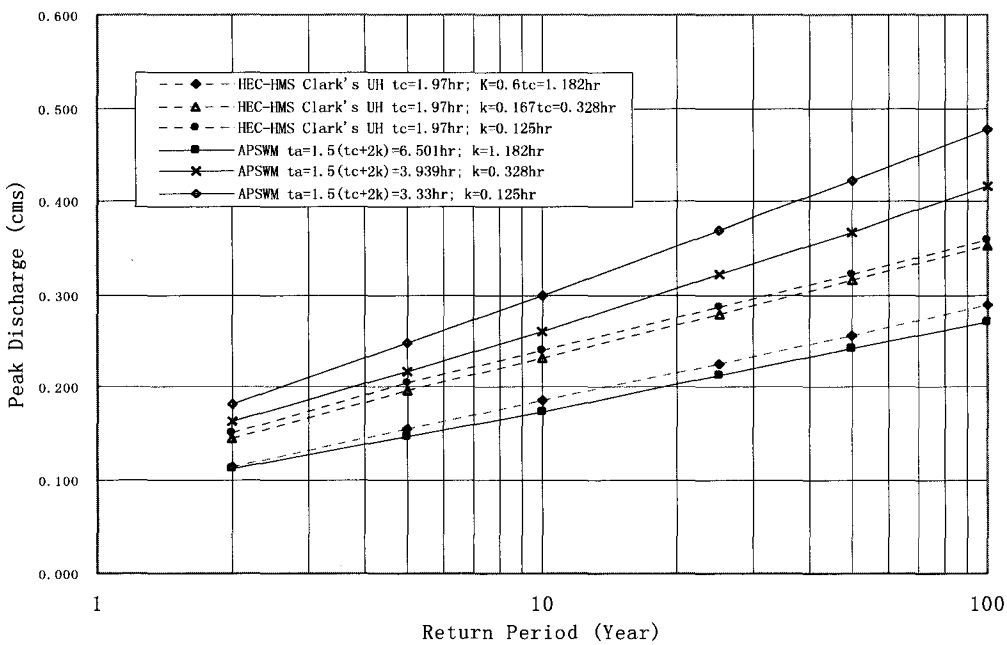

Figure 3.8 Catchment *B*, Routing Comparison Set B-2 (Clark's UH)

Fig. 3.9 presents the results when triangular UH and rectangular UH are adopted in HEC-HMS. The time of concentration t_c in either triangular UH or rectangular UH is 1.97 hours, the same as t_c in Clark's UH. Accordingly t_a in APSWM was selected as $t_a = 2t_c = 3.94$ hr, $t_a = 2.5t_c = 4.925$ hr and $t_a = 3t_c = 5.91$ hr. The results indicate that peak discharges with HEC-HMS triangular UH are about 7% greater than those from rectangular UH, and APSWM models (solid lines) generated close results with triangular and rectangular UH models (dashed lines) when $t_a = 2t_c$ and $t_a = 2.5t_c$.

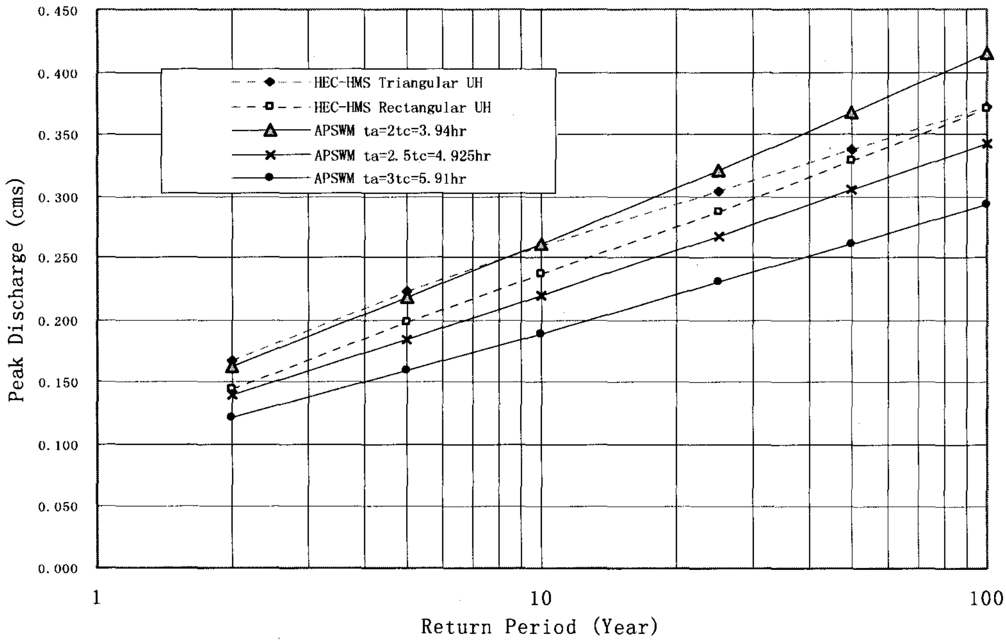

Figure 3.9 Catchment *B*, Routing Comparison Set B-3 (Triangular & Rectangular UH)

3.3.1.3 Catchment C

Fig. 3.10 shows the comparison of using the observed t_c from HEC-HMS as t_a in APSWM for catchment *C*. The average observed t_c from HEC-HMS is 8.38 hour, so use this value as t_c in APSWM and compare the results with those from HEC-HMS. It was found that the peak discharge curves of HEC-HMS (dashed line) and APSWM (solid line) are almost parallel to each other. The average discrepancy is 23.08% based on the 6 return periods of interest.

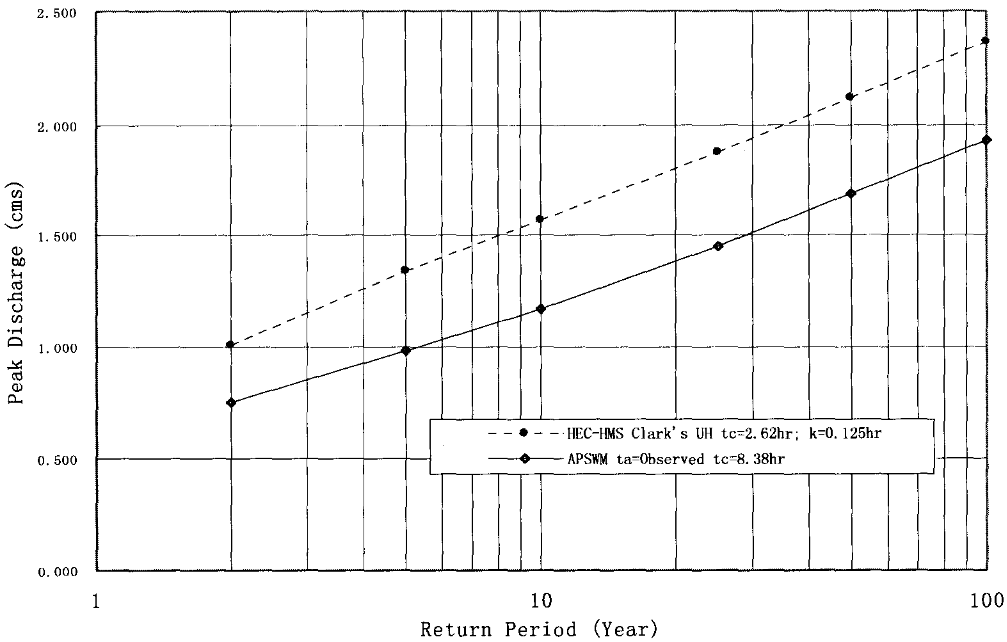

Figure 3.10 Catchment *C*, Routing Comparison Set C-1 (Observed t_c)

Fig. 3.11 illustrates the influence of Clark's UH storage coefficient K on catchment C. The K values were selected as (1) $K = 0.6t_c = 1.572$ hr, (2) $K = 0.167t_c = 0.437$ hr and (3) $K = 0.125$ hr for 3 runs of HEC-HMS continuous simulations, meanwhile t_a in APSWM was chosen as $t_a = 1.5(t_c + 2K)$ using the same K values. The results show that APSWM model results (solid lines) have the same trend as HEC-HMS model results (dashed lines). There is a 35.52% difference when $K = 0.125$ hr between these two models. However the discrepancy will be much less if one uses $t_a = 2(t_c + 2K)$ (not in the figure), only a 6.35% difference will result (See Table 3.2).

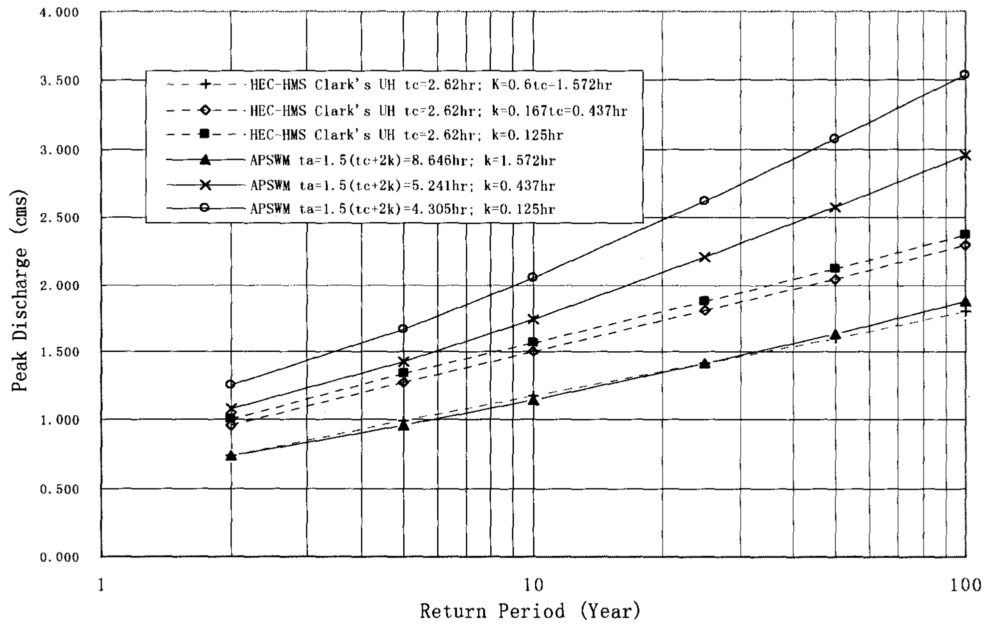

Figure 3.11 Catchment *C* Routing Comparison Set C-2 (Clark's UH)

Fig. 3.12 presents the results when triangular and rectangular UH are adopted in HEC-HMS for catchment *C*. The time of concentration t_c in either the triangular or rectangular UH is 2.62 hours, the same as t_c in Clark's UH. Accordingly t_a in APSWM was selected as $t_a = 2t_c = 5.24$ hr, $t_a = 2.5t_c = 6.55$ hr and $t_a = 3t_c = 7.865$ hr. The results indicate that peak discharge from HEC-HMS triangular UH is about 14% greater than that from rectangular UH, and APSWM models (solid lines) generated close results with triangular and rectangular UH models (dashed lines) when $t_a = 2t_c$ and $t_a = 2.5t_c$.

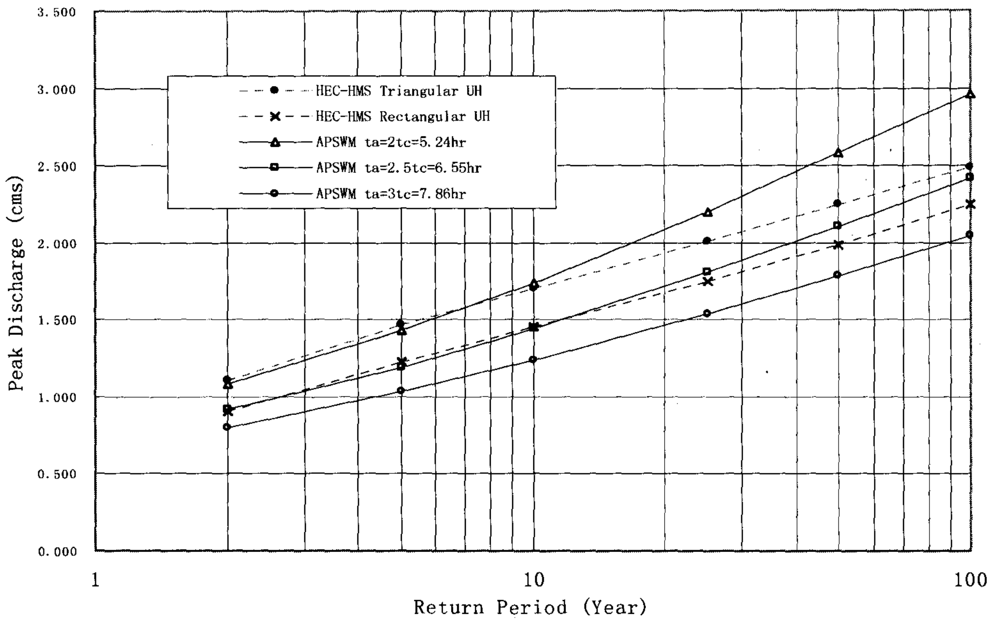

Figure 3.12 Catchment *C*, Routing Comparison Set C-3 (Triangular & Rectangular UH)

In conclusion, Fig. 3.4 through Fig. 3.12 indicate that the peak discharge of HEC-HMS and APSWM can be very close if appropriate time of concentration values are used in APSWM. For catchment *A* and catchment *B*, when $t_a = 2.5\sim3\ t_c$, or t_a = observed t_c, or $t_a = 2(t_c + 2K)$, APSWM generated results close those of HEC-HMS with less than 20% discrepancy. For catchment *C* when $t_a = 2\sim3\ t_c$, or t_a = observed t_c, or $t_a = 2(t_c + 2K)$, the discrepancy is less than 25%.

3.3.2 Comparison for Catchment in Group DEF

As mentioned previously, usually urban catchments do not provide much storage because of their small areas. APSWM does not consider catchment storage separately in its current version. So the large values of K (K = 0.6 t_c and 0.167 t_c) in HEC-HMS simulations were no longer used for Group *DEF*. For those catchments, three HEC-HMS runs were performed with the rectangular, triangular and Clark's UH with K = 0.125 hr. Various t_a values were used in APSWM (i.e., $t_a = 2t_c$, $t_a = 2.5t_c$, $t_a = 3t_c$, $t_a = 1.5(t_c + 2K)$, $t_a = 2(t_c + 2K)$ and t_a = observed t_c).

Fig. 3.13 shows the comparison results for catchment *D*. It can be seen that APSWM results with $t_a = 2(t_c + 2K)$ correspond well with HEC-HMS results with Clark's UH; APSWM results with $t_a = 2.5t_c$ correspond well with HEC-HMS results with Triangular UH; APSWM results with $t_a = 2.5t_c \sim 3t_c$ correspond well with HEC-HMSS results with Rectangular UH. Unlike Group *ABC*, use of observed t_c in APSWM did not generate comparable results.

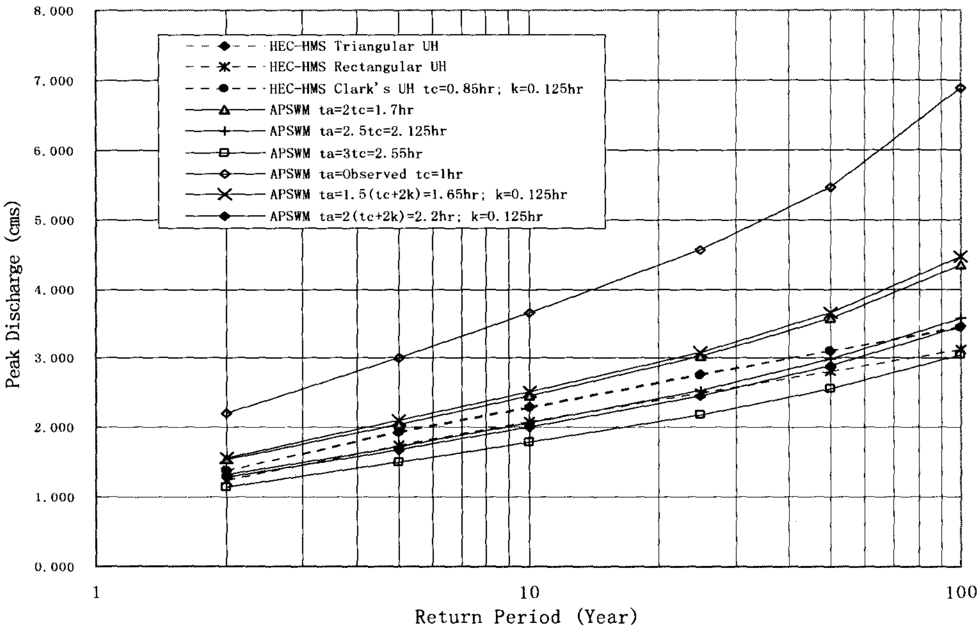

Figure 3.13 Catchment *D*, Routing Comparison Set D-1

The comparisons for catchment *E* is shown in Fig. 3.14, and catchment *F* in Fig. 3.15 are similar to catchment *D*.

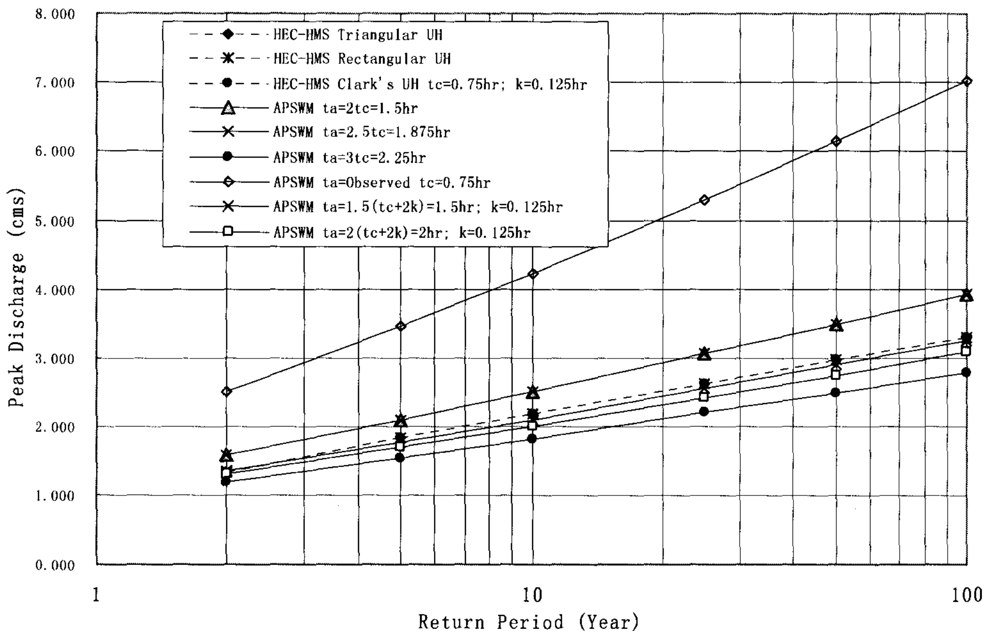

Figure 3.14 Catchment *E*, Routing Comparison Set E-1

Compared to catchments *D* and *E*, catchment *F* has slightly larger differences between the HEC-HMS and APSWM results, the average discrepancy is, however, still less than 25% (see Table 3.2). Also from Fig. 3.15 the eight tests have close results except the APSWM test when t_a = Observed t_c,

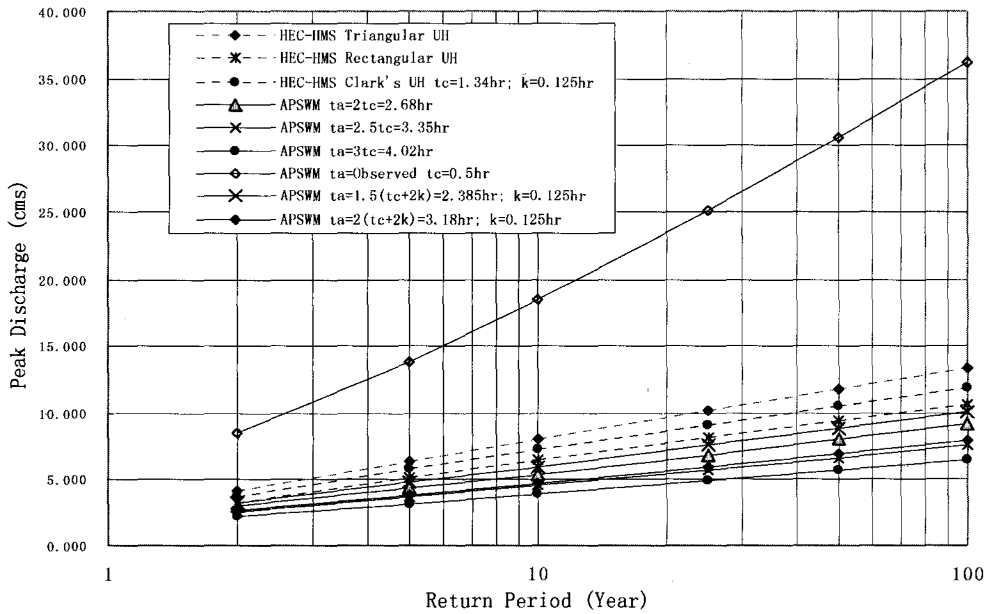

Figure 3.15 Catchment *F*, Routing Comparison Set F-1

3.4 Summary of Findings

Comparison studies focusing on catchment surface runoff routing are conducted in this chapter. Six hypothetical catchments with 57 sets of comparisons were performed using different t_c and t_a values. The findings are summarized in *Table 3.2*, where the average percentage differences between APSWM and HEC-HMS modeled peak discharges with return periods from 2 to 100 years are tabulated so that the overall trends can be identified. The major findings can be summarized as follows.

1) If the triangular UH method is used in HEC-HMS, and if we let t_a = 2~3 t_c in APSWM, the peak discharge discrepancy is less than 20% for the majority of catchments.

2) If the rectangular UH method is used in HEC-HMS, and if we let t_a = 2~3 t_c in APSWM, the peak discharge discrepancy is less than 25% for the majority of catchments.

3) If Clark's UH method is used in HEC-HMS, and if we let t_a = 1.5~2(t_c + 2K) in APSWM, the average peak discharge discrepancy will be less than 25%.

4) When t_c > 1.5 hour, and if we let t_a = observed t_c, the average peak discharge discrepancy is less than 20%. This , however does not valid for t_c < 1.5 hours.

Table 3.2 Average Differences (%) of Peak Discharges from APSWM and HEC-HMS Simulations

	HEC-HMS Using Clark's UH			HEC-HMS Using Triangular UH		HEC-HMS Using Rectangular UH	
Catchment	**APSWM with t_a = Observed**	**APSWM with t_a = 1.5(t_c + 2k)**	**APSWM with t_a = 2(t_c + 2k)**	**APSWM with t_a = 2t_c**	**APSWM with t_a = 3t_c**	**APSWM with t_a = 2t_c**	**APSWM with t_a = 3t_c**
A (t_c = 1.65 hr)	-7.75	46.58	16.61	23.13	-11.13	44.99	4.68
B (t_c = 1.97 hr)	2.70	26.36	0.63	3.66	-25.22	11.48	-19.51
C (tc = 2.62 hr)	-23.08	35.52	6.35	6.79	-24.43	23.81	-12.32
D (tc = 0.85 hr)	69.84	15.45	-8.00	12.18	-18.67	24.48	-9.75
E (tc = 0.75 hr)	98.61	16.78	-6.90	16.80	-15.23	16.79	-15.24
F (tc = 1.34 hr)	165.88	-15.62	-32.96	-31.14	-50.39	-13.80	-37.90

The reasons for APSWM requires longer time of concentration may include:

1) APSWM treats catchments as a lumped area and triangular hydrographs are

always assumed regardless of the duration of rainfall events. Some longer duration rainfall events may result in hydrographs that are more trapezoidal, longer t_a is needed so the peak discharges estimated using the triangular hydrograph assumption can still be reasonably accurate.

2) Continuous simulations combine all the different individual hydrographs generated sequentially from each time step and obtain the total hydrograph. This convolution process may result in lower peak discharges as compared to the event-by-event routing used in APSWM. A longer t_a is necessary to compensate for this difference.

3) For the cases of comparison with Clark's and Rectangular UH method, in addition to the above two reasons, the differences in the shapes of the instantaneous UHs require a longer time of concentration in APSWM. Here we take APSWM's triangular hydrographs as applicable to instantaneous events as well.

CHAPTER 4: A New Probabilistic Channel Flood Routing Method

4.1 Brief Review of the Existing APSWM Channel Routing Method

Traditional hydrologic flow routing uses the continuity equation combined with a linear or curvilinear storage relationship. Another routing approach, i.e., hydraulic routing, uses both the continuity equation and the momentum equation and can simulate more details of the spatial and temporal variations of flow. Both hydraulic and hydrologic routing methods are widely used in deterministic stormwater models.

Currently, APSWM uses a simple probabilistic channel routing procedure developed by *Zhuge* [2005]. This simple approach assumes that the flood wave travel time through a channel affects the peak outflow from the reach in the same way as the t_c affects the peak discharge from a catchment. The routing of hydrographs through a channel reach is combined with the routing of hyetographs through its upstream catchment. The effect of the channel reach is represented by adding the flood wave travel time through the reach to its upstream catchment's t_c. The combination of the catchment and its downstream channel reach is viewed as an equivalent catchment with a time of concentration equaling ($t_c + K$), where K is the Muskingum K value of the reach which is equal to the kinematic wave travel time through the reach. The exceedance probability of peak outflows from a channel reach can therefore be calculated using existing APSWM equations for catchments with minor modifications. These modified analytical equations for peak outflow from a channel reach can be expressed as follows:

For catchment and channel reach combinations with $f_c < \dfrac{S_{dd}}{t_c + K}$,

$$P\left[Q_p > q_p\right] = \begin{cases} \dfrac{2h\lambda}{2h\lambda + \zeta q_p} \exp\left(-\zeta S_{di} - \dfrac{\zeta\left(t_c + K\right)}{2h} q_p\right) & , \quad q_p < 2f_c h \\ \dfrac{2\lambda\zeta(1-h)(q_p - 2f_c h)}{(2h\lambda + \zeta q_p)(2\lambda + \zeta q_p + 2f_c\zeta - 2hf_c\zeta)} \exp\left\{-\dfrac{\left[\zeta S_{il} - \lambda\left(t_c + K\right) - f_c\zeta\left(t_c + K\right)\right] q_p - 2f_c\zeta h S_{di} + 2\lambda h S_{dd}}{q_p - 2f_c h}\right\} & \\ + \dfrac{2h\lambda}{2h\lambda + \zeta q_p} \exp\left[-\zeta S_{di} - \dfrac{\zeta\left(t_c + K\right)}{2h} q_p\right] & , \quad 2f_c h \le q_p < \dfrac{2hS_{dd}}{t_c + K} \\ \dfrac{\lambda}{\lambda + \zeta\left(\dfrac{q_p}{2} + f_c - f_c h\right)} \exp\left[-\zeta S_d - \dfrac{\zeta\left(t_c + K\right)}{2} q_p\right] & , \quad q_p \ge \dfrac{2hS_{dd}}{t_c + K} \end{cases} \tag{4.1}$$

For catchment and channel reach combinations with $f_c \ge \dfrac{S_{dd}}{t_c + K}$,

$$P\left[Q_p > q_p\right] = \begin{cases} \dfrac{2h\lambda}{2h\lambda + \zeta q_p} \exp\left[-\zeta S_{di} - \dfrac{\zeta\left(t_c + K\right)}{2h} q_p\right] & , \quad q_p < \dfrac{2hS_{dd}}{t_c + K} \\ \dfrac{2\lambda\zeta(1-h)(2f_c h - q_p)}{(2h\lambda + \zeta q_p)(2\lambda + \zeta q_p + 2f_c\zeta - 2hf_c\zeta)} \exp\left\{-\dfrac{\left[\zeta S_{il} - \lambda\left(t_c + K\right) - f_c\zeta\left(t_c + K\right)\right] q_p - 2f_c\zeta h S_{di} + 2\lambda h S_{dd}}{q_p - 2f_c h}\right\} & \\ + \dfrac{2\lambda}{2\lambda + \zeta\left(q_p + 2f_c - 2f_c h\right)} \exp\left[-\zeta S_d - \dfrac{\zeta\left(t_c + K\right)}{2} q_p\right] & , \quad \dfrac{2hS_{dd}}{t_c + K} \le q_p < 2f_c h \\ \dfrac{\lambda}{\lambda + \zeta\left(\dfrac{q_p}{2} + f_c - f_c h\right)} \exp\left[-\zeta S_d - \dfrac{\zeta\left(t_c + K\right)}{2} q_p\right] & , \quad q_p \ge 2f_c h \end{cases} \tag{4.2}$$

In the above equations, Q_p is the peak outflow at the downstream end of the channel reach regarded as a random variable; q_p is a given peak discharge value; and $P[Q_p > q_p]$ is the exceedance probability per rainfall event that Q_p is greater than q_p.

The conversion from exceedance probability per rainfall event to return period can also be achieved using Eq. (3.19). Flood routing through channel reaches can therefore be analytically performed, and runoff from the downstream end of a reach can be treated in APSWM as runoff from an equivalent catchment and combined with runoff from other parallel catchments or routed further downstream.

4.2 Improvement on the APSWM Channel Routing Method

With the known value of K for the channel reach downstream of a lumped catchment with parameters S_{di}, S_{il}, f_c, h, t_c, q_p for various return periods of interest can be determined by using equations (Eqs. 4.1, 4.2, and 3.19). However it was found by *Zhuge* (2005) that for some hypothetical reaches, there are considerable differences between APSWM results and design storm modeling results. Further improvement of APSWM's channel routing method is therefore required. Generally the key of *Zhuge*'s approach is to add an appropriate amount to the upstream catchment's t_c to reflect the peak attenuation effect of a river reach. The drawback of *Zhuge*'s approach is that the steepness of the channel reach is not fully considered. For some steep channel reaches, the peak flow of a flood wave is not attenuated as it travels downstream. To correct for this, the following new approach is proposed.

Using the deterministic hydrologic routing methods, the continuity equation is written as

$$Q_i - Q_e = \frac{dS}{dt} \tag{4.3}$$

where Q_i is the inflow; Q_e is the exit flow; S is the amount of water stored within the reach at time t. Using the widely used Muskingum–Cunge method to express storage, we have

$$S = K\left[Q_i X + Q_e(1 - X)\right] \tag{4.4}$$

where K is the Muskingum K value which is equal to the wave travel time through the reach; and X is a weighting factor.

Substitution of (4.4) into (4.3) gives

$$Q_e + K(1 - X)\frac{dQ_e}{dt} = Qi - KX\frac{dQ_i}{dt}$$

Multiplying both sides by $e^{\frac{t}{K(1-X)}}$ allows it to be written as

$$\frac{d}{dt}\left[K(1-X)e^{\frac{t}{K(1-X)}}Q_e\right] = e^{\frac{t}{K(1-X)}}Q_i - KXe^{\frac{t}{K(1-X)}}\frac{dQ_i}{dt}$$

$$= e^{\frac{t}{K(1-X)}}Q_i - KX\frac{d}{dt}\left(e^{\frac{t}{K(1-X)}}Q_i\right) + \frac{KX}{K(1-X)}e^{\frac{t}{K(1-X)}}Q_i$$

$$= -KX\frac{d}{dt}\left(e^{\frac{t}{K(1-X)}}Q_i\right) + \frac{1}{1-X}e^{\frac{t}{K(1-X)}}Q_i$$

Integration of the above equation gives

$$K(1-X)e^{\frac{t}{K(1-X)}}Q_e = -KXe^{\frac{t}{K(1-X)}}Q_i + \frac{1}{1-X}\int_0^t e^{\frac{\tau}{K(1-X)}}Q_i d\tau + \text{constants}$$

Therefore,

$$Q_e = \frac{-X}{1-X}Q_i(t) + \frac{e^{\frac{-t}{K(1-X)}}}{K(1-X)^2}\int_0^t Q_i(\tau)e^{\frac{\tau}{K(1-X)}}d\tau + \text{constants}$$

in which the value of the constant depends on the inflow and outflow rates at $t = 0$, i.e., the initial conditions.

The unit response function of a channel reach is the outflow from the channel reach in response to a unit impulse inflow into the reach at the inflow section at $t = 0$. The unit response function from the channel reach can be obtained by equating $Q_i(t)$ to $\delta(t)$, where $\delta(t)$ is the Dirac delta function of time t, thus

$$u(t) = \frac{e^{\frac{-t}{K(1-X)}}}{K(1-X)^2} - \frac{X\delta(0)}{(1-X)} \tag{4.5}$$

where $u(t)$ is the unit response function of the channel reach. The first moment of the unit response about the origin is

$$u' = \int_0^\infty tu(t)dt$$

$$= \int_0^\infty t\frac{e^{\frac{-t}{K(1-X)}}}{K(1-X)^2}dt - \frac{X}{1-X}\int_0^\infty t\delta(0)dt$$

$$= t\frac{-1}{1-X}e^{\frac{-t}{K(1-X)}}\Big|_0^\infty + \int_0^\infty \frac{e^{\frac{-t}{K(1-X)}}}{1-X}dt + 0$$

$$= -Ke^{\frac{-t}{K(1-X)}}\Big|_0^\infty$$

$$= 0 - (-K)$$

$$= K \tag{4.6}$$

The second moment of the unit response about the origin is

$$\sigma'^2 = \int_0^\infty t^2 u(t)dt$$

$$= \int_0^\infty t^2 \frac{e^{\frac{-t}{K(1-X)}}}{K(1-X)^2} dt - \frac{X}{1-X}\int_0^\infty t^2 \delta(0)dt$$

$$= t^2 \frac{-1}{1-X} e^{\frac{-t}{K(1-X)}}\Big|_0^\infty + \int_0^\infty \frac{e^{\frac{-t}{K(1-X)}}}{1-X} 2tdt + 0$$

$$= 0 - Ke^{\frac{-t}{K(1-X)}} 2t\Big|_0^\infty + \int_0^\infty 2Ke^{\frac{-t}{K(1-X)}} dt$$

$$= 0 + 0 + \left[-2k^2(1-X)e^{\frac{-t}{K(1-X)}}\Big|_0^\infty \right]$$

$$= 0 - \left(-2K^2(1-X)\right)$$

$$= 2K^2(1-X)$$

Thus, the second moment of the unit response about the mean is

$$\sigma^2 = \sigma'^2 - u'^2$$

$$= 2K^2(1-X) - K^2$$

$$= K^2(1-2X) \tag{4.7}$$

The first moment about the origin measures the average time it takes for the flood wave in response to a unit impulse inflow to pass through the reach. The standard deviation σ, that is, the square root of its second moment about the mean, characterizes the increase in the width or average duration of a flood wave as it travels through the reach. Therefore, if the river reach is relatively short and the outflow flood hydrograph can still be approximated as a triangle, the peak of the outflow flood hydrograph resulting from a rainfall event (υ, t) falling on the upstream catchment can be probably estimated as

$$\begin{aligned} Q_0 &= \frac{2\upsilon_r}{t + t_c + m\sigma} \\ &= \frac{2\upsilon_r}{t + t_c + mK\sqrt{1-2X}} \end{aligned} \tag{4.8}$$

where υ_r is the same as in equation 3.16 of Chapter 3; and m denotes some unknown multiplication factor.

Eq. (4.8) is written assuming that the time base of any flood hydrograph would increase by $mK\sqrt{1-2X}$ after passing through a river reach. This may not be exactly true for all individual flood hydrographs, but as shown in the derivation for the response of a channel reach to unit impulse inflows, Eq. (4.8) should provide a reasonable approximation for the majority of flood hydrographs. According to Eq. (4.8), the reduction in peak discharge due to the effect of a channel reach is maximum when $X = 0$; and when $X = 0.5$, there will be no reduction in peak discharge. This is consistent with the conventional interpretation of the X values. That is, when $X = 0$, the channel reach functions in a similar way as a level pool reservoir; and when $X = 0.5$, the flood wave retains its original shape as it travels through the reach. Natural channel reaches or constructed drainage ditches normally have X values between 0 and 0.5.

Use of Eq. (4.8) is obviously an improvement to the method used in *Zhuge* (2005) where only K is included. Since the K and X value of a reach provide complete information about the reach that affects its flood routing function, $K\sqrt{1-2X}$ captures and condenses this complete information. The exact value of m may vary slightly from rainfall event to event and from reach to reach, but the possible range of m variation should be quite small as compared to the possible degrees of variation of the values of $K\sqrt{1-2X}$. Therefore m may be taken as a constant. A reasonable initial guess for m is 2. Initially, we will use this guessed value to test out the overall approach.

Similar to the approach used by *Zhuge* (2005), Eq. (4.8) would be the same as the corresponding equation for a single catchment if the catchment has $(t_c + mK\sqrt{1-2X})$ as its time of concentration. Thus, the APSWM equations for a single catchment can be used for reach routing. The analytical equations are the same as Eq. (4.1) and (4.2) with K replaced by $mK\sqrt{1-2X}$.

4.3 Method of Dealing with Long Reaches

In numerical simulations, the Muskingum–Cunge method is implemented in a numerical calculation procedure with a finite time step Δt. To ensure computational stability and accuracy, the total length of a channel reach is usually subdivided into a number of sub-reaches. The length of sub-reaches Δx should be consistent with the computational time step Δt. For example, in HEC-HMS, Δx is selected to approximately satisfy the following requirement:

$$\Delta x = c\Delta t \tag{4.9}$$

where c is the kinematic wave celerity.

The selection of Δt is based on the time step length of the inflow data, the length of the reach and the desired accuracy. In using the analytical probabilistic approach, reach routing is combined with upstream catchment runoff routing and can be viewed as temporally lumped on an event-by-event basis. To ensure the accuracy of APSWM's spatially and temporally lumped routing calculations, the channel reach cannot be too long. A long channel reach would have a large $mK\sqrt{1-2X}$ value. Therefore, it is necessary to estimate the upper limit of $mK\sqrt{1-2X}$ for the application of the proposed method.

Even for short reaches where the proposed method would provide reasonably accurate estimates of peak discharges, the X values as used in HEC-HMS are calculated based on Δx, i.e., the length of divided sub-reaches, not the entire length of the reach. Therefore, in APSWM, X should also be calculated based on the length of divided sub-reaches if this division is necessary. To examine when the division of a reach into sub-reaches is necessary, the time resolution of APSWM's routing calculation should be examined.

APSWM's event-by-event routing involves two time scales, namely the event duration t and upstream catchment time of concentration t_c. To provide sufficient resolution of the temporal characteristics of flood waves, it stands to reason that the '*time step*' for APSWM routing should be small as compared to $t + t_c$, the time base of flood hydrograph from the upstream catchment. Of course, flood routing calculations conducted by APSWM do not involve any real time steps. But in APSWM, peak discharges are estimated with triangular hydrograph assumptions, and a minimum of three to five points including the start and end points along an approximately triangular hydrograph would be needed to characterize it well for peak estimation purposes. Therefore, an equivalent imaginary '*time step*' of 1/4 to 1/2 of $(t + t_c)$ may be required to ensure accuracy. The event duration is treated as a random variable. For APSWM to work well, t_c should be less than the mean of t. Thus, the mean of $t + t_c$ would be greater than $2t_c$. The required '*time step*' for APSWM should therefore be from 1/2 t_c to t_c. Using these required '*time step*' values (treat them as if they are Δt for HEC-HMS), the corresponding required Δx values can be determined using Eq. (4.9). If the reach's length is shorter than the required Δx, no division into sub-reaches is necessary. Otherwise division can be made according to the required Δx. In this study, the analytical probabilistic routing results with required '*time steps*' of 1/2 t_c and a value equaling that used in continuous simulation (15 minutes) are compared.

To simplify the analytical expressions, if necessary, a channel reach is divided into equal length sub-reaches. Denote n as the number of these identical sub-reaches after division, n would equal to unity if the reach is short and division is not required. The effect of each of the n sub-reaches in series is described by Equations (4.3) and (4.4). As shown by *Nash* (1959), the Muskingum channel reach as governed by Eqs. (4.3) and (4.4) is a linear system, to which the theorem of moment is fully applicable. The theorem of moment states that the second moment about the mean of the unit response of n identical sub-reaches connected in series is

$$\sigma_T^2 = n\sigma^2 = n\left(\frac{K}{n}\right)^2(1-2X)$$

where σ_T^2 is the second moment about the mean for the entire reach; K is the K value for the entire reach while X is for each of the identical sub-reaches. K/n gives the wave travel time through each of the sub-reach. Similar to the case where no subdivision is required, the peak outflow downstream of the reach resulting from a rainfall event (υ, t) can be estimated as

$$\begin{aligned} Q_0 &= \frac{2\upsilon_r}{t+t_c+m\sigma_T} \\ &= \frac{2\upsilon_r}{t+t_c+mK\sqrt{(1-2X)/n}} \end{aligned} \tag{4.10}$$

Longer reaches can therefore be divided into sub-reaches for the calculation of the extra time of concentration that the reach adds to its upstream catchment. Probabilistic routing through a longer reach can then be conducted in the same way as through a short reach for which division into sub-reaches is not required.

4.4 HEC-HMS Channel Routing Overview

There are several channel routing methods available in HEC-HMS including:

- Lag
- Muskingum
- Modified Puls
- Kinematic-wave
- Muskingum-Cunge

In this study, Muskingum-Cunge method is used in order to be consistent with the routing approach used in APSWM. The Muskingum-Cunge method is an extension of the Muskingum routing method and it overcomes the limitations of parameter estimation.

The continuity equation used in the Muskingum-Cunge is:

$$I - O = \frac{ds}{dt} \tag{4.11}$$

Storage S is assumed to be related to the inflow I and outflow O as:

$$S = K[XI + (1 - X)O] \tag{4.12}$$

where K is the flood wave travel time and X is weighting factor with values between 0 and 0.5.

The parameters K and X are estimated using

$$K = \frac{\Delta x}{c} \tag{4.13}$$

$$X = \frac{1}{2}\left(1 - \frac{Q}{BS_0 c\Delta x}\right) \tag{4.14}$$

where B is the water surface width of the channel when the flow rate is Q; c is the flood wave celerity; S_0 is the channel bottom slope; and Δx is the reach length. Thus, using Eq. (4.13) and Eq. (4.14), both the K and X values can be related to the physical characteristics of the channel. The Muskingum-Cunge method blends the accuracy of the diffusion wave method with the simplicity of the Muskingum method, resulting in one of the most recommended techniques for general use. In HEC-HMS simulations, K and X values are not constants since c, Q and B change over time. HEC-HMS recalculates K and X values at each time step. In APSWM, however, fixed K and X values are used. These fixed K and X values are obtained using the Q value corresponding to a return period of 10 years.

4.5 Verification of the New Routing Method

In order to verify the new APSWM channel routing method, results from

HEC-HMS channel routing using the Muskingum-Cunge method are compared with APSWM channel routing results. The hypothetical catchments tested in Chapter 3 were used for runoff generation and a number of hypothetical channel reaches with various physical characteristics are used for comparison purposes. These hypothetical channel reaches are directly connected with an upstream catchment.

4.5.1 Channel Reach Setup

Catchments *C, E, F* in the Chapter 3 are chosen as the test catchments. The areas of the catchments vary from 40 ha for catchment *C*; 22 ha for catchment *E* and 101 ha for catchment *F*. The imperviousness are 70% for catchment *C*; 100% for catchment *E* and 0% for catchment *F*. The times of concentration, t_c, are 2.62 hr for catchment *C*; 0.75 hr for catchment *E* and 1.34 hr for catchment *F*. These three catchments along with their downstream reaches represent a variety of conditions in an urban environment.

The most important channel routing parameters are *K* and *X* values, which are related to the channel reach's physical characteristics as shown in Eq. (4.13) and Eq. (4.14). Channel reach length, slope, roughness (Manning's *n*) and cross-sectional dimensions (Channel shape, bottom width and side slopes) affect these two parameters significantly. From open channel hydraulics, the flow rate of steady uniform flow in a channel reach may be calculated using the Manning's equation (in metric units):

$$Q = \frac{1}{n} A R^{2/3} S_0^{1/2} \tag{4.15}$$

where n is the Manning's roughness coefficient; A is the cross-sectional area; R is the hydraulic radius (area divided by wetted perimeter); S_0 is the channel slope. Using Eq. (4.15) together with Eqs. (4.13) and (4.14), the K and X values can be estimated for a given reach and the Q value with a return period of 10 years as determined based on the upstream catchment. Using these K and X values, APSWM conducts the probabilistic channel routing analytically. Table 4.1 lists the characteristics of the tested reaches for catchment C.

Table 4.1 Reach Characteristics for Catchment C

Reach Name	Length (m)	Slope (%)	Manning's n	X	K	$2K\sqrt{(1\text{-}2X)}$	No. of Sub-Reach
C-1	500	0.05	0.01	0	0.0916	0.1832	1
C-2*	500	0.05	0.08	0	0.4363	0.8726	1
C-3*	500	0.05	0.15	0	0.6993	1.3986	1
C-4*	500	0.5	0.01	0.4652	0.0386	0.0204	1
C-5	500	0.5	0.08	0.4203	0.1839	0.1468	1
C-6*	500	0.5	0.15	0.3985	0.2947	0.2656	1
C-7	500	5	0.01	0.4979	0.0163	0.0021	1
C-8	500	5	0.08	0.4949	0.0775	0.0157	1
C-9	500	5	0.15	0.4935	0.1242	0.0283	1
C-10*	2500	0.05	0.01	0.389	0.458	0.4316	1
C-11*	2500	0.05	0.08	0	2.1814	4.3628	2
C-12	2500	0.05	0.15	0	3.4963	6.9926	3
C-13	2500	0.5	0.01	0.493	0.1931	0.0457	1
C-14	2500	0.5	0.08	0.4841	0.9193	0.3279	1
C-15	2500	0.5	0.15	0.4594	1.4736	0.8398	1

C-16	2500	5	0.01	0.4996	0.0817	0.0046	1
C-17	2500	5	0.08	0.499	0.3874	0.0347	1
C-18	2500	5	0.15	0.4987	0.621	0.0633	1
C-19*	5000	0.05	0.01	0.4445	0.916	0.6104	1
C-20*	5000	0.05	0.08	0	4.3629	8.7258	3
C-21*	5000	0.05	0.15	0	6.9926	13.9852	4
C-22	5000	0.5	0.01	0.4965	0.3861	0.0646	1
C-23	5000	0.5	0.08	0.4841	1.8386	0.6557	1
C-24	5000	0.5	0.15	0.4696	2.9472	1.4534	2
C-25	5000	5	0.01	0.4998	0.1633	0.0065	1
C-26	5000	5	0.08	0.4995	0.7747	0.0490	1
C-27	5000	5	0.15	0.4987	1.2419	0.1266	1
C-28	1000	0.08	0.025	0.0471	0.3055	0.5815	1
C-29	1000	0.09	0.025	0.1065	0.2923	0.5186	1
C-30	1000	0.1	0.025	0.153	0.281	0.4682	1
C-31	1000	0.115	0.025	0.2064	0.2666	0.4086	1
C-32	1000	0.13	0.025	0.2464	0.2546	0.3626	1
C-33	500	0.16	0.025	0.3021	0.1178	0.1482	1
C-34	500	0.205	0.025	0.3529	0.1073	0.1164	1
C-35	1000	0.16	0.025	0.4011	0.2355	0.2095	1
C-36	1000	0.29	0.025	0.4514	0.1884	0.1175	1
C-101*	2500	0.05	0.05	0.2929	1.533	1.9732	1
C-102*	2500	0.05	0.065	0.2712	1.8667	2.5255	1
C-201*	5000	0.05	0.1	0.0958	5.1582	9.2756	3
C-202*	5000	0.05	0.115	0.0738	5.7286	10.5779	3

Note: (1) Each reach has a trapezoidal cross section with 3H:1V side slope; bottom width is 1 meter.

(2) '*' beside the name of reach indicates that HEC-HMS continuous simulation is conducted for that reach.

4.5.2 Influence of the Subdivision of a Reach on APSWM Results

In order to evaluate the routing effects of a channel reach in a lumped but still relatively concise way, the peak discharge reduction rate is defined and used here. The peak discharge (PD) reduction rate for a return period of interest is defined as:

PD Reduction Rate = (PD downstream of Catchment – PD downstream of Reach) / (PD downstream of Catchment) X 100%

where PD stands for peak discharge.

The average PD Reduction Rate (PDRR), is calculated as the average across all the return periods of interest. The return periods of interest included in this research are 2-, 5-, 10-, 25-, 50-, and 100- years. PDRRs calculated for each catchment and channel reach combinations using HEC-HMS continuous simulation results and APSWM results are compared to judge if APSWM provides a good approximation overall.

In this section, the APSWM results for the same catchment and channel reach combinations obtained using different reach subdivision criteria are compared first to ensure that the selected subdivision criterion is sufficiently refined. As previously stated, one of the tested subdivision criterions is that the required '*time step*' be 15 minutes; and the other is that the required '*time step*' be 0.5 t_c, where t_c is the upstream catchment's time of concentration. The PDRRs calculated by APSWM with the two criteria are plotted together in Fig. 4.1. Fig. 4.1 shows that for the majority of the cases, the two criteria do not generate significant differences. The cases where significant differences are observed are those where $X = 0$. These are extreme cases where the channel is very flat or the width of the channel is too small. For these cases, subdivision of the channel would not work with the proposed method because no matter how small the Δx becomes, X will always be zero. Except these extreme cases, the two levels of temporal resolution of APSWM generate similar results and are both acceptable. In the following comparison studies, the criterion that the required '*time step*' be 0.5 t_c is used to decide whether subdivision of a channel reach is necessary and how many sub-reaches that the channel reach need be divided into.

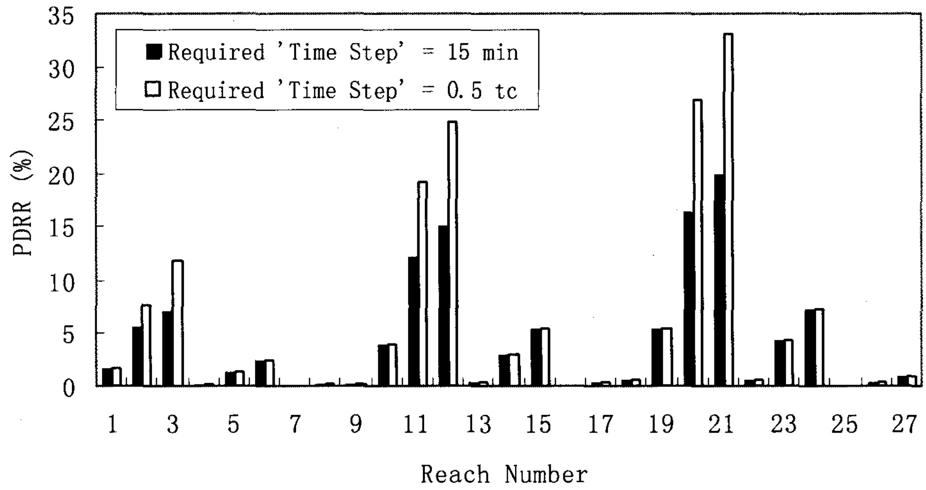

Figure 4.1 'Time Step' Influence on APSWM Reach Routing Results

4.5.3 Comparison of Catchment C and Downstream Reach Combinations

In this section, the proposed new reach routing method is tested. *Zhuge* [2005] incorporates the K value of a channel reach into the time of concentration t_c but ignores the influences of the X value. Figure 4.2 shows the comparison of routing using *Zhuge*'s method, the proposed new approach with $m = 2$, and HEC-HMS. It is clear that the proposed new channel routing method results in closer PDRRs as compared with HEC-HMS, especially when PDRR is more than 10%. As previously stated, when the X value is approaching 0 or the K value is longer than the upstream catchment's time of concentration, the reduction rate increases significantly, as under this condition the reach is acting as a reservoir more than as a channel. The method proposed by *Zhuge* [2005] therefore provides relatively better results for medium X values and short K values but cannot deal well with low X and large K values.

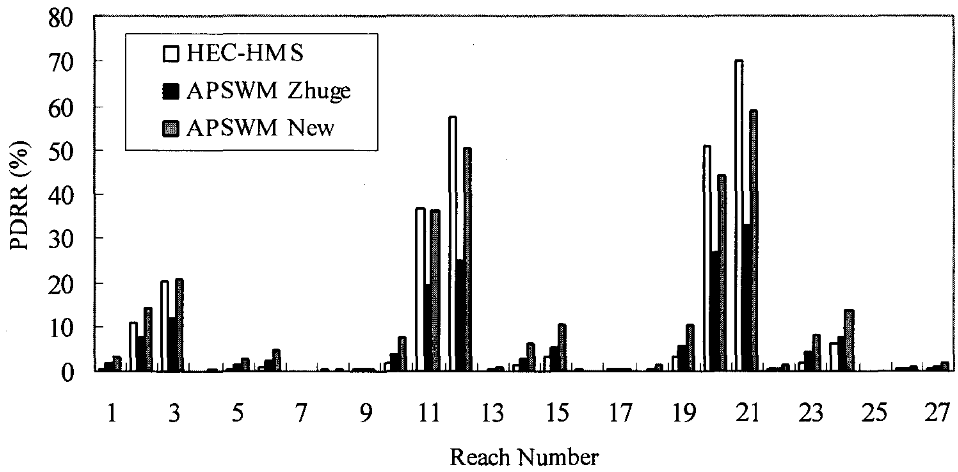

Figure 4.2 Comparisons of PDRRs for Catchment C and Downstream Reach Combinations

The combined effects of X and K, represented by $mK\sqrt{(1-2X)/n}$, should have an approximately liner relationship with the average reduction rate if the approximation made in Eq. (4.8) and Eq. (4.10) is accurate enough. To verify that, the PDRR calculated by APSWM and HEC-HMS for each case are plotted against the reach's $2K\sqrt{(1-2X)/n}$ value in the same figure. Fig. 4.3 shows that both APSWM and HEC-HMS results indicate an approximately liner relationship between PDRR and $2K\sqrt{(1-2X)/n}$. Using HEC-HMS results, the linear regression between PDRR and $2K\sqrt{(1-2X)/n}$ resulted in a R^2 value of 0.9235. Using APSWM results, the R^2 value is 0.9775. Thus, both Eq. (4.8) and (4.10) are accurate enough for the majority of runoff events.

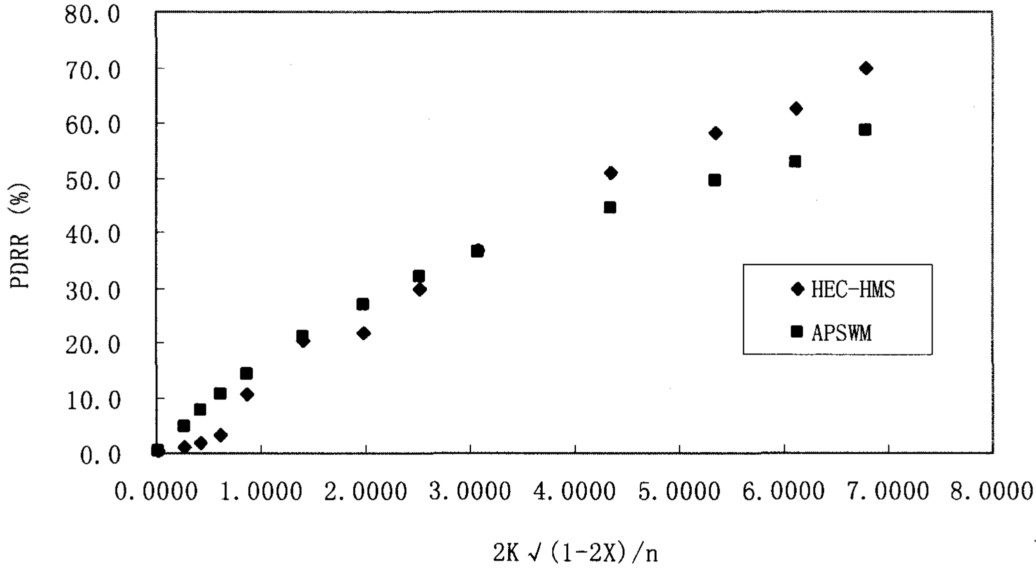

Figure 4.3 Relationship between PDRR and $2K\sqrt{(1-2X)/n}$ for Catchment C and Downstream Reach Combinations

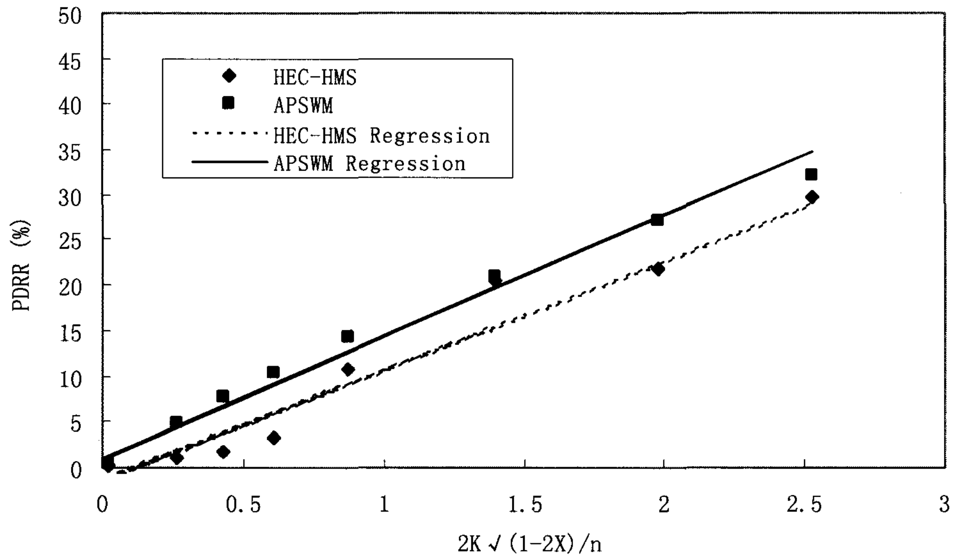

Figure 4.4 Relationship between PDRR and $2K\sqrt{(1-2X)/n}$ for Catchment C and Downstream Reach Combinations (Including cases with $2K\sqrt{(1-2X)/n}$ < 2.5 hr only)

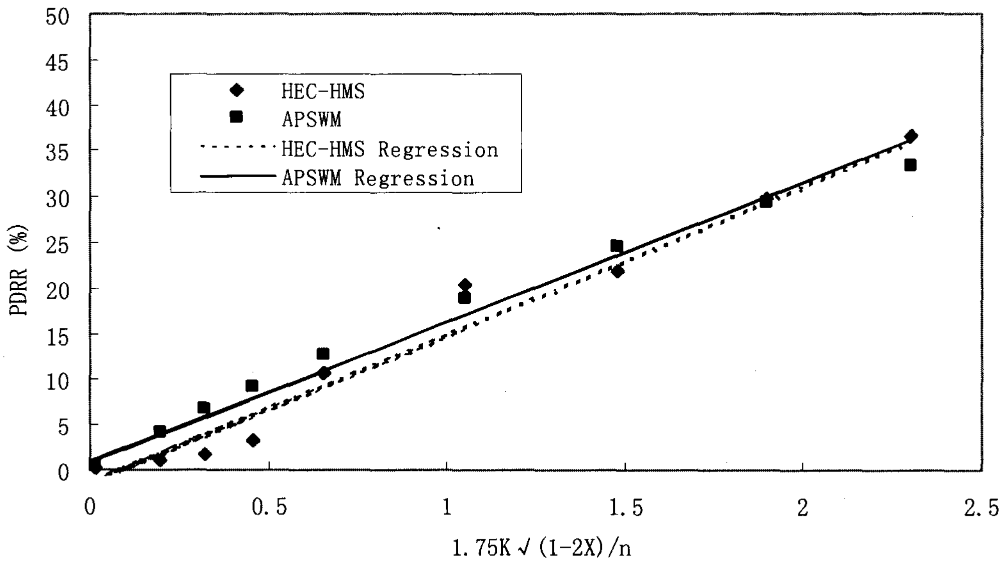

Figure 4.5 Relationship between PDRR and $1.75K\sqrt{(1-2X)/n}$ for Catchment C and Downstream Reach Combinations (Including cases with $2K\sqrt{(1-2X)/n}$ < 2.5 hr only)

Examining the results in Fig. 4.3 in detail indicates that before $2K\sqrt{(1-2X)/n}$ approaches 2.5 hours, APSWM predicts higher PDRRs than those predicted by HEC-HMS. When $2K\sqrt{(1-2X)/n}$ exceeds 2.5 hours, the APSWM calculated PDRRs become smaller than those determined by HEC-HMS. The differences between the APSWM and HEC-HMS predicted PDRRs also increase when $2K\sqrt{(1-2X)/n}$ exceeds 2.5 hours. Hence, the upper application limit of $2K\sqrt{(1-2X)/n}$ for the proposed routing method is probably somewhere close to 2.5 hours in the case of Catchment *C* and its downstream reach combinations. To verify this, we replot the results in Fig. 4.4 excluding cases where $2K\sqrt{(1-2X)/n}$ > 2.5 hours. An even stronger linear relationship is shown in

Fig. 4.4 between PDRRs and $2K\sqrt{(1-2X)/n}$.

As indicated in Section 4.2, the unknown multiplication factor *m* may be determined by minimizing the difference between the PDRRs predicted by APSWM and HEC-HMS. Performing the same APSWM calculations using different *m* values, it was found that an *m* value of 1.75 resulted in the smallest overall difference between PDRRs predicted by APSWM and HEC-HMS. The results are shown in Fig. 4.5.

4.5.4 Comparison for Catchment E and Downstream Reach Combinations

The characteristics of the hypothetical reaches downstream of Catchment *E* are listed in the Table 4.2.

Table 4.2 Hypothetical Reach Characteristics Downstream of Catchment E

Reach Name	Length (m)	Slope (%)	Manning's n	X	K	$2K\surd(1\text{-}2X)$	Sub-Reach
E-2*	200	0.05	0.08	0	0.1368	0.2736	1
E-3*	200	0.05	0.15	0	0.2192	0.4384	1
E-5	200	0. 5	0. 08	0. 2105	0. 0577	0.0878	1
E-11*	500	0. 05	0. 08	0	0. 342	0.6840	1
E-14	500	0. 5	0. 08	0. 3842	0. 1441	0.1387	1
E-16*	500	5	0. 01	0. 4968	0. 0128	0.0020	1
E-20*	1000	0. 05	0. 08	0	0. 684	1.3680	2
E-23	1000	0. 5	0. 08	0. 4421	0. 2883	0.1962	1
E-24	1000	0. 5	0. 15	0. 353	0. 4621	0.5011	2
E-26	1000	5	0. 08	0. 4963	0. 1215	0.0209	1
E-28	1500	0. 05	0. 01	0. 2293	0. 2155	0.3171	1
E-29*	1500	0. 05	0. 08	0	1. 026	2.0520	3

E-30*	1500	0. 05	0. 15	0	1. 6422	3.2844	5
E-32	1500	0. 5	0. 08	0. 4228	0. 4324	0.3398	2
E-34	1500	5	0. 01	0. 4968	0. 2921	0.0467	1
E-37	800	0. 075	0. 025	0. 0553	0. 1963	0.3703	1
E-38	800	0. 083	0. 025	0. 1058	0. 189	0.3356	1
E-39	800	0. 093	0. 025	0. 1558	0. 1811	0.3005	1
E-43	800	0. 13	0. 025	0. 269	0. 1597	0.2171	1
E-44	800	0. 155	0. 025	0. 3127	0. 1495	0.1830	1
E-45	800	0. 27	0. 025	0. 4033	0. 1214	0.1068	1
E-202*	5000	0. 01	0. 2	0	12. 4383	24.8766	34
E-301*	1500	0. 025	0. 15	0	2. 1325	4.2650	6
E-304*	3500	0. 01	0. 15	0	7. 0167	14.0334	19

Note: (1) Each reach has a trapezoidal cross section with 3H:1V side slope; bottom width is 1 meter.
(2) '*' indicates that a HEC-HMS continuous simulation is conducted for that reach.

Analyses similar to what were conducted for catchment *C* and downstream reach combinations were conducted for catchment *E* and downstream reach combinations. The results are shown in Figs. 4.6, 4.7 and 4.8. Fig. 4.6 shows that the proposed new reach routing approach provided results closer to HEC-HMS results than *Zhuge*'s (2005) method for the majority of cases.

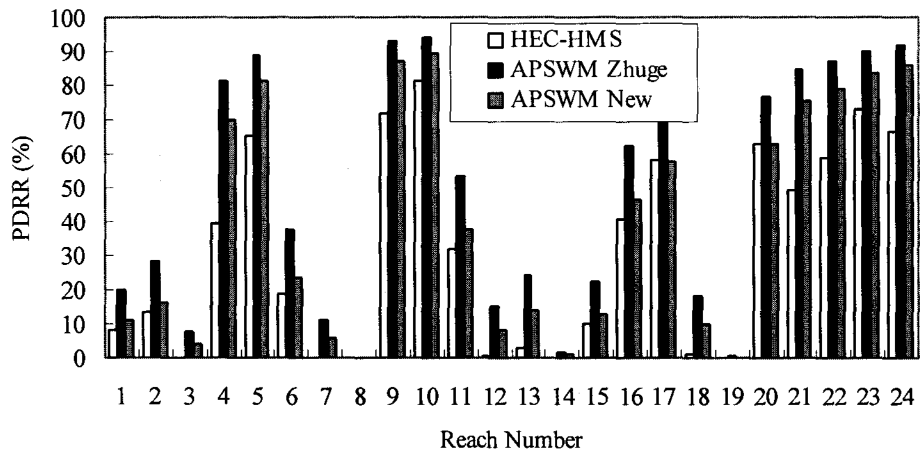

Figure 4.6 Comparisons of PDRR for Catchment E and Downstream Reach Combinations

It can be seen from Figure 4.7 that the PDRR and $2K\sqrt{(1-2X)/n}$ also have an approximately linear relationship when $2K\sqrt{(1-2X)/n}$ is less than about one hour. When $2K\sqrt{(1-2X)/n}$ is greater than 1 hr, the relationship between PDRR and $2K\sqrt{(1-2X)/n}$ flattens and PDRR reaches a maximum of about 90%. catchment E has a t_c of 0.75 hours, reaches that have a $2K\sqrt{(1-2X)/n}$ > 0.75 hours would be so long such that all the lateral inflows into the reach cannot be treated as joining at the downstream end of the reach and modeled as coming from another catchment any more. In other words, the reach should be broken down into several reaches with other catchment inflows joining in between. That is why we are more interested in cases with $2K\sqrt{(1-2X)/n}$ < 1 hour. Figure 4.8 shows the cases where $2K\sqrt{(1-2X)/n}$ is less than 1 hour. The regression line based on APSWM results is parallel to the regression line based on HEC-HMS results; the average difference is less than 15%. Once again, the approximate linear relationship between PDRR and $2K\sqrt{(1-2X)/n}$ is proven to be valid for catchment E and its downstream reach combinations. To obtain a closer match between APSWM and HEC-HMS results, the m value was found to be 1 and the results are shown in Fig. 4.9.

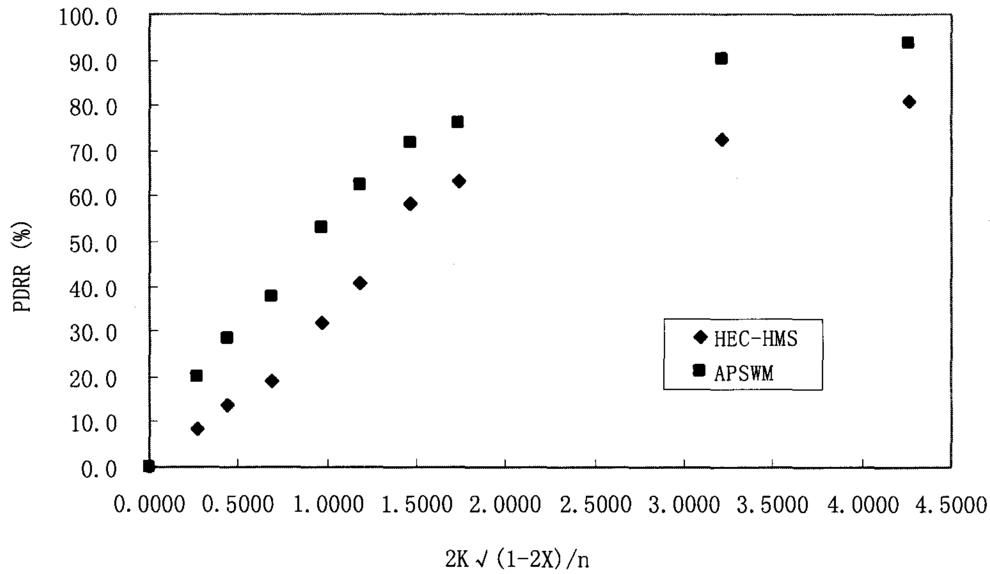

Figure 4.7 Relationship between PDRR and $2K\sqrt{(1-2X)/n}$ for Catchment E and Downstream Reaches

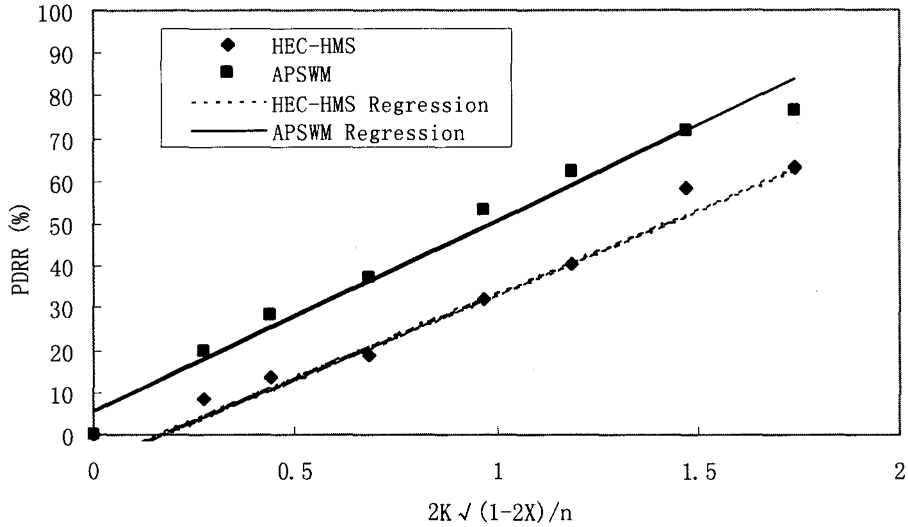

Figure 4.8 Relationship between PDRR and $2K\sqrt{(1-2X)/n}$ for Catchment E and Downstream Reaches (Including cases with $2K\sqrt{(1-2X)/n}$ < 1 hour only)

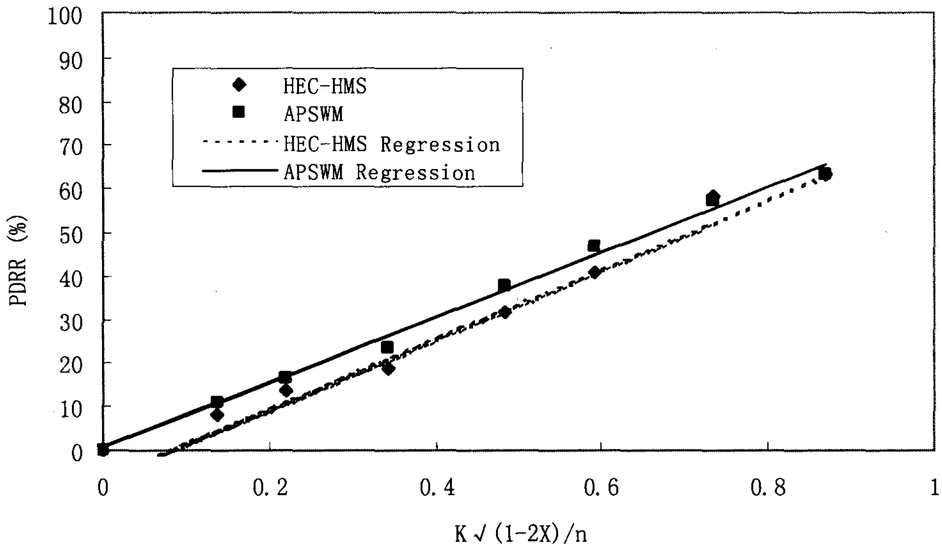

Figure 4.9 Relationship between PDRR and $K\sqrt{(1-2X)/n}$ for Catchment E and Downstream Reach Combinations (Including cases with $K\sqrt{(1-2X)/n}$ < 1 hour only)

4.5.5 Reach Routing Comparisons for Catchment F

Catchment *F* has an area of 101 ha, imperviousness of 0, and a time of concentration of 1.34 hours. Only two reaches representing these extreme conditions were modeled. One of them has an extremely flat slope and consequently has an *X* value of zero; the other one has an extremely steep slope and consequently has an *X* Value of almost 0.5. The details of the two hypothetical reaches are listed in the Table 4.3.

Table 4.3 Routing Reach Characteristics for Catchment F

Reach Name	F-I	F-III
Reach Length (m)	880	5540
Reach Slope (%)	0.01	1.5
Manning's n	0.11	0.1
Reach Shape	Trapezoid	Trapezoid
Bottom Width (m)	1	5
Side Slope (xH:1V)	3	5
X	0	0.4975
K	1.3303	1.3334
Sub-Reach	2	2

Figure 4.10 shows the comparison of results for catchment *F* and its downstream reach combinations. As shown in Fig. 4.10, APSWM with the new reach routing method provides results closer to those from HEC-HMS continuous simulation than APSWM with the old reach routing method proposed by *Zhuge* [2005]. Therefore, as far as extreme cases are concerned, the proposed probabilistic reach routing approach is better.

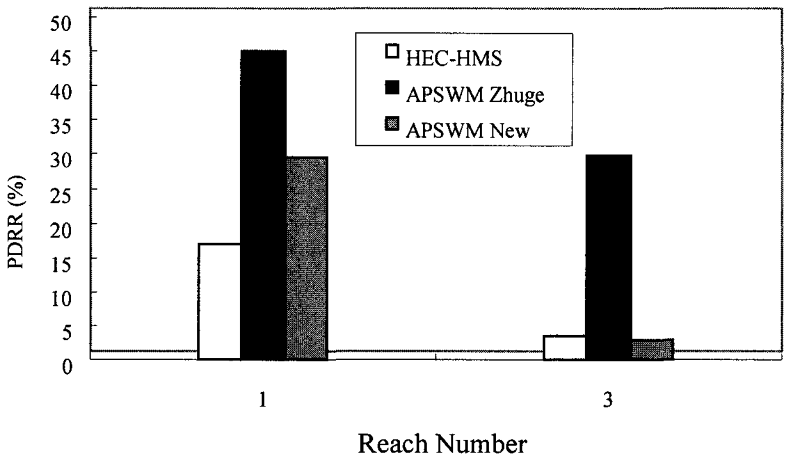

Figure 4.10 Comparisons of PDRR for Catchment F and Downstream Reach Combinations

4.6 Conclusions

The new analytical expressions (Eqs. 4.8 & Eq. 4.10) are derived to provide the basis for the proposed reach routing method. This new method incorporates both K and X values used in the deterministic Muskingum-Cunge routing method. It is shown that this new method significantly improves the accuracy as compared to the previous method. This new method adds $mK\sqrt{(1-2X)/n}$ into the outflow duration (see Fig. 3.1) so that the total duration in the outflow hydrograph is $t+t_c+mK\sqrt{(1-2X)/n}$ (n = 1 when the reach is short) downstream of a channel reach. Thus the peak discharge at a reach outlet decreases proportionally to $mK\sqrt{(1-2X)/n}$.

A number of reaches downstream of three different catchments were tested for comparison purposes. These reaches along with their upstream catchments represent many possible urban catchment conditions because of their different imperviousness, time of concentration, reach length, slope, and Manning's roughness coefficient values. The comparison results can be summarized as follows:

1) A '*time step*' length of $0.5t_c$ would provide as accurate reach routing results as a '*time step*' of 15 minutes using the proposed probabilistic reach routing method.

2) Compared with *Zhuge*'s method, the new routing method provides PDRRs closer to those predicted by HEC-HMS continuous simulations.

3) There appears to be is a linear relationship between $mK\sqrt{(1-2X)/n}$ and PDRR when $mK\sqrt{(1-2X)/n}$ is less than the time of concentration of the upstream catchment.

4) For catchment *C* under Toronto's climate condition, the most suitable multiplication factor *m* seems to be 1.75; while for catchment *E* under Halifax's climate condition, the most suitable multiplication factor *m* seems to be 1.0.

CHAPTER 5: Conclusions and Recommendations

5.1 Overall Summary and Conclusions

In this study, a new probabilistic channel flood routing approach is developed where the interest is not in the determination of the modification that a channel reach make to individual inflow hydrographs but in the determination of the modification that the channel reach makes to the probability distribution of peak flows. This probabilistic approach eliminates the major deficiency of the design storm approach by properly following not only the hydrologic modifications that a river reach makes to individual inflow hydrographs but also the probability transformations taking place to the peak flow from the upstream to the downstream cross-sections of a river reach.

This thesis commences with the rainfall statistical analyses for two Canadian cities: Halifax and Toronto. Following that, APSWM's catchment routing method was further verified by comparing it with results from HEC-HMS continuous simulations using various unit hydrograph methods. A new probabilistic channel reach routing method was then developed and tested by comparing routing results for various hypothetical catchments and downstream reach combinations. The comparison results illustrate that new probabilistic reach routing method provides a significant improvement over the existing one. The main findings and contributions of this study can be summarized as follows:

1) It was found that setting TRV = 1mm and IETD = 9 hours for Halifax and TRV = 1mm and IETD = 6 hours for Toronto resulted in the best fit between the observed relative frequency histograms and theoretical PDF curves. Therefore, these values and the corresponding rainfall statistics are recommended for use in APSWM.

2) Catchment routing method in APSWM was further verified by comparing HEC-HMS continuous simulation and APSWM calculation results. It was found that when t_a = 2~3 t_c in APSWM, the peak discharge discrepancy is less than 25% for the majority of catchments when either the Triangular UH or Rectangular UH method is used in HEC-HMS. When t_a = 1.5~2(t_c + 2K) in APSWM, the average peak discharge discrepancy is less than 25% when the Clark's UH method is used in HEC-HMS. When t_c > 1.5 hour, and if we let t_a = the observed t_c, the average peak discharge discrepancy is less than 20%. But this is not true when t_c < 1.5 hours. Thus, extra care needs to be directed towards cases with t_c < 1.5 hours.

3) The new analytical reach routing method overcomes some of the major limitations of the existing APSWM reach routing method. It incorporates the effects of both K and X values used in the Muskingum-Cunge routing method and provides more accurate results. Using this new method, the total duration of the outflow hydrograph from a river reach is represented as $t + t_c + mK\sqrt{(1-2X)/n}$, where the value of the

multiplication factor m was found to be from 1.0 to 1.75 for the two climate conditions studied.

5.2 Recommendations for Further Research

To further expand and improve APSWM, future research projects may be directed as follows:

1) The new reach routing method may be tested at other locations (besides Halifax and Toronto), and other hypothetical or natural catchment/reach combinations. It's is important to verify if the value of the multiplication factor m is geographic location-dependent.

2) The detention pond routing method proposed by *Zhuge* has not been tested against continuous simulation results. Comparisons similar to those made in this study may be made focusing on detention ponds.

3) Sensitivity analyses may be conducted to determine quantitatively the relative importance of input parameters (e.g., X, K, t_c and a location climate parameter) on reach routing results and the most appropriate m factor values.

REFERENCES

Adams, B. J., Fraser, H. G., Howard, C. D. D. and Hanafy, M. S. 1986 "*Meteorological Data Analysis for Drainage System Design*". Journal of Environmental Engineering, 112(5): 827-847.

Adams, B. J. and Papa, F. 2000 "*Urban Stormwater Management Planning, With Analytical Probabilistic Models*". New York: John Wiley & Sons, Inc.,

Ang, Alfredo H-S. and Tang, Wilson H. 1975 "*Probability Concepts in Engineering Planning and Design, Volume I, Basic Principles*". New York: John Wiley & Sons, Inc.

Aron, G. and E. White, 1982 "*Fitting a Gamma Distribution Over a Synthetic Unit Hydrograph*", Water Resources Bulletin, 18(1): 95-98

Atmospheric Environment Branch Client Services, Ontario Climate Centre. 2002 "IDF Curve Data – Toronto Lester B. Pearson International Airport". AES, Environment Canada.

Bedient, P. B. and Huber, W. C. 1988 "*Hydrology and Floodplain Analysis*". Addison-Wesley Publishing Company.

Benjamin, J. R. and Cornell, C. A. 1970 "*Probability, Statistics and Decision* *for Civil Engineers*". New York: McGraw-Hill, Inc.

Biesenthal, F. M. 1975 "*A Comparison of Kinematic Flood Routing Methods*". M.Eng. Thesis. Hamilton, Ontario: McMaster University.

Boutquin, P., Poremsky, D. and Slovak, K. 2000 "*Beginning Visual Basic 6 Application Development*". Birmingham, UK: Wrox Press Ltd.

Chapra, S. C. and Canale, R. P. 2002 "*Numerical Methods for Engineers, With Software and Programming Applications. 4th ed*". Boston: McGraw-Hill, Inc.

Chow, V. T. 1959 "*Open Channel Hydraulics*". New York: McGraw-Hill, Inc.

Chow, V. T., Maidment, D.R., and Mays, L.W. 1988 "*Applied Hydrology*". New York :McGraw-Hill, Inc.

Clark, C.O. 1945 "*Storage and the Unit Hydrograph.*" Transactions of the American Society of Civil Engineers 110, pp. 1419-1446

Cornell, G. 1998 "*Visual Basic 6: from the Ground Up*". Berkeley, California: Osborne/McGraw-Hill, Inc.

Dooge, J. C. I. 1959 "*A General Theory of the Unit Hydrograph*" Journal of Geophysical Research. 64(2): 241-256.

DeBarry P. A. 2004 "*Watersheds: Processes, Assessment and Management*" London, UK: Wiley, Inc.

Eagleson, P. S. 1972 "*Dynamics of flood frequency*". Water Resources Research, 8(4): 878-898.

Ferguson, B. K. 1998 "*Introduction to Stormwater: Concept, Purpose, Design*". New York: John Wiley & Sons, Inc.

Guo, Y. 2005 "*Analytical Probabilistic Stormwater Models User Manual and Help System.*" Department of Civil Engineering, McMaster University, Hamilton, Ontario.

Guo, Y. 2001 "*Hydrologic design of urban flood Control detention ponds*". Journal of Hydrologic Engineering, Vol. 6, Nov./Dec: 472-479

Guo, Y. 2005 "Introducing APSWM – The Analytical Probabilistic Stormwater Model". 10th International Conference on Urban Drainage, Copenhagen, Denmark.

Guo, Y. and Adams, B. J. 1999a "*Analysis of Detention Ponds for Stormwater Quality Control*". Water Resources Research, 35(8): 2447-2456.

Guo, Y. and Adams, B. J. 1999b "*An Analytical Probabilistic Approach to Sizing Flood Control Detention Facilities*". Water Resources Research, 35(8): 2457-2468.

Guo, Y. and Adams, B. J. 1998a "*Hydrologic Analysis of Urban Catchments with Event-based Probabilistic Models, 1. Runoff Volume*". Water Resources

Research, 34(12): 3421-3431.

Guo, Y. and Adams, B. J. 1998b "*Hydrologic Analysis of Urban Catchments with Event-based Probabilistic Models, 2. Peak Discharge Rate*". Water Resources Research, 34(12): 3433-3443.

Haestad Methods 2003 "*Stormwater Conveyance Modeling and Design*". Waterbury, Connecticut: Haestad Methods Inc.

Hansen, D., Ranade, S. and Hansen, C., R. 2005 "*On the Selection of Rainfall-Runoff Algorithm in Canada*". 10th International Conference on Urban Drainage, Copenhagen, Denmark.

Hotchkiss, R. H. and McCallum, B. E. 1995 "*Peak Discharge for Small Agricultural Watersheds*". Journal of Hydraulic Engineering, 121(1): 36-48.

Huber, W.C. 1993 "*Methods vs. Parameters: the Importance of Parameter Estimation and Sensitivity Analysis in Hydrology*". Water Resources Education: A Lifetime of Learning. AWRA. 1993 pp151-158.

Hydrologic Engineering Center, 2006 "*Hydrologic Modeling System HEC-HMS Users Manual, Ver. 3.0*" Davis, CA: U.S. Army Corps of Engineers.

Hydrologic Engineering Center. 2000 "*Hydrologic Modelling System HEC-HMS, Technical Reference Manual*" Davis, CA: U.S. Army Corps of

Engineers.

Kirpich Z. P. 1940 "*Time of Concentration of Small Agricultural Watersheds*". Journal of Civil Engineering, 10(6): 362.

Marsalek, J. and Watt, W. E. 1984 "*Design Storms for Urban Drainage Design*". Canadian Journal of Civil Engineering, 11, 574-584

Microsoft Corporation. 1998 Electronic References: Microsoft Developer Network (MSDN™) Library, Microsoft® Visual Studio™ 6.0 Development System.

Ministry of Environment Ontario 2003 "*Stormwater Management Planning and Design Manual*". Toronto Ontario: MOE

Ministry of Environment Ontario 2003 "*Understanding Stormwater Management: An Introduction to Stormwater Management Planning and Design*". Toronto Ontario: MOE

Morgali, J. R. and Linsley, R. K. 1965 "*Computer analysis of overland flow*". Journal of Hydraulics Division, Vol. 91, No. HY3.

Nnadi, F. N., Kline, F. X., Wray, H. L., Jr., and Wanielista, M. P. 1999 "*Comparison of Design Storm Concepts Using Continuous Simulation with Short Duration Storms*", Journal of the American Water Resources Association, 35(1): 61-72.

Nash, J.E. 1959 "*Systematic Determination of Unit Hydrograph Parameters*". Journal of Geophysical Research, Vol. 64:111-115.

Overton, D. E. and Meadows, M. E. 1976 "*Stormwater Modeling*". New York: Academic Press, Inc.

Packman, J. C. and Kidd C. H. R. 1980 "*A Logical Approach to the Design Storm Concept*" Water Resources Research. 16(6): 994-1000

Palynchuk, B. 2004 "Comparison of Analytical Probabilistic and Design Storm-based Deterministic Stormwater Models". M.A.Sc. Thesis. Hamilton, Ontario: McMaster University.

Paul A. DeBarry 2004 "*Watersheds: Processes, Assessment and Management*". New York: John Wiley & Sons, Inc.

Ponce, V. M. 1989 "*Engineering Hydrology, Principles and Practices*". Englewood Cliffs, New Jersey Prentice-Hall Inc.

Quader, A. and Guo, Y. 2006 "*Peak Discharge Estimation for Urban Catchments Using Analytical Probabilistic and Design Storm Approaches*". Journal of Hydrologic Engineering, 11(1): 46-54.

Singh, V. P. 1988 "*Hydrologic Systems, Volume I, Rainfall-Runoff Modeling*". Englewood Cliffs, New Jersey: Prentice Hall Inc.

Singh, V. P. 1988 "*Hydrologic Systems, Volume II, Watershed Modeling*".

Englewood Cliffs, New Jersey: Prentice Hall Inc.

Singh, V. P. 1996 "*Kinematic Wave Modeling in Water Resources: Surface-Water Hydrology*". New York: John Wiley & Sons, Inc.

Viessman, W. and Lewis, G. L. 2003 "*Introduction to Hydrology*". 5th ed. Upper Saddle River, New Jersey: Prentice Hall Inc.

Zhuge, Z. 2005 "*Inclusion of Flood Routing in the Analytical Probabilistic Stormwater Model*". MASc Thesis. Hamilton, Ontario: McMaster University.

APPENDIX A: Meteorological Data

Table A-1 Evapotranspiration Rate in the Halifax Area

Month	Rate (mm/day)	Days per month	Rate (mm/month)	Pan Coefficient
April	2.1	30	63.0	0.7
May	2.9	31	89.9	0.7
June	3.4	30	102.0	0.7
July	3.6	31	111.6	0.7
August	3.2	31	99.2	0.7
September	2.3	30	69.0	0.7
October	1.3	31	40.3	0.7

Using Truro ET data since lack of ET data in Toronto

Table A-2 Envaportranspotation Rate in Toronto Area

Month	Rate (mm/day)	Days per month	Rate (mm/month)	Pan Coefficient
April	2.5	30	75.0	0.6
May	3.4	31	105.4	0.6
June	4.1	30	123.0	0.6
July	4.3	31	133.3	0.6
August	3.5	31	108.5	0.6
September	2.2	30	66.0	0.6
October	0.9	31	27.9	0.6

Using Hamilton RBG ET data since lack of ET data in Toronto

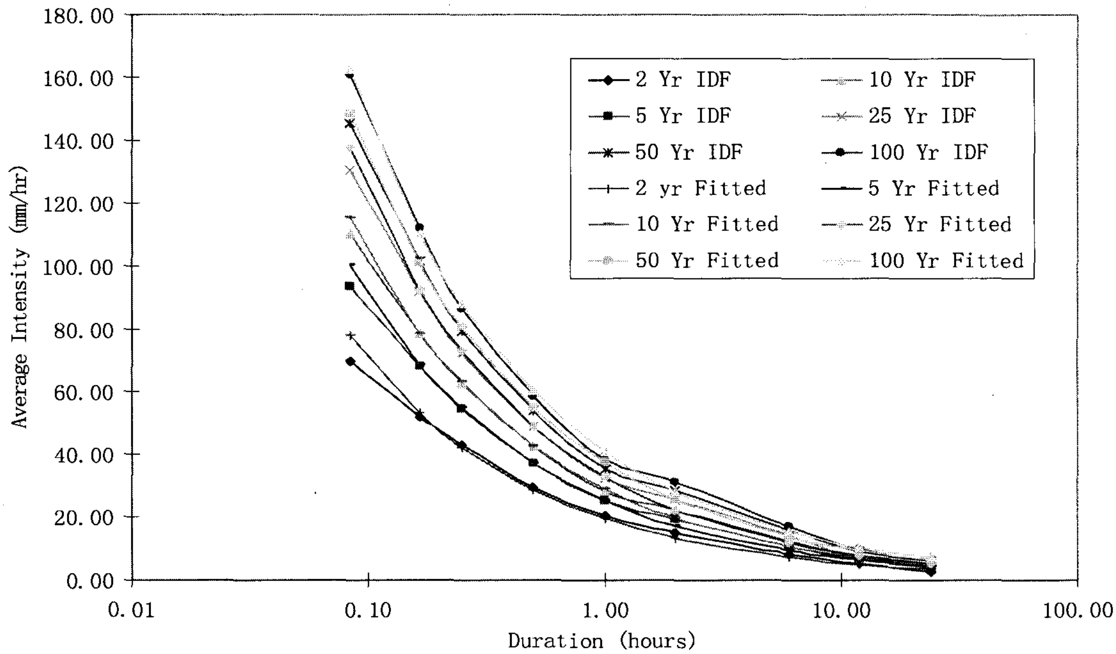

Figure A-1 Measured and Fitted IDF curves in Halifax Area

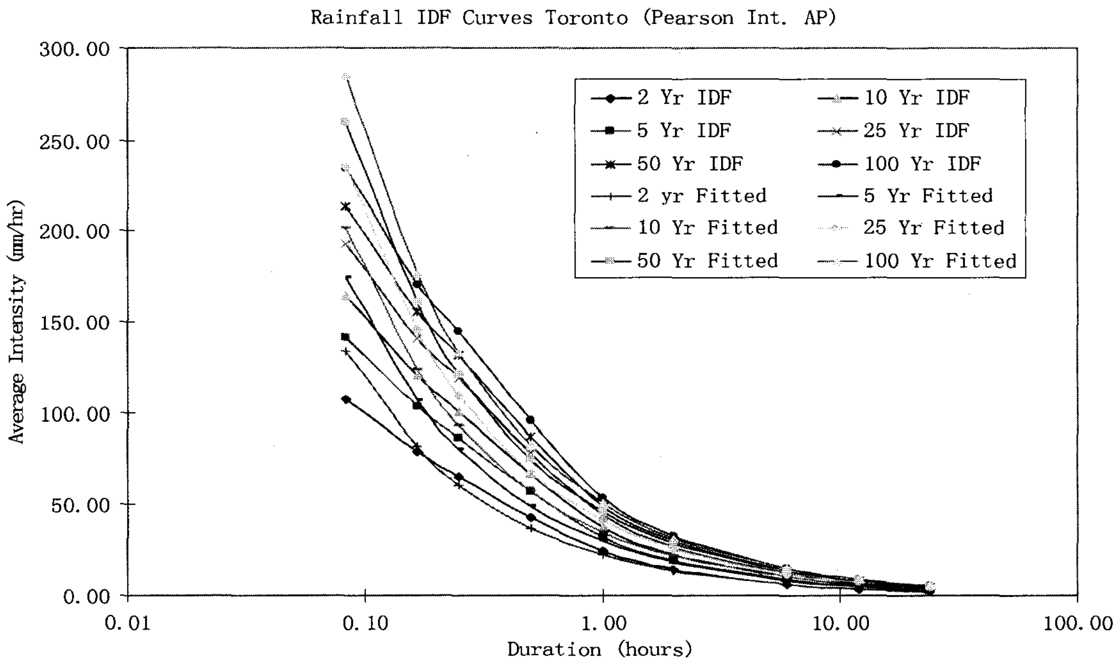

Figure A-2 Measured and Fitted IDF curves in Toronto Area

APPENDIX B: Catchment Time of Concentration

Table B-1 Time of Concentration from the Kinematic Equation

Catchment	L (m)	n	i_e (mm/hr)	S	h	t_c (hr)	Weighted t_c
A (Pervious)	0	0.25	1.456	0.01	1	0.000	**1.629**
A (Impervious)	750	0.014	1.456	0.01	1	1.629	
B (Pervious)	40	0.25	1.456	0.005	0.2	1.948	**1.587**
B (Impervious)	10	0.013	1.456	0.005	0.2	0.144	
C (Pervious)	343	0.25	1.456	0.005	0.7	7.070	**3.929**
C (Impervious)	800	0.02	1.456	0.005	0.7	2.582	
D (Pervious)	380	0.1	1.456	0.005	0.5	4.339	**2.886**
D (Impervious)	400	0.015	1.456	0.005	0.5	1.433	
E (Pervious)	0	0.1	1.456	0.008	1	0.000	**1.220**
E (Impervious)	290	0.02	1.456	0.008	1	1.220	
F (Pervious)	830	0.1	1.456	0.03	0	4.050	**4.050**
F (Impervious)	0	0.015	1.456	0.03	0	0.000	

Table B-2 Time of Concentration from Friend's Equation

Catchment	L (m)	n	S	h	t_c (hr)	Weighted t_c
A (Pervious)	0	0.25	0.01	1	0.000	**0.226**
A (Impervious)	750	0.014	0.01	1	0.226	
B (Pervious)	40	0.25	0.005	0.2	1.749	**1.411**
B (Impervious)	10	0.013	0.005	0.2	0.057	
C (Pervious)	343	0.25	0.005	0.7	3.578	**1.339**
C (Impervious)	800	0.02	0.005	0.7	0.380	
D (Pervious)	380	0.1	0.005	0.5	1.481	**0.853**
D (Impervious)	400	0.015	0.005	0.5	0.226	
E (Pervious)	0	0.1	0.008	1	0.000	**0.246**
E (Impervious)	290	0.02	0.008	1	0.246	
F (Pervious)	830	0.1	0.03	0	1.342	**1.342**
F (Impervious)	0	0.015	0.03	0	0.000	

APPENDIX C: Comparison of Catchment Routing

Table C-1 Comparison of Catchment ABC Routing (K = 0.6 t_c in HEC-HMS)

Catchment A (Imperviousness = 100%)

Peak Discharge (m^3/s)	HEC-HMS Clark's UH	APSWM			Discrepancy (100%)		
Return Period (yr)	t_c = 1.65 hr	t_A = 5.08 hr	$t_A = t_c + 2K$	$t_A = 1.5(t_c + 2K)$	t_A = 5.08 hr	$t_A = t_c + 2K$	$t_A = 1.5(t_c + 2K)$
2	0.988	1.165	1.491	1.106	17.910	50.905	11.939
5	1.312	1.498	1.942	1.418	14.138	47.968	8.042
10	1.537	1.759	2.301	1.663	14.444	49.708	8.198
25	1.833	2.115	2.790	1.996	15.398	52.227	8.905
50	2.063	2.390	3.171	2.253	15.876	53.742	9.234
100	2.300	2.670	3.559	2.515	16.111	54.771	9.370
Average	**t_c = 1.65 hr**	**t_A = 5.08 hr**	**t_A = 3.63 hr**	**t_A = 5.445 hr**	**15.65**	**51.55**	**9.28**

Catchment B (Imperviousness = 20%)

Peak Discharge (m^3/s)	HEC-HMS Clark's UH	APSWM			Discrepancy (100%)		
Return	t_c = 1.97 hr	t_A = 4.33 hr	$t_A = t_c + 2K$	$t_A = 1.5(t_c + 2K)$	t_A = 4.33 hr	$t_A = t_c + 2K$	$t_A = 1.5(t_c + 2K)$

Period (yr)							
2	0.114	0.152	0.152	0.113	33.239	33.239	-0.948
5	0.156	0.203	0.202	0.148	30.231	29.589	-5.054
10	0.186	0.242	0.242	0.175	30.450	30.450	-5.666
25	0.225	0.297	0.297	0.212	31.845	31.845	-5.888
50	0.257	0.340	0.339	0.241	32.480	32.090	-6.095
100	0.289	0.383	0.383	0.270	32.331	32.331	-6.712
Average	**t_c = 1.97 hr**	**t_A = 4.33 hr**	**t_A = 4.334 hr**	**t_A = 6.501 hr**	**31.76**	**31.59**	**-5.06**

Catchment C (Imperviousness = 70%)

Peak Discharge (m^3/s)	HEC-HMS Clark's UH	APSWM			Discrepancy (100%)		
Return Period (yr)	**t_c = 2.62 hr**	**t_A = 8.38 hr**	**$t_A = t_c + 2K$**	**$t_A = 1.5(t_c + 2K)$**	**t_A = 8.38 hr**	**$t_A = t_c + 2K$**	**$t_A = 1.5(t_c + 2K)$**
2	0.742	0.755	1.005	0.737	1.690	35.362	-0.735
5	0.996	0.979	1.325	0.954	-1.717	33.018	-4.227
10	1.175	1.170	1.606	1.140	-0.449	36.649	-3.001
25	1.414	1.454	2.026	1.414	2.800	43.241	-0.028
50	1.603	1.687	2.367	1.640	5.272	47.705	2.339
100	1.799	1.928	2.714	1.874	7.179	50.874	4.177
Average	**t_c = 2.62 hr**	**t_A = 8.38 hr**	**t_A = 5.764 hr**	**t_A = 8.646 hr**	**2.46**	**41.14**	**-0.25**

Note: Halifax Rainfall with IETD = 9 hr, Rainfall threshold = 1 mm; Initial Loss = S_{iw}

Table C-2 Comparison of Catchment ABC Routing (K = 0.167 t_c in HEC-HMS)

Catchment A (Imperviousness = 100%)

Peak Discharge (m^3/s)	HEC-HMS Clark's UH	APSWM			Discrepancy (100%)		
Return Period (yr)	t_c = 1.65 hr	$t_A = t_c$	$t_A = 1.5t_c$	$t_A = 2t_c$	$t_A = t_c$	$t_A = 1.5t_c$	$t_A = 2t_c$
2	1.244	2.567	1.952	1.596	106.307	56.880	28.269
5	1.629	3.488	2.593	2.089	114.097	59.161	28.225
10	1.885	4.232	3.105	2.481	124.568	64.764	31.652
25	2.208	5.264	3.809	3.017	138.354	72.472	36.610
50	2.451	6.074	4.359	3.434	147.831	77.856	40.114
100	2.696	6.904	4.920	3.859	156.121	82.520	43.159
Average	**t_c = 1.65 hr**	**t_A = 1.65 hr**	**t_A = 2.475 hr**	**t_A = 3.3 hr**	**131.21**	**68.94**	**34.67**

Catchment B (Imperviousness = 20%)

Peak Discharge (m^3/s)	HEC-HMS Clark's UH	APSWM			Discrepancy (100%)		
Return Period (yr)	t_c = 1.97 hr	$t_A = t_c$	$t_A = 1.5t_c$	$t_A = 2t_c$	$t_A = t_c$	$t_A = 1.5t_c$	$t_A = 2t_c$
2	0.145	0.261	0.199	0.163	79.643	36.969	12.191
5	0.196	0.362	0.270	0.218	84.230	37.409	10.945
10	0.232	0.444	0.327	0.261	91.315	40.901	12.462

25	0.279	0.558	0.405	0.321	99.970	45.140	15.037
50	0.315	0.648	0.466	0.367	105.395	47.707	16.327
100	0.353	0.741	0.529	0.415	109.811	49.784	17.506
Average	**t_c = 1.97 hr**	**t_A = 1.97 hr**	**t_A = 2.955 hr**	**t_A = 3.94 hr**	**95.06**	**42.99**	**14.08**
Catchment C (Imperviousness = 70%)							
Peak Discharge (m^3/s)	**HEC-HMS Clark's UH**	**APSWM**			**Discrepancy (100%)**		
Return Period	**t_c = 2.62 hr**	**$t_A = t_c$**	**$t_A = 1.5t_c$**	**$t_A = 2t_c$**	**$t_A = t_c$**	**$t_A = 1.5t_c$**	**$t_A = 2t_c$**
2	0.954	1.771	1.332	1.079	85.662	39.639	13.116
5	1.277	2.445	1.792	1.429	91.402	40.283	11.867
10	1.504	3.079	2.209	1.739	104.735	46.885	15.633
25	1.805	4.010	2.833	2.203	122.217	56.993	22.081
50	2.040	4.733	3.327	2.578	132.036	63.107	26.387
100	2.284	5.467	3.828	2.959	139.367	67.605	29.557
Average	**t_c = 2.62 hr**	**t_A = 2.62 hr**	**t_A = 3.93 hr**	**t_A = 5.24 hr**	**112.57**	**52.42**	**19.77**

Note: Halifax Rainfall with IETD = 9 hr, Rainfall threshold = 1 mm; Initial Loss = S_{iw}

Table C-3 Comparison of Catchment ABC Routing (K = 0.125 hr in HEC-HMS)

Catchment A (Imperviousness = 100%)

Peak Discharge (m^3/s)	HEC-HMS Clark's UH	APSWM			Discrepancy (100%)		
Return Period	t_c = 1.65 hr	$t_A = 2t_c$	$t_A = 2.25t_c$	$t_A = 2.5t_c$	$t_A = 2t_c$	$t_A = 2.25t_c$	$t_A = 2.5t_c$
2	1.295	1.596	1.467	1.358	23.201	13.243	4.829
5	1.690	2.089	1.910	1.761	23.580	12.991	4.176
10	1.949	2.481	2.260	2.078	27.269	15.932	6.596
25	2.275	3.017	2.739	2.512	32.626	20.405	10.427
50	2.516	3.434	3.112	2.849	36.465	23.669	13.217
100	2.759	3.859	3.491	3.191	39.886	26.546	15.671
Average	**t_c = 1.65 hr**	**tA = 3.3 hr**	**t_A = 3.71 hr**	**t_A = 4.125 hr**	**30.50**	**18.80**	**9.15**

Catchment B (Imperviousness = 20%)

Peak Discharge (m^3/s)	HEC-HMS Clark's UH	APSWM			Discrepancy (100%)		
Return Period	t_c = 1.97 hr	$t_A = 2t_c$	$t_A = 2.25t_c$	$t_A = 2.5t_c$	$t_A = 2t_c$	$t_A = 2.25t_c$	$t_A = 2.5t_c$
2	0.150	0.163	0.150	0.139	8.461	-0.189	-7.509
5	0.204	0.218	0.199	0.184	6.985	-2.339	-9.701
10	0.242	0.261	0.238	0.219	7.961	-1.553	-9.412
25	0.293	0.321	0.291	0.267	9.668	-0.581	-8.781
50	0.333	0.367	0.333	0.305	10.229	0.017	-8.393

100	0.375	0.415	0.375	0.343	10.650	-0.015	-8.547
Average	**t_c = 1.97 hr**	**t_A = 3.94 hr**	**t_A = 4.43 hr**	**t_A = 4.925 hr**	**8.99**	**-0.78**	**-8.72**
Catchment C (Imperviousness = 70%)							
Peak Discharge (m^3/s)	**HEC-HMS Clark's UH**	**APSWM**			**Discrepancy (100%)**		
Return Period	**t_c = 2.62 hr**	**$t_A = 2t_c$**	**$t_A = 2.25t_c$**	**$t_A = 2.5t_c$**	**$t_A = 2t_c$**	**$t_A = 2.25t_c$**	**$t_A = 2.5t_c$**
2	1.004	1.079	0.989	0.913	7.507	-1.460	-9.033
5	1.340	1.429	1.301	1.196	6.665	-2.889	-10.727
10	1.572	1.739	1.576	1.442	10.612	0.244	-8.279
25	1.878	2.203	1.986	1.810	17.289	5.736	-3.635
50	2.116	2.578	2.319	2.109	21.846	9.605	-0.320
100	2.361	2.959	2.660	2.417	25.347	12.681	2.387
Average	**t_c = 2.62 hr**	**t_A = 5.24 hr**	**t_A = 5.895 hr**	**t_A = 6.55 hr**	**14.88**	**3.99**	**-4.93**

Note: Halifax Rainfall with IETD = 9 hr, Rainfall threshold = 1 mm; Initial Loss = S_{iw}

Table C-4 Comparison of Catchment DEF Routing (K = 0.125 hr in HEC-HMS)

Catchment D (Imperviousness = 50%)

Peak Discharge (m^3/s)	HEC-HMS Clark's UH	APSWM			Discrepancy (100%)		
Return Period	$t_c = 0.85$ hr	t_A = Observed	$t_A = t_c + 2K$	$t_A = 1.5(t_c + 2K)$	t_A = Observed	$t_A = t_c + 2K$	$t_A = 1.5(t_c + 2K)$
2	1.375	2.189	2.056	1.569	59.176	49.505	14.092
5	1.917	2.998	2.803	2.086	56.363	46.192	8.797
10	2.281	3.657	3.405	2.501	60.326	49.278	9.646
25	2.745	4.572	4.243	3.087	66.568	54.582	12.466
50	3.094	5.478	5.077	3.661	77.079	64.117	18.344
100	3.444	6.872	6.335	4.457	99.528	83.937	29.409
Average	**$t_c = 0.85$ hr**	**$t_A = 1$ hr**	**$t_A = 1.1$ hr**	**$t_A = 1.65$ hr**	**69.84**	**57.94**	**15.46**

Catchment E (Imperviousness = 100%)

Peak Discharge (m^3/s)	HEC-HMS Clark's UH	APSWM			Discrepancy (100%)		
Return Period	$t_c = 0.75$ hr	t_A = Observed	$t_A = t_c + 2K$	$t_A = 1.5(t_c + 2K)$	t_A = Observed	$t_A = t_c + 2K$	$t_A = 1.5(t_c + 2K)$
2	1.322	2.521	2.093	1.591	90.758	58.372	20.387
5	1.843	3.465	2.823	2.097	88.041	53.201	13.802
10	2.192	4.233	3.413	2.502	93.091	55.686	14.130
25	2.638	5.304	4.231	3.059	101.052	60.379	15.953
50	2.973	6.148	4.872	3.494	106.771	63.856	17.511

100	3.310	7.014	5.529	3.938	111.879	67.020	18.959
Average	**t_c = 0.75 hr**	**t_A = 0.75 hr**	**t_A = 1 hr**	**t_A = 1.5 hr**	**98.60**	**59.75**	**16.79**
Catchment F (Imperviousness = 0%)							
Peak Discharge (m^3/s)	**HEC-HMS Clark's UH**	**APSWM**			**Discrepancy (100%)**		
Return Period	**t_c = 1.34 hr**	**t_A = Observed**	**$t_A = t_c + 2K$**	**$t_A = 1.5(t_c + 2K)$**	**t_A = Observed**	**$t_A = t_c + 2K$**	**$t_A = 1.5(t_c + 2K)$**
2	3.632	8.477	4.329	3.286	133.376	19.179	-9.535
5	5.763	13.824	6.431	4.772	139.870	11.589	-17.198
10	7.335	18.446	8.129	5.953	151.470	10.821	-18.844
25	9.486	25.145	10.485	7.575	165.076	10.532	-20.145
50	11.200	30.558	12.333	8.839	172.837	10.115	-21.081
100	13.001	36.202	14.226	10.128	178.452	9.421	-22.099
Average	**t_c = 1.34 hr**	**t_A = 0.5 hr**	**t_A = 1.59 hr**	**t_A = 2.385 hr**	**156.85**	**11.94**	**-18.15**

Note: Toronto Rainfall with IETD = 6 hr, Rainfall threshold = 1 mm; Initial Loss = S_{iw}

Table C-5 Comparison of Catchment DEF Routing (K = 0.125 hr in HEC-HMS)

Catchment D (Imperviousness = 50%)

Peak Discharge (m^3/s)	HEC-HMS Triangular IUH	APSWM			Discrepancy (100%)		
Return Period	t_c = 0.85 hr	$t_A = t_c$	$t_A = 1.5t_c$	$t_A = 2t_c$	$t_A = t_c$	$t_A = 1.5t_c$	$t_A = 2t_c$
2	1.383	2.428	1.868	1.537	75.622	35.116	11.175
5	1.929	3.362	2.520	2.040	74.295	30.644	5.759
10	2.296	4.125	3.046	2.444	79.691	32.688	6.464
25	2.764	5.191	3.780	3.015	87.839	36.781	9.099
50	3.115	6.233	4.511	3.573	100.069	44.796	14.688
100	3.469	7.882	5.578	4.342	127.193	60.782	25.155
Average	**t_c = 0.85 hr**	**t_A = 0.85 hr**	**t_A = 1.275 hr**	**t_A = 1.7 hr**	**90.78**	**40.13**	**12.06**

Catchment E (Imperviousness = 100%)

Peak Discharge (m^3/s)	HEC-HMS Triangular IUH	APSWM			Discrepancy (100%)		
Return Period	t_c = 0.75 hr	$t_A = t_c$	$t_A = 1.5t_c$	$t_A = 2t_c$	$t_A = t_c$	$t_A = 1.5t_c$	$t_A = 2t_c$
2	1.321	2.521	1.934	1.591	90.813	46.384	20.422
5	1.842	3.465	2.592	2.097	88.073	40.688	13.821
10	2.192	4.233	3.121	2.502	93.110	42.380	14.142
25	2.638	5.304	3.853	3.059	101.058	46.055	15.957
50	2.973	6.148	4.425	3.494	106.768	48.820	17.509

100	3.311	7.014	5.012	3.938	111.867	51.394	18.952
Average	**t_c = 0.75 hr**	**t_A = 0.75 hr**	**t_A = 1.125 hr**	**t_A = 1.5 hr**	**98.61**	**45.95**	**16.80**
Catchment F (Imperviousness = 0%)							
Peak Discharge (m^3/s)	**HEC-HMS Triangular IUH**	**APSWM**			**Discrepancy (100%)**		
Return Period	**t_c = 1.34 hr**	**$t_A = t_c$**	**$t_A = 1.5t_c$**	**$t_A = 2t_c$**	**$t_A = t_c$**	**$t_A = 1.5t_c$**	**$t_A = 2t_c$**
2	4.081	4.840	3.699	3.025	18.596	-9.362	-25.877
5	6.410	7.260	5.421	4.367	13.257	-15.432	-31.874
10	8.116	9.237	6.799	5.430	13.812	-16.228	-33.096
25	10.437	11.992	8.698	6.888	14.900	-16.661	-34.003
50	12.278	14.161	10.181	8.020	15.333	-17.081	-34.682
100	14.206	16.388	11.698	9.174	15.356	-17.657	-35.424
Average	**t_c = 1.34 hr**	**t_A = 1.34 hr**	**t_A = 2.01 hr**	**t_A = 2.68 hr**	**15.21**	**-15.40**	**-32.49**

Note: Toronto Rainfall with IETD = 6 hr, Rainfall threshold = 1 mm; Initial Loss = S_{iw}

APPENDIX D: Comparison of Channel Reach Routing

Table D-1 Comparison of Reach Routing for Catchment C (m = 1.75 for $mK\sqrt{(1-2X)/n}$)

Catchment C (Impervious = 70%)

Catchment-Reach	**C-2**	**C-3**	**C-4**	**C-6**	**C-10**	**C-101**	**C102**	**C-11**	**C-19**	**C-201**	**C-202**	**C-20**	**C-21**
X	0.000	0.000	0.465	0.399	0.389	0.293	0.271	0.005	0.445	0.096	0.074	0.129	0.029
K	0.436	0.699	0.039	0.295	0.458	1.533	1.867	2.181	0.916	5.158	5.729	4.363	6.993
n	1	1	1	1	1	1	1	2	1	3	3	3	4

Comparison of Peak Discharge (m3/s)														
HEC-HMS Continuous Simulations														
Return Period (Year)	C	C-2	C-3	C-4	C-6	C-10	C-101	C102	C-11	C-19	C-201	C-202	C-20	C-21
2.000	1.004	0.876	0.769	0.998	0.992	0.980	0.760	0.684	0.619	0.961	0.417	0.373	0.488	0.297
5.000	1.340	1.182	1.046	1.334	1.325	1.311	1.030	0.928	0.839	1.287	0.560	0.503	0.656	0.401
10.000	1.572	1.398	1.243	1.568	1.555	1.542	1.222	1.099	0.993	1.516	0.658	0.591	0.772	0.473
25.000	1.878	1.687	1.508	1.876	1.860	1.847	1.478	1.328	1.197	1.820	0.785	0.705	0.923	0.567
50.000	2.116	1.914	1.717	2.116	2.096	2.085	1.680	1.507	1.357	2.058	0.882	0.792	1.039	0.640
100.000	2.361	2.151	1.936	2.363	2.341	2.331	1.891	1.694	1.522	2.305	0.981	0.881	1.159	0.716

APSWM ($t_{c\text{-channel}} = t_c + 1.75K \sqrt{(1-X)/n}$)														
Return Period (Year)	C	C-2	C-3	C-4	C-6	C-10	C-101	C102	C-11	C-19	C-201	C-202	C-20	C-21
2.000	1.173	1.042	0.978	1.169	1.129	1.104	0.916	0.866	0.820	1.078	0.677	0.641	0.733	0.571
5.000	1.595	1.404	1.310	1.590	1.531	1.493	1.223	1.150	1.086	1.455	0.885	0.836	0.964	0.741

10.000	1.974	1.724	1.604	1.968	1.890	1.842	1.491	1.397	1.317	1.792	1.064	1.002	1.162	0.884
25.000	2.542	2.205	2.043	2.533	2.429	2.363	1.892	1.768	1.661	2.296	1.328	1.247	1.457	1.095
50.000	2.995	2.591	2.397	2.984	2.859	2.780	2.217	2.069	1.941	2.700	1.545	1.448	1.698	1.268
100.000	3.453	2.984	2.759	3.441	3.295	3.203	2.550	2.377	2.229	3.110	1.769	1.658	1.947	1.448

Differences (%)														
Return Period (Year)	C	C-2	C-3	C-4	C-6	C-10	C-101	C102	C-11	C-19	C-201	C-202	C-20	C-21
2.000	16.873	19.009	27.133	17.142	13.802	12.671	20.507	26.574	32.512	12.224	62.529	71.684	50.265	91.959
5.000	19.056	18.793	25.243	19.161	15.563	13.867	18.700	23.940	29.421	13.021	57.933	66.321	46.886	84.718
10.000	25.560	23.304	29.051	25.532	21.507	19.470	22.041	27.090	32.618	18.185	61.605	69.597	50.505	86.922
25.000	35.337	30.700	35.522	35.026	30.605	27.941	28.012	33.161	38.725	26.135	69.076	76.847	57.806	93.014
50.000	41.555	35.344	39.620	41.035	36.370	33.342	31.959	37.282	43.063	31.182	75.132	82.779	63.378	98.029
100.000	46.273	38.696	42.504	45.595	40.768	37.410	34.835	40.346	46.453	34.907	80.275	88.105	68.040	102.337
Average Difference	30.776	27.641	33.179	30.582	26.436	24.117	26.009	31.399	37.132	22.609	67.758	75.889	56.147	92.830

Comparison of Reach Inflow and Outflow														
HEC-HMS														
Return Period (Year)		C-2	C-3	C-4	C-6	C-10	C-101	C102	C-11	C-19	C-201	C-202	C-20	C-21
2.00		-12.76	-23.35	-0.57	-1.15	-2.37	-24.26	-31.83	-38.34	-4.29	-58.50	-62.80	-51.40	-70.36
5.00		-11.78	-21.93	-0.40	-1.11	-2.13	-23.09	-30.74	-37.37	-3.91	-58.17	-62.48	-51.01	-70.06
10.00		-11.07	-20.94	-0.28	-1.06	-1.93	-22.29	-30.08	-36.83	-3.55	-58.12	-62.42	-50.89	-69.92
25.00		-10.18	-19.74	-0.12	-0.98	-1.67	-21.31	-29.31	-36.25	-3.09	-58.18	-62.46	-50.84	-69.80
50.00		-9.52	-18.86	0.00	-0.91	-1.46	-20.59	-28.77	-35.87	-2.72	-58.30	-62.56	-50.88	-69.74
100.00		-8.86	-17.98	0.12	-0.84	-1.26	-19.89	-28.25	-35.53	-2.35	-58.43	-62.66	-50.92	-69.68

Average Difference		-10.69	-20.47	-0.21	-1.01	-1.80	-21.91	-29.83	-36.70	-3.32	-58.29	-62.56	-50.99	-69.93

APSWM ($t_{c\text{-}channel} = t_c + 1.75K \sqrt{(1-X)/n}$)														
Return Period (Year)		C-2	C-3	C-4	C-6	C-10	C-101	C102	C-11	C-19	C-201	C-202	C-20	C-21
2.00		-11.17	-16.62	-0.34	-3.75	-5.88	-21.91	-26.17	-30.09	-8.10	-42.28	-45.35	-37.51	-51.32
5.00		-11.97	-17.87	-0.31	-4.01	-6.39	-23.32	-27.90	-31.91	-8.78	-44.51	-47.59	-39.56	-53.54
10.00		-12.66	-18.74	-0.30	-4.26	-6.69	-24.47	-29.23	-33.28	-9.22	-46.10	-49.24	-41.13	-55.22
25.00		-13.26	-19.63	-0.35	-4.45	-7.04	-25.57	-30.45	-34.66	-9.68	-47.76	-50.94	-42.68	-56.92
50.00		-13.49	-19.97	-0.37	-4.54	-7.18	-25.98	-30.92	-35.19	-9.85	-48.41	-51.65	-43.31	-57.66
100.00		-13.58	-20.10	-0.35	-4.58	-7.24	-26.15	-31.16	-35.45	-9.93	-48.77	-51.98	-43.61	-58.07
Average Difference		-12.69	-18.82	-0.34	-4.26	-6.74	-24.57	-29.30	-33.43	-9.26	-46.31	-49.46	-41.30	-55.46

Peak Reduction HEC-HMS	**10.69**	**20.47**	**0.21**	**1.01**	**1.80**	**21.91**	**29.83**	**36.70**	**3.32**	**58.29**	**62.56**	**50.99**	**69.93**
Peak Reduction APSWM	**12.69**	**18.82**	**0.34**	**4.26**	**6.74**	**24.57**	**29.30**	**33.43**	**9.26**	**46.31**	**49.46**	**41.30**	**55.46**
Regression HEC-HMS	**14.01**	**22.86**	**-0.33**	**3.80**	**6.59**	**32.53**	**41.82**	**50.99**	**9.60**	**89.43**	**102.08**	**72.38**	**113.55**
Regression APSWM	**14.76**	**22.14**	**2.82**	**6.26**	**8.58**	**30.19**	**37.93**	**45.57**	**11.09**	**77.60**	**88.14**	**63.40**	**97.70**
$1.75K\sqrt{(1-2X)}/n$	**0.65**	**1.05**	**0.02**	**0.20**	**0.32**	**1.48**	**1.89**	**2.30**	**0.46**	**4.02**	**4.58**	**3.26**	**5.09**
K	**0.44**	**0.70**	**0.04**	**0.29**	**0.46**	**1.53**	**1.87**	**2.18**	**0.92**	**5.16**	**5.73**	**4.36**	**6.99**

HEC-HMS R-Square	**0.96603**
APSWM R-Square	**0.98613**

Table D-2 Comparison of Reach Routing for Catchment C (m = 2 for $mK\sqrt{(1-2X)/n}$)

Catchment C (Impervious = 70%)

Catchment-Reach	**C-2**	**C-3**	**C-4**	**C-6**	**C-10**	**C-101**	**C102**	**C-11**	**C-19**	**C-201**	**C-202**	**C-20**
X	**0.000**	**0.000**	**0.465**	**0.399**	**0.389**	**0.293**	**0.271**	**0.005**	**0.445**	**0.096**	**0.074**	**0.129**
K	**0.436**	**0.699**	**0.039**	**0.295**	**0.458**	**1.533**	**1.867**	**2.181**	**0.916**	**5.158**	**5.729**	**4.363**
n	**1**	**1**	**1**	**1**	**1**	**1**	**1**	**2**	**1**	**3**	**3**	**3**

Comparison of Peak Discharge (m3/s)

HEC-HMS Continuous Simulations

Return Period (Year)	C	C-2	C-3	C-4	C-6	C-10	C-101	C102	C-11	C-19	C-201	C-202	C-20
2	1.004	0.876	0.769	0.998	0.992	0.980	0.760	0.684	0.619	0.961	0.417	0.373	0.488
5	1.340	1.182	1.046	1.334	1.325	1.311	1.030	0.928	0.839	1.287	0.560	0.503	0.656
10	1.572	1.398	1.243	1.568	1.555	1.542	1.222	1.099	0.993	1.516	0.658	0.591	0.772
25	1.878	1.687	1.508	1.876	1.860	1.847	1.478	1.328	1.197	1.820	0.785	0.705	0.923
50	2.116	1.914	1.717	2.116	2.096	2.085	1.680	1.507	1.357	2.058	0.882	0.792	1.039
100	2.361	2.151	1.936	2.363	2.341	2.331	1.891	1.694	1.522	2.305	0.981	0.881	1.159

APSWM ($t_{c\text{-}channel} = t_c + 2K\sqrt{(1-X)/n}$)

Return Period (Year)	C	C-2	C-3	C-4	C-6	C-10	C-101	C102	C-11	C-19	C-201	C-202	C-20
2	1.173	1.026	0.956	1.169	1.123	1.095	0.890	0.834	0.788	1.066	0.640	0.603	0.698
5	1.595	1.380	1.278	1.589	1.522	1.480	1.184	1.106	1.041	1.438	0.835	0.785	0.914
10	1.974	1.694	1.562	1.967	1.879	1.824	1.442	1.343	1.259	1.769	1.001	0.938	1.100
25	2.542	2.164	1.988	2.532	2.413	2.339	1.826	1.695	1.584	2.265	1.246	1.165	1.375
50	2.995	2.542	2.331	2.982	2.840	2.752	2.139	1.982	1.849	2.663	1.447	1.351	1.601

100	3.453	2.927	2.682	3.439	3.274	3.171	2.459	2.277	2.123	3.067	1.656	1.545	1.834

Differences (%)

Return Period (Year)	C	C-2	C-3	C-4	C-6	C-10	C-101	C102	C-11	C-19	C-201	C-202	C-20
2	16.9	17.2	24.3	17.1	13.2	11.8	17.1	21.9	27.3	11.0	53.6	61.5	43.1
5	19.1	16.8	22.2	19.1	14.9	12.9	14.9	19.2	24.1	11.7	49.0	56.2	39.3
10	25.6	21.2	25.7	25.5	20.8	18.3	18.0	22.2	26.8	16.7	52.0	58.8	42.5
25	35.3	28.3	31.9	35.0	29.7	26.6	23.5	27.7	32.3	24.4	58.6	65.2	48.9
50	41.6	32.8	35.8	40.9	35.5	32.0	27.3	31.5	36.3	29.4	64.0	70.5	54.0
100	46.3	36.0	38.5	45.5	39.9	36.0	30.0	34.4	39.5	33.0	68.8	75.3	58.3
Average Difference	30.8	25.4	29.7	30.5	25.7	22.9	21.8	26.1	31.0	21.0	57.7	64.6	47.7

Comparison of Reach Inflow and Outflow

HEC-HMS

Return Period (Year)	C-2	C-3	C-4	C-6	C-10	C-101	C102	C-11	C-19	C-201	C-202	C-20
2	-12.8	-23.4	-0.6	-1.2	-2.4	-24.3	-31.8	-38.3	-4.3	-58.5	-62.8	-51.4
5	-11.8	-21.9	-0.4	-1.1	-2.1	-23.1	-30.7	-37.4	-3.9	-58.2	-62.5	-51.0
10	-11.1	-20.9	-0.3	-1.1	-1.9	-22.3	-30.1	-36.8	-3.6	-58.1	-62.4	-50.9
25	-10.2	-19.7	-0.1	-1.0	-1.7	-21.3	-29.3	-36.3	-3.1	-58.2	-62.5	-50.8
50	-9.5	-18.9	0.0	-0.9	-1.5	-20.6	-28.8	-35.9	-2.7	-58.3	-62.6	-50.9
100	-8.9	-18.0	0.1	-0.8	-1.3	-19.9	-28.3	-35.5	-2.3	-58.4	-62.7	-50.9
Average Difference	-10.7	-20.5	-0.2	-1.0	-1.8	-21.9	-29.8	-36.7	-3.3	-58.3	-62.6	-51.0

APSWM ($t_{c\text{-channel}} = t_c + 2K\sqrt{(1-X)/n}$)

Return Period (Year)	C-2	C-3	C-4	C-6	C-10	C-101	C102	C-11	C-19	C-201	C-202	C-20
2	-12.5	-18.5	-0.3	-4.3	-6.6	-24.1	-28.9	-32.8	-9.1	-45.4	-48.6	-40.5
5	-13.5	-19.9	-0.4	-4.6	-7.2	-25.8	-30.7	-34.7	-9.8	-47.6	-50.8	-42.7
10	-14.2	-20.9	-0.4	-4.8	-7.6	-27.0	-32.0	-36.2	-10.4	-49.3	-52.5	-44.3
25	-14.9	-21.8	-0.4	-5.1	-8.0	-28.2	-33.3	-37.7	-10.9	-51.0	-54.2	-45.9
50	-15.1	-22.2	-0.4	-5.2	-8.1	-28.6	-33.8	-38.3	-11.1	-51.7	-54.9	-46.5
100	-15.2	-22.3	-0.4	-5.2	-8.2	-28.8	-34.1	-38.5	-11.2	-52.0	-55.3	-46.9
Average Difference	-14.2	-20.9	-0.4	-4.8	-7.6	-27.1	-32.1	-36.4	-10.4	-49.5	-52.7	-44.5

Peak Reduction HEC-HMS	10.7	20.5	0.2	1.0	1.8	21.9	29.8	36.7	3.3	58.3	62.6	51.0
Peak Reduction APSWM	14.2	20.9	0.4	4.8	7.6	27.1	32.1	36.4	10.4	49.5	52.7	44.5
Regression HEC-HMS	18.9	30.7	-0.2	5.3	9.0	43.6	56.0	68.2	13.0	119.5	136.3	96.7
Regression APSWM	18.8	28.7	2.9	7.5	10.6	39.4	49.7	59.9	13.9	102.6	116.7	83.7
$2K\sqrt{(1-2X)/n}$	0.8726	1.3986	0.0204	0.2656	0.4316	1.9732	2.5255	3.0701	0.6104	5.3553	6.1072	4.3419
K	0.4363	0.6993	0.0386	0.2947	0.4580	1.5330	1.8667	2.1814	0.9160	5.1582	5.7286	4.3629

HEC-HMS R-Square	**0.94366**
APSWM R-Square	**0.9853**

Table D-3 Comparison of Reach Routing for Catchment E (m = 1 for $mK\sqrt{(1-2X)/n}$)

Catchment E (Impervious = 100%)

Catchment-Reach	**E-2**	**E-3**	**E-11**	**E-16**	**E-202**	**E-20**	**E-29**	**E-30**	**E-301**	**E-304**
X	**0**	**0**	**0**	**0.4968**	**0**	**0**	**0**	**0**	**0**	**0**
K	**0.1368**	**0.2192**	**0.342**	**0.0128**	**12.4383**	**0.684**	**1.026**	**1.6442**	**2.1325**	**7.0167**
n	**1**	**1**	**1**	**1**	**34**	**2**	**3**	**5**	**6**	**19**

Comparison of Peak Discharge (m3/s)

HEC-HMS Continuous Simulations

Return Period (Year)	E	E-2	E-3	E-11	E-16	E-202	E-20	E-29	E-30	E-301	E-304
2	1.147	1.028	0.966	0.876	1.147	0.047	0.680	0.586	0.414	0.352	0.162
5	1.463	1.328	1.254	1.157	1.463	0.135	0.928	0.805	0.567	0.505	0.342
10	1.664	1.521	1.436	1.342	1.664	0.232	1.104	0.960	0.675	0.607	0.463
25	1.909	1.760	1.660	1.574	1.909	0.411	1.342	1.170	0.819	0.737	0.602
50	2.088	1.936	1.822	1.746	2.088	0.592	1.530	1.336	0.932	0.833	0.692
100	2.263	2.111	1.981	1.919	2.263	0.821	1.726	1.510	1.049	0.929	0.771

APSWM ($t_{c\text{-channel}} = t_c + 1K\sqrt{(1-X)/n}$)

Return Period (Year)	E	E-2	E-3	E-11	E-16	E-202	E-20	E-29	E-30	E-301	E-304
2	2.834	2.577	2.445	2.280	2.831	0.388	1.926	1.681	1.379	1.214	0.589
5	4.139	3.712	3.498	3.228	4.136	0.489	2.677	2.302	1.855	1.617	0.752
10	5.237	4.655	4.370	4.012	5.231	0.566	3.289	2.806	2.238	1.940	0.880
25	6.795	5.991	5.601	5.114	6.789	0.671	4.144	3.506	2.767	2.384	1.053
50	8.039	7.054	6.578	5.987	8.031	0.751	4.819	4.056	3.180	2.730	1.187

100	9.327	8.152	7.587	6.887	9.317	0.832	5.512	4.620	3.603	3.084	1.322

Differences (%)

Return Period (Year)	E	E-2	E-3	E-11	E-16	E-202	E-20	E-29	E-30	E-301	E-304
2	147.0	150.6	153.0	160.3	146.8	724.9	183.3	186.7	233.2	244.9	263.5
5	182.8	179.5	179.0	179.0	182.6	262.8	188.5	186.1	226.9	220.2	119.6
10	214.8	206.0	204.2	199.0	214.4	144.3	197.8	192.2	231.3	219.5	90.0
25	255.9	240.3	237.4	224.9	255.6	63.4	208.8	199.7	237.7	223.5	74.9
50	285.1	264.3	261.0	242.8	284.7	26.8	215.1	203.6	241.1	227.6	71.4
100	312.1	286.2	282.9	258.8	311.7	1.4	219.3	206.0	243.3	231.8	71.6
Average Difference	232.9	221.2	219.6	210.8	232.6	203.9	202.1	195.7	235.6	227.9	115.2

Comparison of Reach Inflow and Outflow

HEC-HMS

Return Period (Year)	E-2	E-3	E-11	E-16	E-202	E-20	E-29	E-30	E-301	E-304
2	-10.4	-15.8	-23.6	0.0	-95.9	-40.7	-48.9	-63.9	-69.3	-85.9
5	-9.3	-14.3	-20.9	0.0	-90.8	-36.6	-45.0	-61.2	-65.5	-76.6
10	-8.6	-13.7	-19.4	0.0	-86.1	-33.6	-42.3	-59.4	-63.5	-72.2
25	-7.8	-13.1	-17.6	0.0	-78.5	-29.7	-38.7	-57.1	-61.4	-68.5
50	-7.3	-12.7	-16.4	0.0	-71.6	-26.7	-36.0	-55.4	-60.1	-66.8
100	-6.7	-12.4	-15.2	0.0	-63.7	-23.7	-33.3	-53.6	-58.9	-65.9
Average Difference	-8.3	-13.7	-18.8	0.0	-81.1	-31.9	-40.7	-58.4	-63.1	-72.6

APSWM ($t_{c\text{-channel}} = t_c + 1K\sqrt{(1-X)/n}$)

Return Period (Year)	E-2	E-3	E-11	E-16	E-202	E-20	E-29	E-30	E-301	E-304
2	-9.1	-13.7	-19.5	-0.1	-86.3	-32.0	-40.7	-51.3	-57.2	-79.2
5	-10.3	-15.5	-22.0	-0.1	-88.2	-35.3	-44.4	-55.2	-60.9	-81.8
10	-11.1	-16.6	-23.4	-0.1	-89.2	-37.2	-46.4	-57.3	-63.0	-83.2
25	-11.8	-17.6	-24.7	-0.1	-90.1	-39.0	-48.4	-59.3	-64.9	-84.5
50	-12.3	-18.2	-25.5	-0.1	-90.7	-40.1	-49.5	-60.4	-66.0	-85.2
100	-12.6	-18.7	-26.2	-0.1	-91.1	-40.9	-50.5	-61.4	-66.9	-85.8
Average Difference	-11.2	-16.7	-23.6	-0.1	-89.3	-37.4	-46.7	-57.5	-63.2	-83.3

Peak Reduction HEC-HMS	**8.3**	**13.7**	**18.8**	**0.0**	**81.1**	**31.9**	**40.7**	**58.4**	**63.1**	**72.6**
Peak Reduction APSWM	**11.2**	**16.7**	**23.6**	**0.1**	**89.3**	**37.4**	**46.7**	**57.5**	**63.2**	**83.3**
Regression HEC-HMS	**7.8**	**11.2**	**16.3**	**2.2**	**90.3**	**22.2**	**26.7**	**32.6**	**38.2**	**68.7**
Regression APSWM	**22.0**	**25.9**	**31.8**	**15.5**	**117.6**	**38.6**	**43.8**	**50.7**	**57.1**	**92.6**
$1K\sqrt{(1-2X)}/n$	**0.1368**	**0.2192**	**0.3420**	**0.0010**	**2.1332**	**0.4837**	**0.5924**	**0.7353**	**0.8706**	**1.6097**
K	**0.1368**	**0.2192**	**0.3420**	**0.0128**	**12.4383**	**0.6840**	**1.0260**	**1.6442**	**2.1325**	**7.0167**

HEC-HMS R-Square	**0.93253314**
APSWM R-Square	**0.99668376**

Table D-4 Comparison of Reach Routing for Catchment E (m = 2 for $mK\sqrt{(1-2X)/n}$)

Catchment E (Impervious = 100%)

Catchment-Reach	E-2	E-3	E-11	E-16	E-202	E-20	E-29	E-30	E-301	E-304
X	0	0	0	0.4968	0	0	0	0	0	0
K	0.1368	0.2192	0.342	0.0128	12.4383	0.684	1.026	1.6442	2.1325	7.0167
n	1	1	1	1	34	2	3	5	6	19

Comparison of Peak Discharge (m3/s)

HEC-HMS Continuous Simulations

Return Period (Year)	E	E-2	E-3	E-11	E-16	E-202	E-20	E-29	E-30	E-301	E-304
2	1.147	1.028	0.966	0.876	1.147	0.047	0.680	0.586	0.414	0.352	0.162
5	1.463	1.328	1.254	1.157	1.463	0.135	0.928	0.805	0.567	0.505	0.342
10	1.664	1.521	1.436	1.342	1.664	0.232	1.104	0.960	0.675	0.607	0.463
25	1.909	1.760	1.660	1.574	1.909	0.411	1.342	1.170	0.819	0.737	0.602
50	2.088	1.936	1.822	1.746	2.088	0.592	1.530	1.336	0.932	0.833	0.692
100	2.263	2.111	1.981	1.919	2.263	0.821	1.726	1.510	1.049	0.929	0.771

APSWM ($t_{c\text{-channel}} = t_c + 2K\sqrt{(1-X)/n}$)

Return Period (Year)	E	E-2	E-3	E-11	E-16	E-202	E-20	E-29	E-30	E-301	E-304
2	2.834	2.369	2.163	1.926	2.828	0.224	1.498	1.239	0.957	0.817	0.354
5	4.139	3.371	3.047	2.677	4.132	0.278	2.029	1.652	1.254	1.062	0.444
10	5.237	4.203	3.774	3.289	5.227	0.320	2.457	1.983	1.490	1.254	0.514
25	6.795	5.373	4.793	4.144	6.782	0.375	3.050	2.439	1.813	1.517	0.608
50	8.039	6.301	5.598	4.819	8.022	0.418	3.515	2.795	2.063	1.720	0.680

100	9.327	7.258	6.428	5.512	9.307	0.461	3.991	3.158	2.319	1.928	0.753

Differences (%)

Return Period (Year)	E	E-2	E-3	E-11	E-16	E-202	E-20	E-29	E-30	E-301	E-304
2	147.0	130.4	123.9	119.8	146.5	376.2	120.3	111.3	131.2	132.1	118.5
5	182.8	153.9	143.0	131.4	182.4	106.3	118.7	105.3	121.0	110.3	29.7
10	214.8	176.3	162.7	145.1	214.2	38.1	122.5	106.5	120.6	106.5	11.0
25	255.9	205.2	188.7	163.3	255.2	-8.7	127.3	108.5	121.3	105.9	1.0
50	285.1	225.4	207.2	175.9	284.2	-29.4	129.8	109.2	121.3	106.4	-1.8
100	312.1	243.9	224.4	187.2	311.3	-43.8	131.2	109.1	121.0	107.4	-2.3
Average Difference	232.9	189.2	175.0	153.8	232.3	73.1	125.0	108.3	122.7	111.4	26.0

Comparison of Reach Inflow and Outflow

HEC-HMS

Return Period (Year)	E-2	E-3	E-11	E-16	E-202	E-20	E-29	E-30	E-301	E-304
2	-10.4	-15.8	-23.6	0.0	-95.9	-40.7	-48.9	-63.9	-69.3	-85.9
5	-9.3	-14.3	-20.9	0.0	-90.8	-36.6	-45.0	-61.2	-65.5	-76.6
10	-8.6	-13.7	-19.4	0.0	-86.1	-33.6	-42.3	-59.4	-63.5	-72.2
25	-7.8	-13.1	-17.6	0.0	-78.5	-29.7	-38.7	-57.1	-61.4	-68.5
50	-7.3	-12.7	-16.4	0.0	-71.6	-26.7	-36.0	-55.4	-60.1	-66.8
100	-6.7	-12.4	-15.2	0.0	-63.7	-23.7	-33.3	-53.6	-58.9	-65.9
Average Difference	-8.3	-13.7	-18.8	0.0	-81.1	-31.9	-40.7	-58.4	-63.1	-72.6

APSWM $(t_{c\text{-channel}} = t_c + 2K\sqrt{(1-X)/n})$

Return Period (Year)	E-2	E-3	E-11	E-16	E-202	E-20	E-29	E-30	E-301	E-304
2	-16.4	-23.7	-32.0	-0.2	-92.1	-47.1	-56.3	-66.2	-71.2	-87.5
5	-18.6	-26.4	-35.3	-0.2	-93.3	-51.0	-60.1	-69.7	-74.3	-89.3
10	-19.7	-27.9	-37.2	-0.2	-93.9	-53.1	-62.1	-71.5	-76.1	-90.2
25	-20.9	-29.5	-39.0	-0.2	-94.5	-55.1	-64.1	-73.3	-77.7	-91.1
50	-21.6	-30.4	-40.1	-0.2	-94.8	-56.3	-65.2	-74.3	-78.6	-91.5
100	-22.2	-31.1	-40.9	-0.2	-95.1	-57.2	-66.1	-75.1	-79.3	-91.9
Average Difference	-19.9	-28.2	-37.4	-0.2	-93.9	-53.3	-62.3	-71.7	-76.2	-90.2

Peak Reduction HEC-HMS	8.3	13.7	18.8	0.0	81.1	31.9	40.7	58.4	63.1	72.6
Peak Reduction APSWM	19.9	28.2	37.4	0.2	93.9	53.3	62.3	71.7	76.2	90.2
Regression HEC-HMS	13.5	20.3	30.4	2.3	178.4	42.1	51.1	62.9	74.1	135.2
Regression APSWM	28.5	36.4	48.2	15.5	219.8	61.8	72.2	85.9	98.9	169.7
$2K\sqrt{(1-2X)}/n$	0.2736	0.4384	0.6840	0.0020	4.2663	0.9673	1.1847	1.4706	1.7412	3.2195
K	0.1368	0.2192	0.3420	0.0128	12.4383	0.6840	1.0260	1.6442	2.1325	7.0167

HEC-HMS R-Square	**0.93253314**
APSWM R-Square	**0.97749005**

Table D-5 Comparison of Reach Routing for Catchment F (m = 2 for $mK\sqrt{(1-2X)/n}$)

Catchment F (Impervious = 0%)

Catchment-Reach Combination	F-I	F-II	F-III	F-IV
X	0	0	0.497	0.4932
K	1.1947	4.7726	1.196	4.7699

Comparison of Peak Discharge (m3/s)

HEC-HMS Continuous Simulations

Return Period (Year)	F	F-I	F-II	F-III	F-IV
2	3.699	2.844	3.561	3.562	1.687
5	5.788	4.710	5.619	5.586	2.795
10	7.239	6.025	7.020	6.993	3.590
25	9.124	7.737	8.801	8.822	4.639
50	10.550	9.036	10.126	10.207	5.440
100	11.988	10.336	11.435	11.604	6.274

APSWM ($t_{c\text{-channel}} = t_c + 2K\sqrt{(1-X)}$)

Return Period (Year)	F	F-I	F-II	F-III	F-IV
2	4.517	3.384	1.986	4.410	3.916
5	6.689	4.899	2.804	6.508	5.729
10	8.439	6.102	3.439	8.198	7.179
25	10.858	7.748	4.295	10.533	9.171
50	12.755	9.028	4.955	12.363	10.727
100	14.696	10.332	5.623	14.235	12.316

Differences (%)

Return Period (Year)	F	F-I	F-II	F-III	F-IV
2	22.1	19.0	-44.2	23.8	132.2
5	15.6	4.0	-50.1	16.5	104.9
10	16.6	1.3	-51.0	17.2	100.0
25	19.0	0.1	-51.2	19.4	97.7
50	20.9	-0.1	-51.1	21.1	97.2
100	22.6	0.0	-50.8	22.7	96.3
Average Difference	19.5	4.1	-49.7	20.1	104.7

Comparison of Reach Inflow and Outflow

HEC-HMS

Return Period (Year)	F-I	F-II	F-III	F-IV
2	-23.1	-3.7	-3.7	-54.4
5	-18.6	-2.9	-3.5	-51.7
10	-16.8	-3.0	-3.4	-50.4
25	-15.2	-3.5	-3.3	-49.2
50	-14.4	-4.0	-3.3	-48.4
100	-13.8	-4.6	-3.2	-47.7
Average Difference (100%)	-17.0	-3.6	-3.4	-50.3

APSWM ($t_{c\text{-channel}} = t_c + 2K\sqrt{(1-X)}$)

Return Period (Year)	F-I	F-II	F-III	F-IV
2	-25.1	-56.0	-2.4	-13.3
5	-26.8	-58.1	-2.7	-14.4
10	-27.7	-59.2	-2.9	-14.9
25	-28.6	-60.4	-3.0	-15.5
50	-29.2	-61.2	-3.1	-15.9
100	-29.7	-61.7	-3.1	-16.2
Average Difference (100%)	-27.8	-59.4	-2.9	-15.0